ADVANCED HANDLING AND SORTING TECHNIQUES FOR ULTRASMALL PARTICLES

Stuart J. Hemple, et al

Block Engineering, Incorporated

Prepared for:

Advanced Research Projects Agency
Air Force Technical Applications Center

15 April 1975

BEI-75-649

ADVANCED HANDLING AND SORTING TECHNIQUES FOR ULTRASMALL PARTICLES

FINAL REPORT

AFTAC PROJECT AUTHORIZATION NO: AFTAC/VT/3428

CONTRACT NUMBER: F08606-73-C-0042

PREPARED BY: S. J. HEMPLE
H. J. CAULFIELD
K. DUTTA

Effective Date of Contract: 3 July 1973
Contract Expiration Data: 16 February 1975

Sponsored by:
Advanced Research Projects Agency
ARPA Order No. 1702

Submitted by:
BLOCK ENGINEERING, INC.
19 Blackstone Street
Cambridge, Mass. 02139
(617) 868-6050

and one-at-a-time sorting. In addition, particle aerosolization by plasma ashing, gas dynamic transport and positioning of particles, and particle deposition from gas flow were studied to interface the three techniques.

An extensive study of the effects of plasma ashing on particles and substrates was made. These results should prove useful in the removal of particles from organic substrates and in removing unwanted organic particles from samples. A wide range of material and commercial substrates were ashed and a large number of gas compositions and relative ratios were tested. The particles formed upon oxygen ashing appear under a microscope to be 0.1 μm and should be easily separated from the larger inorganic particles remaining.

An extensive theoretical investigation of dielectrophoresis was made. This resulted in the theoretical determination of particle size dependence, a dielectric sorter module design, and likely operating conditions.

A technique for producing a one-at-a-time particle flow in a gas was developed. Interesting particles were to be detected by their characteristic fluorescence which is excited by a focused laser beam and sensed by filtered photo cells. The interesting particles were then to be deflected by an ion wind created by a high voltage pulse between two electrodes. Work on the breadboard was terminated before these ideas could be tested.

As advanced testing progressed, it slowly became apparent that the pressure and gas flow rate requirements of the three separate techniques were irreconcilably incompatible. That is, as the likely operating conditions for each stage became known, it became apparent that there was no way to interface them into one simple instrument as proposed.

Unclassified

SECURITY CLASSIFICATION OF THIS PAGE (When Data Entered)

REPORT DOCUMENTATION PAGE		READ INSTRUCTIONS BEFORE COMPLETING FORM
1. REPORT NUMBER	2. GOVT ACCESSION NO.	3. RECIPIENT'S CATALOG NUMBER
4. TITLE (and Subtitle) Advanced Handling and Sorting Techniques for Ultrasmall Particles		5. TYPE OF REPORT & PERIOD COVERED Final Report 6. PERFORMING ORG. REPORT NUMBER BEI-75-649
7. AUTHOR(s) Stuart J. Hemple H. John Caulfield Kalyan Dutta		8. CONTRACT OR GRANT NUMBER(s) F08606-73-C-0042
9. PERFORMING ORGANIZATION NAME AND ADDRESS Block Engineering, Inc. 19 Blackstone Street Cambridge, MA 02139		10. PROGRAM ELEMENT, PROJECT, TASK AREA & WORK UNIT NUMBERS
11. CONTROLLING OFFICE NAME AND ADDRESS AFTAC/VT 3428 Patrick AFB, FL 32925		12. REPORT DATE 15 April 1975 13. NUMBER OF PAGES 114
14. MONITORING AGENCY NAME & ADDRESS (if different from Controlling Office) Advanced Research Projects Agency of the Department of Defense ARPA Order No. 1702		15. SECURITY CLASS. (of this report) Unclassified 15a. DECLASSIFICATION/DOWNGRADING SCHEDULE

16. DISTRIBUTION STATEMENT (of this Report)

Distribution of this document is unlimited.

17. DISTRIBUTION STATEMENT (of the abstract entered in Block 20, if different from Report)

18. SUPPLEMENTARY NOTES

19. KEY WORDS (Continue on reverse side if necessary and identify by block number)

Plasma Ashing
Particle Handling
Dielectrophoresis
Particle Sorting

20. ABSTRACT (Continue on reverse side if necessary and identify by block number)

The goal of this particle handling project was to design and construct an automatic particle sorter. This instrument was to be capable of sorting out particles of interest rapidly and with low loss. The particle diameter range, over which this instrument was to be effective was 5 μm to 0.1 μm. The following techniques were investigated for use in a breadboard particle sorter: plasma ashing, dielectrophoresis,

DD FORM 1 JAN 73 1473 EDITION OF 1 NOV 65 IS OBSOLETE

Unclassified

SECURITY CLASSIFICATION OF THIS PAGE (When Data Entered)

This research was supported by the Advanced Research Projects Agency of the Department of Defense and was monitored by AFTAC/VT 3428, Patrick AFB FL 32925, under Contract No. F08606-73-C-0042.

TABLE OF CONTENTS

TABLE OF CONTENTS

TABLE OF FIGURES

LIST OF TABLES

SUMMARY

The goal of this particle handling project was to design and construct an automatic particle sorter. This instrument was to be capable of sorting out particles of interest rapidly and with low loss. The particle diameter range, over which this instrument was to be effective, was 5 μm to 0.1 μm. The techniques utilized were to be highly independent of particle shape or size and present minimal damage and contamination. The following techniques were investigated for use in a breadboard particle sorter: plasma ashing, dielectrophoresis, and one-at-a-time sorting. In addition, particle aerosolization by plasma ashing, gas dynamic transport and positioning of particles, and particle deposition from gas flow were studied to interface the three techniques.

An extensive study of the effects of plasma ashing on particles and substrates was made. These results should prove useful in the removal of particles from organic substrates and in removing unwanted organic particles from samples. A wide range of material and commercial substrates were ashed and a large number of gas compositions and relative ratios were tested. The particles formed upon oxygen ashing appear under a scanning electron microscope to be less than 0.1 μm and should be easily separated from the larger inorganic particles remaining. However, in oxygen plasmas, samples of UO_2 showed a slight increase in weight indicating the formation of higher oxides of uranium.

An extensive theoretical investigation of dielectrophoresis was made. This resulted in the theoretical determination of particle size dependence, a dielectric sorter module design, and likely operating conditions. However, since the operating conditions conflicted with pressure and flow requirements, we were not able to test these theoretical results.

A technique for producing a one-at-a-time particle flow in

a gas was developed. Interesting particles were to be detected by their characteristic fluorescence which is excited by a focused laser beam and sensed by filtered photo cells. The interesting particles were then to be deflected by an ion wind created by a high voltage pulse between two electrodes. Work on the breadboard was terminated before these ideas could be tested.

As advanced testing progressed, it slowly became apparent that the pressure and gas flow rate requirements of the three separate techniques were irreconcilably incompatible. That is, as the likely operating conditions for each stage became known, it became apparent that there was no way to interface them into one simple instrument as proposed.

In addition, other difficulties came to light. The dielectic constant to density ratios of particles of interest were found not to be unique as first proposed. Plasma ashing did not put the remaining particles evenly and completely into a flowing gas stream. As a consequence of these insoluble problems, it was necessary to abort plans to construct a breadboard instrument. For the balance of the contract period, our effort was directed entirely toward the only stand-alone component of the system - plasma ashing.

SECTION I

INTRODUCTION

1.0 Historical Perspective

This is the final report for a two phase program on "Advanced Handling and Sorting Techniques for Ultrasmall Particles". By early 1972, Block Engineering had conceived of a variety of particle handling techniques which seemed unique and promising. These techniques were described in an unsolicited proposal. That proposal led to the funding of the first two phases of a proposed three phase program to test those techniques, select from among them the most useful ones, and construct a breadboard automatic particle sorting instrument.

In Phase I, a large number of techniques were developed and given preliminary testing. The primary accomplishments are enumerated:

(1) The diverse concepts proposed were organized into a unified system concept which carries out the desired functions in a logical order.

(2) A concept of avoiding liquids altogether to prevent contamination was developed.

(3) Plasma ashing was tested and found to be adequate for suspending the particles and introducing them into a fluidic sorter.

(4) It was demonstrated that most of the uninteresting organic particles could be eliminated by selective ashing.

(5) A fluidic system was demonstrated to be a low loss technique.

(6) Bulk sorting techniques were considered to eliminate uninteresting particles early in the fluidic sorting procedure.

(7) Suitable modular sorter section construction methods were devised.

(8) One-at-a-time sorting in a fluidic system was investigated.

(9) Two new deflection methods were devised and tested.

(10) Storage in the vapor state was demonstrated.

(11) Laser levitation of particles 1/10 of the diameter of the smallest previously-levitated particles was accomplished.

(12) Photophoretic separation of relatively large particles from relatively small particles was indicated.

At the end of Phase I, it was decided that a breadboard automatic particle sorter based on the concepts developed during Phase I could be constructed. Thus, the goal of Phase II was to construct a breadboard particle sorter using the following techniques: plasma ashing, dielectrophoresis, and one-at-a-time sorting. In addition, the techniques of particle aerosolization by plasma ashing, particle transport and positioning by flowing gases, and particle deposition from a gas stream would be utilized.

1.1 Performance Goals for Automatic Particle Sorter

A review of particle analysis problems determined for us the following specific requirements for this program which have guided our work.

First, it is necessary that particle selection be only species dependent and be relatively independent of particle shape or size.

Second, it is necessary that the system have low losses. To be specific, losses must be considerably fewer than losses of available methods. It is clear that currently losses approach 100% for particles below, say, 0.5 μm. Thus, any significant efficiency in the 0.1 μm to 0.5 μm range would be helpful. Furthermore, the number of these particles is likely to greatly exceed the number in the 1 μm to 5 μm range. Thus, although the goal is no loss for all sizes, even a high loss rate (e.g., 20%) would offer a very dramatic improvement.

Third, damage and contamination must be minimized.

Fourth, the sorting rate must be rapid.

1.2 Techniques Chosen for Utilization in Automatic Particle Sorter

1.2.1 Plasma Ashing

A plasma is a state of matter composed entirely of electrons and bare nuclei. However, at very high temperatures or in the presence of strong electric or magnetic fields, a glowing and partially ionized gas composed of ions, electrons, and neutral species is also referred to as a plasma. In plasmas produced by radio frequency (RF) fields, free electrons gain energy from the imposed electric field and lose this energy through collisions with neutral gas molecules. The transfer of energy to the molecules leads to the formation of a variety of new species including metastables, atoms, free radicals, and ions. These products are all chemically active and can be used to react with solid matter to form gaseous products. An additional characteristic of such plasmas is the lack of equilibrium between the electron temperature, T_e, and the gas

temperature, T_g. While the electrons are sufficiently energetic to cause the rupture of molecular bonds, the gas temperature may only be slightly above ambient values, hence the term cold or low temperature ashing.

In Phase II, cold plasma ashing was to be used in two separate ways. First, to remove all the organic and some of the inorganic particles which contaminate samples. While leaving particles of interest unaltered, plasma ashing removes most of the unwanted particles by reactions to form volatile products. Secondly, plasma ashing appeared to be useful in the removal of the original substrate. As ashing progressed, the remaining particles could be picked up by a flowing gas stream and carried into the succeeding stages of separation.

1.2.2 Dielectrophoresis

Dielectric particles can be deflected by inhomogeneous electric fields. At low pressures (0.1 torr), this deflection is in the first order independent of particle size. Size dependence enters as a second order term which depends on mean free path and gas viscosity. At pressures of 10 torr and greater, this size dependent term becomes significant and at higher pressures even dominant. In this second stage, particles of one dielectric constant-to-density ratio were to have been separated from those unwanted particles having very different ratios. After this stage, those particles of a certain dielectric constant to density ratio range will be passed on to the final stage.

1.2.3 One-at-a-Time Sorting

Once the great bulk of uninteresting particles have been removed by the first two stages, the number of remaining particles should be small enough to sort one particle at a time. The par-

ticles in the transporting gas are so constricted that they pass one-at-a-time with constant velocity through a laser beam. The laser light produces a characteristic fluorescence emission which can be detected by an array of filter photocells. Shortly downstream, the interesting particles can be deflected by a strong electric field into a separate gas stream for final deposition or any other type of processing.

1.3 Organization of Phase II

The primary goal of Phase II was to assemble and test a workable breadboard particle sorter based on the concepts examined in Phase I. The breadboard should have been suitable as a basis for a deliverable model for Phase III. Phase II as planned involved three separate steps:

(1) To do advanced testing and theoretical investigation of the three techniques, plasma ashing, dielectrophoresis, and one-at-a-time sorting, that are the basis for the three operating stages of the automatic fluidic sorter. Also to do advanced testing of the interfacing of the three stages and of the final particle deposition.

(2) To develop by using the data from step one, a detailed instrument design that is suitable for rapid, inexpensive construction.

(3) To construct a breadboard instrument and test its capability and efficiency with standards and unknown samples.

Steps one and two were to run simultaneously over the first two thirds of the contract period. These two steps were to interact with each other and culminate in a complete system design

to be built in step three. The system assembly would demonstrate the concepts used and the solutions to the interfacing problems. Of course, the system would have been improved considerably in transmission efficiency, sorting versatility, and transmission rate in going from the breadboard model to the deliverable system in Phase III. Nevertheless, all of the basic features would have been present in the breadboard model.

1.4 Results of Phase II

An extensive study of the effects of plasma ashing on particles and substrates was made. The results of this investigation, presented in Section III, should prove useful in the removal of particles from organic substrates and in removing unwanted organic particles from their samples. A wide range of natural substrates were ashed and a large number of gas compositions and relative ratios were tested.

An extensive theoretical investigation of dielectrophoresis, presented in Appendix A, was made. This led to the determination of particle size dependence, a dielectric sorter module design and likely operating conditions. Also, the problems in utilizing this technique have been outlined in Section II.

As the proper operating conditions became known for each stage of the sorter, it became apparent that there was no way to interface them into one simple instrument as proposed. Since steps one and two could not yield a detailed instrument design suitable for construction, step three had to be aborted. Consequently, we could not complete that part of the original tasking dealing with construction and testing with both standards and unknowns of a fluidic particle sorter. The system design, at the point of termination, is presented in Section IV.

SECTION II

DIELECTROPHORETIC SEPARATION

2.0 Introduction

The thorough theoretical analysis of dielectrophoresis, presented in Appendix A, is elucidated by a series of numerical computations aimed at determining the theoretical effectiveness of dielectric particle separation in our various designs. The equations of motion derived in Appendix A are in the form of second order differential equations, and are analytically solvable. However, th. approach taken here is an iterative solution method, well suited to implementation on a digital computer. A computer simulation of the dielectric separation is presented with results showing the separate effects of particle size, initial position, and other parameters on the efficiency of separation.

Also, the behavior of an ensemble of dielectric particles of two different species (UO_2 and SiO_2) and of various sizes is analyzed. UO_2 and SiO_2 were selected because there was a great difference in their dielectric constant to density ratios. Numerical results show the theoretically derived distribution of these particles in a separation stage, and indicate the degree to which these species can be separated.

2.1 A Computer Simulation of the Dielectrophoretic Separation Technique

2.1.1 Preliminary Experiments

In order to gain insight into the behavior of particles of various sizes, dielectric constants and densities, the equation of motion for dielectrophoresis in a gas was solved. The starting point for these computations are the equations

$$\ddot{x} = \frac{-\varepsilon_o (K - 1) V_o^2}{\rho P^2 r_1^4} \frac{(1 - x)}{(x - \frac{1}{2}x^2)^3} - \frac{18\eta \dot{x}}{\rho d^2 + \rho dL(a + be^{-cd/L})} \qquad (2\text{-}1)$$

for the planar geometry and its counterpart

$$\ddot{x} = \frac{-\epsilon_o (K - 1)\, V_o^2}{\rho\, p'^2\, r_1^4} \quad \frac{1}{x^3} - \frac{18\eta\, \dot{x}}{\rho d^2 + \rho dL(a + be^{-cd/L})} \tag{2-2}$$

for the cylindrical electrode geometry (see Equations A-39, A-40, and A-52).

Here x is defined as a normalized position coordinate (see Equations A-37 and A-38) and $\dot{x}$ and $\ddot{x}$ are the corresponding normalized velocity and acceleration.

Although Equations 2-1 and 2-2 are solvable by analytic means, it was decided to simulate the behavior of a general particle by computing its trajectory with a simultaneous evaluation of the accelerations produced by the field and by the drag forces, in order to decide when drag forces became considerable.

The method for the solution of the differential equations 2-1 and 2-2 are very similar. In both cases almost identical FORTRAN source programs were generated. A listing of the programs to compute the trajectories in the planar and cylindrical cases, names FIELD and FIELD 3 respectively, is attached in Appendix B.

In each case a number of parameters are capable of being entered under program control, to be used as initial values, etc. These include the initial position of the particle; its size; the applied voltage; etc. Also, the geometrical dimensions of the electrode configuration was variable, with the inner electrode radius being fixed at 1/50 of the distance of the outer electrode. Initially, only two choices for the possible use of the viscosity coefficient were provided: one

corresponding to air at standard temperature and pressure, and the other corresponding to hydrogen at 1/100 atmospheres pressure.

The technique for the solution of the equations of motion was to update iteratively the position, velocity, and accelerations due to field and drag respectively, for each particle. For a convenient compromise between speed of computation and the accuracy of the results, the iterations were done on 1 μsec intervals, with the results being displayed at intervals of 0.1 milliseconds, or every 100 iterations.

Some of the results from executing the programs FIELD and FIELD 3 are shown in Tables 2-1 and 2-5 on the following pages. In each case, the results have been displayed simultaneously for identical particles under identical electrode geometry and accelerating voltage conditions. In reading these data, a minor discrepancy between the description of the equation of motion for the planar geometry and its implementation in FIELD must be mentioned. In FIELD, the particle moves from its initial normalized position (typically 0.95 cm) out to a normalized final position (typically 0.98 cm). Thus its velocity and acceleration are both positive. This is in contrast with FIELD 3 where the particle is moving inwards and its velocity and acceleration are consequently negative. Apart from the minor differences, the absolute values of the velocities and acceleration can be compared for both programs at each instant of time.

Tables 2-1, 2-2 and 2-3 show the rapidly increasing effect of drag when the size is reduced, for a particle of dielectric constant of 20, and a density of 3 gm/cc. A comparison of the field and drag accelerations indicates that

```
FIELD
ETA? (TYPE 0.0 FOR DEFAULT)1E-6
POSN? 0.95
ELECTRODE SPACING IN CM. ? (F4.2)

1.0
PARTICLE DIAMETER IN MICRONS ? (F5.1)

 10.0
VOLTAGE ? (F7.1)

 4220.0
```

POSITION CM.		VELOCITY CM/SEC		ACCELERATION CM/SECSQ		FIELD ACCN CM/SECSQ		DRAG ACCN CM/SECSQ		TIME MSEC
0.9500E	0	0.5148E	0	0.1658E	5					
0.9521E	0	0.1647E	1	0.1648E	5	0.1658E	5	0.9834E	2	0.100
0.9553E	0	0.3321E	1	0.1663E	5	0.1682E	5	0.1981E	3	0.200
0.9607E	0	0.4972E	1	0.1695E	5	0.1725E	5	0.2937E	3	0.300
0.9712E	0	0.6697E	1	0.1747E	5	0.1787E	5	0.4018E	3	0.400
0.9921E	0	0.8479E	1	0.1822E	5	0.1870E	5	0.5087E	3	0.500
0.9520E	0	0.1035E	2	0.1924E	5	0.1986E	5	0.6209E	3	0.600
0.9542E	0	0.1234E	2	0.2062E	5	0.2136E	5	0.7403E	3	0.700
0.9565E	0	0.1449E	2	0.2247E	5	0.2334E	5	0.8693E	3	0.800
0.9571E	0	0.1685E	2	0.2495E	5	0.2596E	5	0.1011E	4	0.900
0.9589E	0	0.1951E	2	0.2853E	5	0.2953E	5	0.1170E	4	1.000
0.9612E	0	0.2256E	2	0.3317E	5	0.3458E	5	0.1354E	4	1.100
0.9634E	0	0.2621E	2	0.4725E	5	0.4132E	5	0.1572E	4	1.200
0.9662E	0	0.3074E	2	0.5137E	5	0.5321E	5	0.1844E	4	1.300
0.9696E	0	0.3673E	2	0.7055E	5	0.7275E	5	0.2204E	4	1.400
0.9757E	0	0.4544E	2	0.1091E	6	0.1118E	6	0.2726E	4	1.500
0.9789E	0	0.6048E	2	0.2127E	6	0.2163E	6	0.3629E	4	1.600
0.9865E	0	0.1037E	3	0.5194E	6	0.5254E	6	0.6039E	4	1.700
0.1079E	1	0.2344E	4	-0.1445E	6	-0.3875E	4	0.1487E	6	1.INT

```
FIELD3
ETA? (TYPE 0.0 FOR DEFAULT)1E-6
POSN? 0.05
ELECTRODE DIAMETER IN CM. ? (F4.2)

2.0
PARTICLE DIAMETER IN MICRONS ? (F5.1)

 10.0
VOLTAGE ? (F7.1)

 4002.0
```

POSITION CM.		VELOCITY CM/SEC		ACCELERATION CM/SECSQ		FIELD ACCN CM/SECSQ		DRAG ACCN CM/SECSQ		TIME MSEC
0.5000E	-1	0.0000E	0	-0.2221E	5					
0.4989E	-1	-0.2219E	1	-0.2222E	5	-0.2235E	5	-0.1331E	3	0.100
0.4956E	-1	-0.4454E	1	-0.2254E	5	-0.2381E	5	-0.2673E	3	0.200
0.4900E	-1	-0.6738E	1	-0.2319E	5	-0.2560E	5	-0.4043E	3	0.300
0.4821E	-1	-0.9105E	1	-0.2433E	5	-0.2878E	5	-0.5463E	3	0.400
0.4717E	-1	-0.1165E	2	-0.2575E	5	-0.2645E	5	-0.6959E	3	0.500
0.4588E	-1	-0.1427E	2	-0.2789E	5	-0.2874E	5	-0.8564E	3	0.600
0.4431E	-1	-0.1722E	2	-0.3088E	5	-0.3191E	5	-0.1030E	4	0.700
0.4243E	-1	-0.2049E	2	-0.3512E	5	-0.3635E	5	-0.1229E	4	0.800
0.4019E	-1	-0.2428E	2	-0.4109E	5	-0.4275E	5	-0.1457E	4	0.900
0.3758E	-1	-0.2834E	2	-0.5072E	5	-0.5245E	5	-0.1731E	4	1.000
0.3439E	-1	-0.3461E	2	-0.6600E	5	-0.6820E	5	-0.2077E	4	1.100
0.3015E	-1	-0.4248E	2	-0.9477E	5	-0.9732E	5	-0.2549E	4	1.200
0.2575E	-1	-0.5465E	2	-0.1593E	6	-0.1626E	6	-0.3279E	4	1.300
0.1925E	-1	-0.7891E	2	-0.3845E	6	-0.3893E	6	-0.4735E	4	1.400
0.7452E	-2	-0.2179E	3	-0.8694E	7	-0.6787E	7	-0.1307E	5	1.500
0.2845E	0	0.3521E	4	-0.2114E	6	-0.1225E	3	0.2113E	6	1.600
0.6356E	0	0.3528E	4	-0.2180E	6	-0.1081E	2	0.2160E	6	1.700
0.9845E	0	0.3479E	4	-0.2287E	6	-0.2909E	1	0.2287E	6	1.800
0.1331E	1	0.3450E	4	-0.2875E	6	-0.1176E	1	0.2875E	6	1.900

TABLE 2-1. Motion of a 10 μm Particle in H_2 at 1/100 atm.

```
FIELD
ETA? (TYPE 0.0 FOR DEFAULT)1E-6
POSN? 0.95
ELECTRODE SPACING IN CM. ? (F4.2)

1.2
PARTICLE DIAMETER IN MICRONS ? (F5.1)

  5.0
VOLTAGE ? (F7.1)

 4002.0
```

POSITION CM.		VELOCITY CM/SEC		ACCELERATION CM/SECSQ		FIELD ACCN CM/SECSQ		DRAG ACCN CM/SECSQ		TIME MSEC
0.9500E	0	0.5140E	0	0.1650E	5					
0.9321E	0	0.1650E	1	0.1619E	5	0.1658E	5	0.3917E	3	0.100
0.9500E	0	0.3240E	1	0.1634E	5	0.1632E	5	0.7703E	3	0.200
0.9507E	0	0.4847E	1	0.1607E	5	0.1723E	5	0.1163E	4	0.300
0.9513E	0	0.6463E	1	0.1609E	5	0.1784E	5	0.1551E	4	0.400
0.9522E	0	0.8111E	1	0.1671E	5	0.1866E	5	0.1947E	4	0.500
0.9537E	0	0.9812E	1	0.1720E	5	0.1973E	5	0.2355E	4	0.600
0.9540E	0	0.1160E	2	0.1809E	5	0.2113E	5	0.2763E	4	0.700
0.9552E	0	0.1329E	2	0.1978E	5	0.2294E	5	0.3208E	4	0.800
0.9567E	0	0.1555E	2	0.2157E	5	0.2531E	5	0.3730E	4	0.900
0.9584E	0	0.1730E	2	0.2417E	5	0.2845E	5	0.4378E	4	1.000
0.9603E	0	0.2048E	2	0.2782E	5	0.3278E	5	0.4979E	4	1.100
0.9625E	0	0.2244E	2	0.3211E	5	0.3874E	5	0.5626E	4	1.200
0.9650E	0	0.2712E	2	0.4115E	5	0.4766E	5	0.6509E	4	1.300
0.9679E	0	0.3183E	2	0.5426E	5	0.6199E	5	0.7629E	4	1.400
0.9714E	0	0.3838E	2	0.7807E	5	0.8726E	5	0.9193E	4	1.500
0.9757E	0	0.4830E	2	0.1302E	6	0.1418E	6	0.1159E	5	1.600
0.9814E	0	0.6765E	2	0.2972E	6	0.3134E	6	0.2624E	5	1.700
0.9908E	0	0.1475E	3	0.2525E	7	0.2561E	7	0.3543E	5	1.800

```
FIELD3
ETA? (TYPE 0.0 FOR DEFAULT)1E-6
POSN? 0.05
ELECTRODE DIAMETER IN CM. ? (F4.2)

2.0
PARTICLE DIAMETER IN MICRONS ? (F5.1)

  5.0
VOLTAGE ? (F7.1)

 4000.0
```

POSITION CM.		VELOCITY CM/SEC		ACCELERATION CM/SECSQ		FIELD ACCN CM/SECSQ		DRAG ACCN CM/SECSQ		TIME MSEC
0.5000E	-1	0.2870E	2	-0.2021E	5					
0.4939E	-1	-0.2100E	1	-0.2103E	5	-0.2035E	5	-0.5075E	3	0.100
0.4956E	-1	-0.4076E	1	-0.2175E	5	-0.2230E	5	-0.1005E	4	0.200
0.4981E	-1	-0.6960E	1	-0.2385E	5	-0.2357E	5	-0.1504E	4	0.300
0.4985E	-1	-0.8787E	1	-0.2261E	5	-0.2471E	5	-0.2109E	4	0.400
0.4725E	-1	-0.1109E	2	-0.2364E	5	-0.2631E	5	-0.2660E	4	0.500
0.4600E	-1	-0.1352E	2	-0.2522E	5	-0.2847E	5	-0.3243E	4	0.600
0.4454E	-1	-0.1616E	2	-0.2752E	5	-0.3141E	5	-0.3879E	4	0.700
0.4278E	-1	-0.1907E	2	-0.3067E	5	-0.3545E	5	-0.4577E	4	0.800
0.4071E	-1	-0.2230E	2	-0.3576E	5	-0.4113E	5	-0.5372E	4	0.900
0.3829E	-1	-0.2600E	2	-0.4316E	5	-0.4946E	5	-0.6311E	4	1.000
0.3540E	-1	-0.3115E	2	-0.5477E	5	-0.6248E	5	-0.7476E	4	1.100
0.3221E	-1	-0.3756E	2	-0.7565E	5	-0.8467E	5	-0.9215E	4	1.200
0.2781E	-1	-0.4693E	2	-0.1177E	6	-0.1290E	6	-0.1126E	5	1.300
0.2240E	-1	-0.6324E	2	-0.2319E	6	-0.2471E	6	-0.1515E	5	1.400
0.1435E	-1	-0.1075E	3	-0.9129E	6	-0.9687E	6	-0.2581E	5	1.500
-0.1529E	0	-0.4413E	4	0.1060E	7	0.7763E	3	-0.1259E	7	1.600

TABLE 2-2. Motion of a 5 μm Particle in H_2 at 1/100 atm.

FIELD
ETA? (TYPE 0.0 FOR DEFAULT)1E-6
POSN? 0.95
ELECTRODE SPACING IN CM. ? (F4.2)

1.0
PARTICLE DIAMETER IN MICRONS ? (F5.1)

1.0
VOLTAGE ? (F7.1)

4000.0

POSITION CM.	VELOCITY CM/SEC	ACCELERATION CM/SECSQ	FIELD ACCN CM/SECSQ	DRAG ACCN CM/SECSQ	TIME MSEC
0.9500E 0	0.2517E-80	0.1652E 5			
0.9501E 0	0.1245E 1	0.9392E 4	0.1656E 5	0.7471E 4	0.100
0.9502E 0	0.1937E 1	0.5125E 4	0.1673E 5	0.1163E 5	0.200
0.9504E 0	0.2330E 1	0.2962E 4	0.1694E 5	0.1398E 5	0.300
0.9507E 0	0.2562E 1	0.1814E 4	0.1719E 5	0.1536E 5	0.400
0.9512E 0	0.2711E 1	0.1223E 4	0.1747E 5	0.1627E 5	0.500
0.9512E 0	0.2814E 1	0.8834E 3	0.1777E 5	0.1688E 5	0.600
0.9515E 0	0.2893E 1	0.7202E 3	0.1803E 5	0.1736E 5	0.700
0.9518E 0	0.2961E 1	0.6432E 3	0.1841E 5	0.1777E 5	0.800
0.9521E 0	0.3024E 1	0.6127E 3	0.1875E 5	0.1814E 5	0.900
0.9524E 0	0.3085E 1	0.6081E 3	0.1912E 5	0.1851E 5	1.000
0.9527E 0	0.3146E 1	0.6132E 3	0.1949E 5	0.1887E 5	1.100
0.9530E 0	0.3206E 1	0.6274E 3	0.1989E 5	0.1925E 5	1.200
0.9534E 0	0.3273E 1	0.6624E 3	0.2030E 5	0.1964E 5	1.300
0.9537E 0	0.3341E 1	0.6914E 3	0.2074E 5	0.2005E 5	1.400
0.9542E 0	0.3412E 1	0.7239E 3	0.2119E 5	0.2047E 5	1.500
0.9544E 0	0.3486E 1	0.7591E 3	0.2167E 5	0.2092E 5	1.600
0.9547E 0	0.3564E 1	0.7993E 3	0.2218E 5	0.2138E 5	1.700
0.9551E 0	0.3646E 1	0.8415E 3	0.2272E 5	0.2187E 5	1.800
0.9555E 0	0.3732E 1	0.8876E 3	0.2328E 5	0.2239E 5	1.900
0.9558E 0	0.3823E 1	0.9386E 3	0.2333E 5	0.2294E 5	2.000

FIELD3
ETA? (TYPE 0.0 FOR DEFAULT)1E-6
POSN? 0.05
ELECTRODE DIAMETER IN CM. ? (F4.2)

2.0
PARTICLE DIAMETER IN MICRONS ? (F5.1)

1.0
VOLTAGE ? (F7.1)

4000.0

POSITION CM.	VELOCITY CM/SEC	ACCELERATION CM/SECSQ	FIELD ACCN CM/SECSQ	DRAG ACCN CM/SECSQ	TIME MSEC
0.5000E -1	0.2000E 0	-0.2221E 5			
0.4991E -1	-0.1677E 1	-0.1027E 5	-0.2230E 5	-0.1826E 5	0.100
0.4969E -1	-0.2613E 1	-0.6948E 4	-0.2262E 5	-0.1568E 5	0.200
0.4943E -1	-0.3153E 1	-0.4112E 4	-0.2303E 5	-0.1592E 5	0.300
0.4907E -1	-0.3481E 1	-0.2611E 4	-0.2352E 5	-0.2089E 5	0.400
0.4871E -1	-0.3699E 1	-0.1827E 4	-0.2402E 5	-0.2220E 5	0.500
0.4833E -1	-0.3860E 1	-0.1431E 4	-0.2459E 5	-0.2316E 5	0.600
0.4793E -1	-0.3993E 1	-0.1245E 4	-0.2520E 5	-0.2396E 5	0.700
0.4753E -1	-0.4112E 1	-0.1174E 4	-0.2585E 5	-0.2468E 5	0.800
0.4711E -1	-0.4230E 1	-0.1167E 4	-0.2655E 5	-0.2539E 5	0.900
0.4668E -1	-0.4348E 1	-0.1197E 4	-0.2728E 5	-0.2609E 5	1.000
0.4624E -1	-0.4472E 1	-0.1252E 4	-0.2807E 5	-0.2682E 5	1.100
0.4579E -1	-0.4598E 1	-0.1322E 4	-0.2891E 5	-0.2739E 5	1.200
0.4532E -1	-0.4735E 1	-0.1407E 4	-0.2982E 5	-0.2841E 5	1.300
0.4484E -1	-0.4880E 1	-0.1504E 4	-0.3078E 5	-0.2903E 5	1.400
0.4435E -1	-0.5036E 1	-0.1613E 4	-0.3183E 5	-0.3022E 5	1.500
0.4383E -1	-0.5203E 1	-0.1737E 4	-0.3296E 5	-0.3122E 5	1.600
0.4331E -1	-0.5384E 1	-0.1877E 4	-0.3415E 5	-0.3228E 5	1.700
0.4276E -1	-0.5579E 1	-0.2036E 4	-0.3551E 5	-0.3347E 5	1.800
0.4219E -1	-0.5791E 1	-0.2217E 4	-0.3697E 5	-0.3475E 5	1.900
0.4162E -1	-0.6023E 1	-0.2423E 4	-0.3856E 5	-0.3614E 5	2.000

TABLE 2-3. Motion of a 1 μm Particle in H_2 at 1/100 atm.

while 10 μm particles are not drag-limited at 1/100 of an atmosphere H_2 pressure, 5 μm particles are more so, and 1 μm particles are almost completely governed by viscous drag.

Table 2-4 indicates the effect of the initial position on the trajectory of identical particles, while Table 2-5 indicates its motion in air under normal atmospheric pressure.

2.1.2 Determination of Particle Trajectories for a Specified Distribution of Particle Sizes and Dielectric Constants

Following the initial numerical work, a more flexible series of programs was developed to investigate the behaviour of dielectric particle trajectories. The programs FIELD, FIELD 2, and FIELD 3, listed in Appendix C, each determine different aspects of dielectric paticle behaviour. Each is capable of accepting the complete range of relevant variable parameters.

The new version of FIELD takes into account the Millikan version of Stoke's Law for very small spheres in a gas; that is, the mean free path considerations referred to in Section A-5.1 have been incorporated in the computation. Also, the program is capable of treating either the cylindrical or the planar geometry, with the coordinates being identically defined in both cases. Thus in both modes, the particle is travelling inwards, towards x = 0, and thus the velocity and acceleration are both expressed as negative quantities. A sample run to compare the behaviour of a 10μm diameter particle in a) air at standard pressure and b) in hydrogen at 1/100 atmospheres pressure is shown in Table 2-6.
The behaviour of the particle in air is seen to be predominantly drag-determined, whereas at the lower pressure in hydrogen, the drag effects are at worst an order of magnitude lower than field effects.

```
FIELD
ETA? (TYPE 0.0 FOR DEFAULT)1E-6
POSN? 0.9
ELECTRODE SPACING IN CM. ? (F4.2)

0.5
PARTICLE DIAMETER IN : CRONS ? (F5.1)

  1.0
VOLTAGE ? (F7.1)

 4000.0
POSITION      VELOCITY      ACCELERATION  FIELD ACCN    DRAG ACCN     TIME
CM.           CM/SEC        CM/SEC$Q      CM/SEC$Q      CM/SEC$Q      MSEC

0.4500E  0    0.5148E  0    0.1689E  5
0.4991E  0    0.1275E  1    0.9313E  4    0.1696E  5    0.7652E  4    0.100
0.4982E  0    0.1984E  1    0.5231E  4    0.1713E  5    0.1198E  5    0.200
0.4955E  0    0.2887E  1    0.3838E  4    0.1736E  5    0.1432E  5    0.300
0.4907E  0    0.3986E  1    0.1864E  4    0.1762E  5    0.1579E  5    0.400
0.4818E  0    0.2779E  1    0.1240E  4    0.1791E  5    0.1667E  5    0.500
0.4813E  0    0.2885E  1    0.9130E  3    0.1820E  5    0.1734E  5    0.600
0.4516E  0    0.2967E  1    0.7472E  3    0.1838E  5    0.1780E  5    0.700
0.4519E  0    0.2037E  1    0.6692E  3    0.1869E  5    0.1820E  5    0.800
0.4528E  0    0.3102E  1    0.6209E  3    0.1905E  5    0.1861E  5    0.900
0.4555E  0    0.3166E  1    0.6050E  3    0.1963E  5    0.1899E  5    1.000
0.4593E  0    0.3230E  1    0.6465E  3    0.2003E  5    0.1938E  5    1.100
0.4501E  0    0.3295E  1    0.6475E  3    0.2044E  5    0.1977E  5    1.200
0.4505E  0    0.3360E  1    0.6945E  3    0.2087E  5    0.2018E  5    1.300
0.4536E  0    0.3424E  1    0.7259E  3    0.2133E  5    0.2061E  5    1.400
0.4541E  0    0.3509E  1    0.7611E  3    0.2181E  5    0.2105E  5    1.500
0.4545E  0    0.3587E  1    0.7997E  3    0.2232E  5    0.2152E  5    1.600
0.4549E  0    0.3669E  1    0.8421E  3    0.2285E  5    0.2201E  5    1.700
0.4552E  0    0.3755E  1    0.8883E  0    0.2342E  5    0.2252E  5    1.800
0.4556E  0    0.3846E  1    0.9386E  3    0.2402E  5    0.2308E  5    1.900
0.4560E  0    0.3943E  1    0.9936E  3    0.2465E  5    0.2366E  5    2.000
```

```
FIELD3
ETA? (TYPE 0.0 FOR DEFAULT)1E-6
POSN? 0.1
ELECTRODE DIAMETER IN CM. ? (F4.2)

1.0
PARTICLE DIAMETER IN MICRONS ? (F5.1)

  1.0
VOLTAGE ? (F7.1)

 4000.0
POSITION      VELOCITY      ACCELERATION  FIELD ACCN    DRAG ACCN     TIME
CM.           CM/SEC        CM/SEC$Q      CM/SEC$Q      CM/SEC$Q      MSEC

0.5000E -1    0.0000E  0   -0.2221E  5
0.4991E -1   -0.1677E  1   -0.1227E  5   -0.2203E  5   -0.1206E  5    0.100
0.4969E -1   -0.3613E  1   -0.6943E  4   -0.2263E  5   -0.1568E  5    0.200
0.4940E -1   -0.5130E  1   -0.4112E  4   -0.2303E  5   -0.1838E  5    0.300
0.4907E -1   -0.6481E  1   -0.2611E  4   -0.2350E  5   -0.2059E  5    0.400
0.4871E -1   -0.7699E  1   -0.1807E  4   -0.2402E  5   -0.2222E  5    0.500
0.4830E -1   -0.8860E  1   -0.1431E  4   -0.2459E  5   -0.2316E  5    0.600
0.4790E -1   -0.9990E  1   -0.1245E  4   -0.2520E  5   -0.2396E  5    0.700
0.4750E -1   -0.1113E  2   -0.1174E  4   -0.2585E  5   -0.2468E  5    0.800
0.4711E -1   -0.1230E  1   -0.1167E  4   -0.2654E  5   -0.2538E  5    0.900
0.4660E -1   -0.1348E  1   -0.1197E  4   -0.2728E  5   -0.2609E  5    1.000
0.4624E -1   -0.1470E  1   -0.1281E  4   -0.2807E  5   -0.2682E  5    1.100
0.4579E -1   -0.1593E  1   -0.1300E  4   -0.2891E  5   -0.2759E  5    1.200
0.4530E -1   -0.1720E  1   -0.1407E  4   -0.2981E  5   -0.2841E  5    1.300
0.4484E -1   -0.1850E  1   -0.1584E  4   -0.3078E  5   -0.2928E  5    1.400
0.4435E -1   -0.1986E  1   -0.1813E  4   -0.3183E  5   -0.3021E  5    1.500
0.4383E -1   -0.2128E  1   -0.2077E  4   -0.3296E  5   -0.3123E  5    1.600
0.4331E -1   -0.2278E  1   -0.2377E  4   -0.3416E  5   -0.3233E  5    1.700
0.4276E -1   -0.2436E  1   -0.2706E  4   -0.3551E  5   -0.3347E  5    1.800
0.4219E -1   -0.2604E  1   -0.3069E  4   -0.3698E  5   -0.3475E  5    1.900
0.4160E -1   -0.2783E  1   -0.3466E  4   -0.3856E  5   -0.3614E  5    2.000
```

TABLE 2-4. Effect of Changed Initial Position of Particle Motion. 1 μm Particle in H_2 at 1/100 atm.

```
FIELD
ETA? (TYPE 0.0 FOR DEFAULT)0.18E-4
POSN? 0.95
ELECTRODE SPACING IN CM. ? (F4.2)

1.0
PARTICLE DIAMETER IN MICRONS ? (F5.1)

  5.0
VOLTAGE ? (F7.1)
```

4222.0 POSITION CM.		VELOCITY CM/SEC		ACCELERATION CM/SEC/SEC		FIELD ACCN CM/SEC/SEC		DRAG ACCN CM/SEC/SEC		TIME MSEC
0.9500E	0	0.5142E	0	0.1600E	5					
0.9501E	0	0.1044E	1	0.1876E	5	0.1657E	5	0.9866E	4	0.100
0.9503E	0	0.2227E	1	0.7129E	4	0.1673E	5	0.9619E	4	0.200
0.9505E	0	0.2317E	1	0.4835E	4	0.1700E	5	0.1217E	5	0.300
0.9508E	0	0.3224E	1	0.3393E	4	0.1738E	5	0.1393E	5	0.400
0.9511E	0	0.3915E	1	0.2494E	4	0.1786E	5	0.1513E	5	0.500
0.9515E	0	0.4735E	1	0.1941E	4	0.1847E	5	0.1613E	5	0.600
0.9519E	0	0.5911E	1	0.1611E	4	0.1921E	5	0.1689E	5	0.700
0.9523E	0	0.6262E	1	0.1428E	4	0.1997E	5	0.1755E	5	0.800
0.9527E	0	0.6199E	1	0.1309E	4	0.1947E	5	0.1814E	5	0.900
0.9531E	0	0.6300E	1	0.1226E	4	0.2000E	5	0.1870E	5	1.000
0.9536E	0	0.6409E	1	0.1304E	4	0.2057E	5	0.1926E	5	1.100
0.9542E	0	0.6591E	1	0.1340E	4	0.2118E	5	0.1983E	5	1.200
0.9548E	0	0.6722E	1	0.1402E	4	0.2183E	5	0.2042E	5	1.300
0.9555E	0	0.6872E	1	0.1481E	4	0.2253E	5	0.2105E	5	1.400
0.9555E	0	0.6835E	1	0.1575E	4	0.2328E	5	0.2171E	5	1.500
0.9562E	0	0.6108E	1	0.1685E	4	0.2412E	5	0.2241E	5	1.600
0.9569E	0	0.5362E	1	0.1812E	4	0.2498E	5	0.2317E	5	1.700
0.9578E	0	0.5558E	1	0.1956E	4	0.2593E	5	0.2398E	5	1.800
0.9576E	0	0.5754E	1	0.2120E	4	0.2693E	5	0.2481E	5	1.900
0.9582E	0	0.5975E	1	0.2305E	4	0.2812E	5	0.2581E	5	2.000

```
FIELD3
ETA? (TYPE 0.0 FOR DEFAULT)0.18E-4
POSN? 0.95
ELECTRODE DIAMETER IN CM. ? (F4.2)

2.0
PARTICLE DIAMETER IN MICRONS ? (F5.1)

5-  5.0
VOLTAGE ? (F7.1)
```

4000.0 POSITION CM.		VELOCITY CM/SEC		ACCELERATION CM/SEC/SEC		FIELD ACCN CM/SEC/SEC		DRAG ACCN CM/SEC/SEC		TIME MSEC
0.5000E	-1	0.0000E	0	-0.2021E	5					
0.4990E	-1	-0.1810E	1	-0.1450E	5	-0.8834E	5	-0.7800E	4	0.100
0.4956E	-1	-0.3004E	1	-0.9690E	4	-0.2267E	5	-0.1895E	5	0.200
0.4900E	-1	-0.3812E	1	-0.6676E	4	-0.2814E	5	-0.1647E	5	0.300
0.4830E	-1	-0.4550E	1	-0.4812E	4	-0.2373E	5	-0.1592E	5	0.400
0.4844E	-1	-0.4800E	1	-0.3678E	4	-0.2442E	5	-0.2074E	5	0.500
0.4700E	-1	-0.5132E	1	-0.2913E	4	-0.2518E	5	-0.2217E	5	0.600
0.4740E	-1	-0.5410E	1	-0.2448E	4	-0.2603E	5	-0.2338E	5	0.700
0.4637E	-1	-0.5665E	1	-0.2480E	4	-0.2697E	5	-0.2449E	5	0.800
0.4579E	-1	-0.5914E	1	-0.2440E	4	-0.2799E	5	-0.2555E	5	0.900
0.4508E	-1	-0.6160E	1	-0.2504E	4	-0.2912E	5	-0.2661E	5	1.000
0.4505E	-1	-0.6417E	1	-0.2633E	4	-0.3035E	5	-0.2772E	5	1.100
0.4440E	-1	-0.6689E	1	-0.2821E	4	-0.3172E	5	-0.2890E	5	1.200
0.4372E	-1	-0.6982E	1	-0.3063E	4	-0.3320E	5	-0.3016E	5	1.300
0.4300E	-1	-0.7300E	1	-0.3361E	4	-0.3491E	5	-0.3155E	5	1.400
0.4225E	-1	-0.7656E	1	-0.3721E	4	-0.3696E	5	-0.3298E	5	1.500
0.4147E	-1	-0.8049E	1	-0.4153E	4	-0.3892E	5	-0.3477E	5	1.600
0.4064E	-1	-0.8489E	1	-0.4674E	4	-0.4138E	5	-0.3667E	5	1.700
0.3977E	-1	-0.8987E	1	-0.5300E	4	-0.4413E	5	-0.3882E	5	1.800
0.3884E	-1	-0.9555E	1	-0.6039E	4	-0.4737E	5	-0.4128E	5	1.900
0.3785E	-1	-0.1021E	2	-0.7862E	4	-0.5117E	5	-0.4411E	5	2.000

TABLE 2-5. The Effect of Increased Pressure on Particle Motion.
5 μm Particle in Air at Standard Pressure.

FIELD

CYLINDRICAL(1) OR PLANAR(2) GEOMETRY ? 1
OUTER ELECTRODE RADIUS IN CM. ? 1.00
INNER ELECTRODE RADIUS IN CM. ? 0.02
INITIAL POSITION IN CM. ? 0.10
AIR(1) OR HYDROGEN(2) ? 1
PRESSURE IN ATMOSPHERES ? 1.00
PARTICLE DIAMETER IN MICRONS ? 10.0
DIELECTRIC CONSTANT ? 10.0
PARTICLE DENSITY IN GM/CM**3 ? 3.00
APPLIED VOLTAGE ? 4000.0

POSITION CM.	VELOCITY CM/SEC	ACCN CM/SECSQ	FIELD ACCN CM/SECSQ	DRAG ACCN CM/SECSQ	TIME MSEC
0.1000E 0	0.0000E 0	-0.2776E 4			
0.9999E -1	-0.2603E 0	-0.2494E 4	-0.2777E 4	0.2831E 3	0.100
0.9995E -1	-0.5020E 0	-0.2243E 4	-0.2780E 4	0.5376E 3	0.200
0.9959E -1	-0.7122E 0	-0.2019E 4	-0.2735E 4	0.7645E 3	0.300
0.9981E -1	-0.9045E 0	-0.1619E 4	-0.2792E 4	0.9727E 3	0.400
0.9971E -1	-0.1072E 1	-0.1642E 4	-0.2800E 4	0.1158E 4	0.500
0.9959E -1	-0.1227E 1	-0.1432E 4	-0.2810E 4	0.1323E 4	0.600
0.9946E -1	-0.1375E 1	-0.1343E 4	-0.2821E 4	0.1472E 4	0.700
0.9932E -1	-0.1503E 1	-0.1217E 4	-0.2833E 4	0.1616E 4	0.800
0.9916E -1	-0.1619E 1	-0.1104E 4	-0.2847E 4	0.1741E 4	0.900
0.9899E -1	-0.1725E 1	-0.1007E 4	-0.2861E 4	0.1854E 4	1.000
0.9882E -1	-0.1821E 1	-0.9139E 3	-0.2877E 4	0.1957E 4	1.100
0.9863E -1	-0.1909E 1	-0.8437E 3	-0.2893E 4	0.2032E 4	1.200
0.9843E -1	-0.1990E 1	-0.7713E 3	-0.2710E 4	0.2129E 4	1.300
0.9823E -1	-0.2064E 1	-0.7073E 3	-0.2929E 4	0.2217E 4	1.400
0.9802E -1	-0.2132E 1	-0.6552E 3	-0.2947E 4	0.2292E 4	1.500
0.9781E -1	-0.2195E 1	-0.6871E 3	-0.2747E 4	0.2367E 4	1.600
0.9759E -1	-0.2252E 1	-0.5644E 3	-0.2987E 4	0.2423E 4	1.700
0.9736E -1	-0.2303E 1	-0.5368E 3	-0.3007E 4	0.2461E 4	1.800
0.9712E -1	-0.2357E 1	-0.4937E 3	-0.3032E 4	0.2536E 4	1.900
0.9688E -1	-0.2407E 1	-0.4646E 3	-0.3050E 4	0.2587E 4	2.000
0.9664E -1	-0.2452E 1	-0.4292E 3	-0.3075E 4	0.2636E 4	2.100
0.9639E -1	-0.2495E 1	-0.4169E 3	-0.3099E 4	0.2653E 4	2.200
0.9614E -1	-0.2536E 1	-0.3974E 3	-0.3122E 4	0.2726E 4	2.300
0.9589E -1	-0.2570E 1	-0.3867E 3	-0.3149E 4	0.2763E 4	2.400
0.9563E -1	-0.2610E 1	-0.3663E 3	-0.3174E 4	0.2383E 4	2.500
0.9536E -1	-0.2643E 1	-0.3533E 3	-0.3200E 4	0.2347E 4	2.600
0.9510E -1	-0.2680E 1	-0.3434E 3	-0.3226E 4	0.2894E 4	2.700
0.9483E -1	-0.2717E 1	-0.3346E 3	-0.3255E 4	0.2921E 4	2.800
0.9455E -1	-0.2750E 1	-0.3274E 3	-0.3284E 4	0.2956E 4	2.900
0.9427E -1	-0.2782E 1	-0.3214E 3	-0.3310E 4	0.2991E 4	3.000
0.9400E -1	-0.2814E 1	-0.3160E 3	-0.3342E 4	0.3025E 4	3.100
0.9372E -1	-0.2846E 1	-0.3100E 3	-0.3372E 4	0.3059E 4	3.200
0.9343E -1	-0.2877E 1	-0.3187E 3	-0.3474E 4	0.3093E 4	3.300
0.9314E -1	-0.2908E 1	-0.3273E 3	-0.3403E 4	0.3126E 4	3.400
0.9285E -1	-0.2939E 1	-0.3278E 3	-0.3460E 4	0.3159E 4	3.500
0.9255E -1	-0.2972E 1	-0.3083E 3	-0.3501E 4	0.3197E 4	3.600
0.9225E -1	-0.3000E 1	-0.3096E 3	-0.3535E 4	0.3226E 4	3.700
0.9195E -1	-0.3031E 1	-0.3112E 3	-0.3570E 4	0.3257E 4	3.800
0.9165E -1	-0.3062E 1	-0.3133E 3	-0.3606E 4	0.3293E 4	3.900
0.9134E -1	-0.3074E 1	-0.3161E 3	-0.3640E 4	0.3326E 4	4.000
0.9103E -1	-0.3126E 1	-0.3193E 3	-0.3680E 4	0.3361E 4	4.100
0.9071E -1	-0.3150E 1	-0.3222E 3	-0.3713E 4	0.3395E 4	4.200
0.9040E -1	-0.3191E 1	-0.3274E 3	-0.3758E 4	0.3429E 4	4.300
0.9008E -1	-0.3224E 1	-0.3324E 3	-0.3790E 4	0.3465E 4	4.400
0.8975E -1	-0.3257E 1	-0.3276E 3	-0.3839E 4	0.3502E 4	4.500

FIELD

CYLINDRICAL(1) OR PLANAR(2) GEOMETRY ? 1
OUTER ELECTRODE RADIUS IN CM. ? 1.00
INNER ELECTRODE RADIUS IN CM. ? 0.02
INITIAL POSITION IN CM. ? 0.10
AIR(1) OR HYDROGEN(2) ? 2
PRESSURE IN ATMOSPHERES ? 0.01
PARTICLE DIAMETER IN MICRONS ? 10.0
DIELECTRIC CONSTANT ? 10.0
PARTICLE DENSITY IN GM/CM**3 ? 3.00
APPLIED VOLTAGE ? 4000.0

POSITION CM.	VELOCITY CM/SEC	ACCN CM/SECSQ	FIELD ACCN CM/SECSQ	DRAG ACCN CM/SECSQ	TIME MSEC
0.1000E 0	0.0000E 0	-0.2776E 4			
0.9999E -1	-0.2769E 0	-0.2762E 4	-0.2777E 4	0.1445E 2	0.100
0.9994E -1	-0.5526E 0	-0.2752E 4	-0.2780E 4	0.2854E 2	0.200
0.9988E -1	-0.8272E 0	-0.2742E 4	-0.2786E 4	0.4317E 2	0.300
0.9978E -1	-0.1101E 1	-0.2737E 4	-0.2794E 4	0.5747E 2	0.400
0.9966E -1	-0.1375E 1	-0.2733E 4	-0.2803E 4	0.7174E 2	0.500
0.9950E -1	-0.1648E 1	-0.2731E 4	-0.2817E 4	0.8600E 2	0.600
0.9933E -1	-0.1921E 1	-0.2732E 4	-0.2833E 4	0.1002E 3	0.700
0.9912E -1	-0.2194E 1	-0.2736E 4	-0.2850E 4	0.1145E 3	0.800
0.9889E -1	-0.2468E 1	-0.2742E 4	-0.2871E 4	0.1288E 3	0.900
0.9863E -1	-0.2743E 1	-0.2752E 4	-0.2893E 4	0.1431E 3	1.000
0.9834E -1	-0.3018E 1	-0.2761E 4	-0.2919E 4	0.1575E 3	1.100
0.9802E -1	-0.3295E 1	-0.2770E 4	-0.2947E 4	0.1720E 3	1.200
0.9768E -1	-0.3574E 1	-0.2792E 4	-0.2978E 4	0.1865E 3	1.300
0.9731E -1	-0.3854E 1	-0.2811E 4	-0.3013E 4	0.2011E 3	1.400
0.9691E -1	-0.4135E 1	-0.2824E 4	-0.3050E 4	0.2155E 3	1.500
0.9648E -1	-0.4431E 1	-0.2860E 4	-0.3091E 4	0.2307E 3	1.600
0.9602E -1	-0.4706E 1	-0.2887E 4	-0.3135E 4	0.2457E 3	1.700
0.9554E -1	-0.4999E 1	-0.2922E 4	-0.3183E 4	0.2605E 3	1.800
0.9502E -1	-0.5297E 1	-0.2959E 4	-0.3235E 4	0.2762E 3	1.900
0.9445E -1	-0.5593E 1	-0.2999E 4	-0.3291E 4	0.2917E 3	2.000
0.9391E -1	-0.5892E 1	-0.3044E 4	-0.3350E 4	0.3072E 3	2.100
0.9330E -1	-0.6197E 1	-0.3094E 4	-0.3417E 4	0.3225E 3	2.200
0.9267E -1	-0.6511E 1	-0.3143E 4	-0.3488E 4	0.3398E 3	2.300
0.9200E -1	-0.6829E 1	-0.3203E 4	-0.3565E 4	0.3564E 3	2.400
0.9130E -1	-0.7150E 1	-0.3274E 4	-0.3647E 4	0.3733E 3	2.500
0.9057E -1	-0.7484E 1	-0.3346E 4	-0.3736E 4	0.3926E 3	2.600
0.8980E -1	-0.7835E 1	-0.3424E 4	-0.3833E 4	0.4080E 3	2.700
0.8900E -1	-0.8167E 1	-0.3511E 4	-0.3937E 4	0.4263E 3	2.800
0.8817E -1	-0.8528E 1	-0.3600E 4	-0.4050E 4	0.4447E 3	2.900
0.8730E -1	-0.8890E 1	-0.3733E 4	-0.4170E 4	0.4627E 3	3.000
0.8639E -1	-0.9267E 1	-0.3821E 4	-0.4300E 4	0.4336E 3	3.100
0.8545E -1	-0.9655E 1	-0.3944E 4	-0.4440E 4	0.5029E 3	3.200
0.8446E -1	-0.1006E 2	-0.4003E 4	-0.4602E 4	0.5240E 3	3.300
0.8342E -1	-0.1047E 2	-0.4223E 4	-0.4779E 4	0.5468E 3	3.400
0.8237E -1	-0.1090E 2	-0.4397E 4	-0.4968E 4	0.5570E 3	3.500
0.8126E -1	-0.1125E 2	-0.4562E 4	-0.5174E 4	0.5924E 3	3.600
0.8007E -1	-0.1183E 2	-0.4785E 4	-0.5400E 4	0.6165E 3	3.700
0.7889E -1	-0.1231E 2	-0.5011E 4	-0.5654E 4	0.6424E 3	3.800
0.7763E -1	-0.1282E 2	-0.5264E 4	-0.5933E 4	0.6692E 3	3.900
0.7632E -1	-0.1336E 2	-0.5546E 4	-0.6243E 4	0.6972E 3	4.000
0.7496E -1	-0.1372E 2	-0.5862E 4	-0.6590E 4	0.7271E 3	4.100
0.7354E -1	-0.1454E 2	-0.6222E 4	-0.6981E 4	0.7586E 3	4.200
0.7205E -1	-0.1518E 2	-0.6629E 4	-0.7421E 4	0.7921E 3	4.300
0.7050E -1	-0.1584E 2	-0.7094E 4	-0.7922E 4	0.8277E 3	4.400
0.6888E -1	-0.1660E 2	-0.7629E 4	-0.8495E 4	0.8660E 3	4.500
0.6718E -1	-0.1729E 2	-0.8249E 4	-0.9156E 4	0.9076E 3	4.600
0.6540E -1	-0.1822E 2	-0.8973E 4	-0.9725E 4	0.9528E 3	4.700
0.6352E -1	-0.1919E 2	-0.9827E 4	-0.1083E 5	0.1001E 4	4.800
0.6155E -1	-0.2025E 2	-0.1078E 5	-0.1179E 5	0.1055E 4	4.900
0.5948E -1	-0.2137E 2	-0.1201E 5	-0.1319E 5	0.1111E 4	5.000
0.5728E -1	-0.2262E 2	-0.1317E 5	-0.1477E 5	0.1180E 4	5.100
0.5494E -1	-0.2407E 2	-0.1543E 5	-0.1674E 5	0.1257E 4	5.200
0.5248E -1	-0.2576E 2	-0.1733E 5	-0.1924E 5	0.1344E 4	5.300
0.4978E -1	-0.2762E 2	-0.2104E 5	-0.2250E 5	0.1448E 4	5.400
0.4692E -1	-0.2987E 2	-0.2524E 5	-0.2691E 5	0.1566E 4	5.500
0.4376E -1	-0.3258E 2	-0.3146E 5	-0.3312E 5	0.1713E 4	5.600
0.4031E -1	-0.3603E 2	-0.4047E 5	-0.4237E 5	0.1098E 4	5.700
0.3640E -1	-0.4102E 2	-0.5517E 5	-0.5721E 5	0.2144E 4	5.800
0.3193E -1	-0.4772E 2	-0.8198E 5	-0.8447E 5	0.2492E 4	5.900
0.2677E -1	-0.5840E 2	-0.1417E 6	-0.1448E 6	0.3222E 4	6.000
0.1979E -1	-0.8017E 2	-0.3423E 6	-0.3474E 6	0.4184E 4	6.100

STOP

TABLE 2-6. Comparison of Trajectories at Normal and Low Pressures for a 10 μm Particle.

The main aim of this series of simulations was implemented in the programs FIELD 2 and FIELD 3. This aim consists of generating the distribution of particles at a specific time instant as a function of their size, dielectric constant, and density.

The program FIELD 2 is almost identical with FIELD, except that the particle motion is determined on a logarithmically varying time scale rather than at equal intervals of time. The minimum iterative interval, as before, is still 1μsec. Thus no additional error has been introduced. The main aim of this program was to determine the total time of flight for the particles suffering the highest acceleration. This then determined the time for which the entire range of particles should be allowed to accelerate. Accordingly, the transit time obtained from FIELD 2 was entered into FIELD 3 as a parameter to determine the distribution of the particles.

The program FIELD 3 determines the final position for particles of various sizes, densities, and dielectric constants, which have been allowed to accelerate for a specific time. At the end of this time, each particle position, velocity, and accelerations are output.

A typical output result from FIELD 3 is shown on the following two pages. In these records, the particle population consists of a mixture of particle sizes ranging from 10μm to 0.1μm in diameter.

Also, two specific particle types were selected for analysis, namely particles of uranium dioxide having a density of 10.0 and a dielectric constant of 21.00, and particle of silica, with a density of 2.20 and dielectric constant

```
FIELD2
CYLINDRICAL(1) OR PLANAR(2) GEOMETRY ?          1
OUTER ELECTRODE RADIUS IN CM. ?                 0.02
INNER ELECTRODE RADIUS IN CM. ?                 .005
INITIAL POSITION IN CM. ?                       .0145
ZIP(1) OR HYDROGEN(2) ?                         2
PRESSURE IN ATMOSPHERES ?                       0.01
PARTICLE DENSITY IN CM/CM**3 ?                  10.0
APPLIED VOLTAGE ?                               210

 POSITION      VELOCITY      ACCN          FIELD ACCN    DRAG ACCN.    TIME
 CM.           CM/SEC        CM/SEC/SEC    CM/SEC/SEC    CM/SEC/SEC    MSEC

 0.1450E -1    0.0000E  0   -0.3785E  4
 0.1059E -1   -0.4147E  1   -0.5436E  4   -0.5784E  4    0.2951E  3   0.982
DIELECTRIC CONST. =  2.25  PARTICLE DIA = 10.00

 POSITION      VELOCITY      ACCN          FIELD ACCN    DRAG ACCN     TIME
 CM.           CM/SEC        CM/SEC/SEC    CM/SEC/SEC    CM/SEC/SEC    MSEC

 0.1450E -1    0.0000E  0   -0.3785E  4
 0.1072E -1   -0.3740E  1   -0.4547E  4   -0.5611E  4    0.1065E  4   0.982
DIELECTRIC CONST. =  2.25  PARTICLE DIA =  5.00

 POSITION      VELOCITY      ACCN          FIELD ACCN    DRAG ACCN     TIME
 CM.           CM/SEC        CM/SEC/SEC    CM/SEC/SEC    CM/SEC/SEC    MSEC

 0.1450E -1    0.0000E  0   -0.3785E  4
 0.1333E -1   -0.2005E  1   -0.1309E  4   -0.4871E  4    0.3563E  4   0.982
DIELECTRIC CONST. =  2.25  PARTICLE DIA =  2.00

 POSITION      VELOCITY      ACCN          FIELD ACCN    DRAG ACCN     TIME
 CM.           CM/SEC        CM/SEC/SEC    CM/SEC/SEC    CM/SEC/SEC    MSEC

 0.1450E -1    0.0000E  0   -0.3785E  4
 0.1403E -1   -0.1373E  0   -0.3921E  1   -0.3357E  4    0.3933E  4   0.982
DIELECTRIC CONST. =  2.25  PARTICLE DIA =  0.50

 POSITION      VELOCITY      ACCN          FIELD ACCN    DRAG ACCN     TIME
 CM.           CM/SEC        CM/SEC/SEC    CM/SEC/SEC    CM/SEC/SEC    MSEC

 0.1450E -1    0.0000E  0   -0.3785E  4
 0.1446E -1   -0.3167E -1   -0.1050E  0   -0.3801E  4    0.3801E  4   0.982
DIELECTRIC CONST. =  2.25  PARTICLE DIA =  0.20

 POSITION      VELOCITY      ACCN          FIELD ACCN    DRAG ACCN     TIME
 CM.           CM/SEC        CM/SEC/SEC    CM/SEC/SEC    CM/SEC/SEC    MSEC

 0.1450E -1    0.0000E  0   -0.3785E  4
 0.1449E -1   -0.5478E -2   -0.6210E -2   -0.3758E  4    0.3759E  4   0.982
DIELECTRIC CONST. =  2.25  PARTICLE DIA =  0.10
```

```
FIELD1
CYLINDRICAL(1) OR PLANAR(2) GEOMETRY ?          1
OUTER ELECTRODE RADIUS IN CM. ?                 0.02
INNER ELECTRODE RADIUS IN CM. ?                 .005
INITIAL POSITION IN CM. ?                       .0145
ZIP(1) OR HYDROGEN(2) ?                         2
PRESSURE IN ATMOSPHERES ?                       0.01
PARTICLE DENSITY IN CM/CM**3 ?                  10.0
APPLIED VOLTAGE ?                               210

 POSITION      VELOCITY      ACCN          FIELD ACCN    DRAG ACCN     TIME
 CM.           CM/SEC        CM/SEC/SEC    CM/SEC/SEC    CM/SEC/SEC    MSEC

 0.1450E -1    0.0000E  0   -0.3785E  4
 0.1059E -1   -0.4147E  1   -0.5436E  4   -0.5784E  4    0.2951E  3   0.982
DIELECTRIC CONST. =  2.25  PARTICLE DIA = 10.00

 POSITION      VELOCITY      ACCN          FIELD ACCN    DRAG ACCN     TIME
 CM.           CM/SEC        CM/SEC/SEC    CM/SEC/SEC    CM/SEC/SEC    MSEC

 0.1450E -1    0.0000E  0   -0.3785E  4
 0.1072E -1   -0.3740E  1   -0.4547E  4   -0.5611E  4    0.1065E  4   0.982
DIELECTRIC CONST. =  2.25  PARTICLE DIA =  5.00

 POSITION      VELOCITY      ACCN          FIELD ACCN    DRAG ACCN     TIME
 CM.           CM/SEC        CM/SEC/SEC    CM/SEC/SEC    CM/SEC/SEC    MSEC

 0.1450E -1    0.0000E  0   -0.3785E  4
 0.1333E -1   -0.2005E  1   -0.1309E  4   -0.4871E  4    0.3563E  4   0.982
DIELECTRIC CONST. =  2.25  PARTICLE DIA =  2.00

 POSITION      VELOCITY      ACCN          FIELD ACCN    DRAG ACCN     TIME
 CM.           CM/SEC        CM/SEC/SEC    CM/SEC/SEC    CM/SEC/SEC    MSEC

 0.1450E -1    0.0000E  0   -0.3785E  4
 0.1403E -1   -0.1373E  0   -0.3921E  1   -0.3357E  4    0.3933E  4   0.982
DIELECTRIC CONST. =  2.25  PARTICLE DIA =  0.50

 POSITION      VELOCITY      ACCN          FIELD ACCN    DRAG ACCN     TIME
 CM.           CM/SEC        CM/SEC/SEC    CM/SEC/SEC    CM/SEC/SEC    MSEC

 0.1450E -1    0.0000E  0   -0.3785E  4
 0.1446E -1   -0.3167E -1   -0.1050E  0   -0.3801E  4    0.3801E  4   0.982
DIELECTRIC CONST. =  2.25  PARTICLE DIA =  0.20

 POSITION      VELOCITY      ACCN          FIELD ACCN    DRAG ACCN     TIME
 CM.           CM/SEC        CM/SEC/SEC    CM/SEC/SEC    CM/SEC/SEC    MSEC

 0.1450E -1    0.0000E  0   -0.3785E  4
 0.1449E -1   -0.5478E -2   -0.6210E -2   -0.3758E  4    0.3759E  4   0.982
DIELECTRIC CONST. =  2.25  PARTICLE DIA =  0.10
```

```
FIELDS
CYLINDRICAL(1) OR PLANAR(2) GEOMETRY ?      1
OUTER ELECTRODE RADIUS IN CM. ?             0.08
INNER ELECTRODE RADIUS IN CM. ?             .005
INITIAL POSITION IN CM. ?                   .0155
AIR(1) OR HYDROGEN(2) ?                     2
PRESSURE IN ATMOSPHERES ?                   0.01
PARTICLE DENSITY IN GM/CM**3 ?              10.0
APPLIED VOLTAGE ?                           210

POSITION     VELOCITY      ACCN          FIELD ACCN      DRAG ACCN     TIME
CM.          CM/SEC        CM/SECSQ      CM/SECSQ        CM/SECSQ      MSEC

0.1550E -1    0.0000E  0  -0.1091E  5
0.9301E -2   -0.1067E  2  -0.5867E  5  -0.5897E  5    0.2924E  3  0.982
DIELECTRIC CONST. = 21.00  PARTICLE DIA = 10.00

POSITION     VELOCITY      ACCN          FIELD ACCN      DRAG ACCN     TIME
CM.          CM/SEC        CM/SECSQ      CM/SECSQ        CM/SECSQ      MSEC

0.1550E -1    0.0000E  0  -0.1091E  5
0.3944E -2   -0.1816E  2  -0.5559E  5  -0.5673E  5    0.1137E  4  0.982
DIELECTRIC CONST. = 21.00  PARTICLE DIA =  5.00

POSITION     VELOCITY      ACCN          FIELD ACCN      DRAG ACCN     TIME
CM.          CM/SEC        CM/SECSQ      CM/SECSQ        CM/SECSQ      MSEC

0.1550E -1    0.0000E  0  -0.1091E  5
0.9669E -2   -0.1542E  2  -0.3906E  5  -0.4494E  5    0.5877E  4  0.982
DIELECTRIC CONST. = 21.00  PARTICLE DIA =  2.00

POSITION     VELOCITY      ACCN          FIELD ACCN      DRAG ACCN     TIME
CM.          CM/SEC        CM/SECSQ      CM/SECSQ        CM/SECSQ      MSEC

0.1550E -1    0.0000E  0  -0.1091E  5
0.1144E -1   -0.3550E  1  -0.1379E  5  -0.2712E  5    0.1333E  5  0.982
DIELECTRIC CONST. = 21.00  PARTICLE DIA =  1.00

POSITION     VELOCITY      ACCN          FIELD ACCN      DRAG ACCN     TIME
CM.          CM/SEC        CM/SECSQ      CM/SECSQ        CM/SECSQ      MSEC

0.1550E -1    0.0000E  0  -0.1091E  5
0.1349E -1   -0.2149E  1  -0.1040E  4  -0.1514E  5    0.1412E  5  0.982
DIELECTRIC CONST. = 21.00  PARTICLE DIA =  0.50

POSITION     VELOCITY      ACCN          FIELD ACCN      DRAG ACCN     TIME
CM.          CM/SEC        CM/SECSQ      CM/SECSQ        CM/SECSQ      MSEC

0.1550E -1    0.0000E  0  -0.1091E  5
0.1528E -1   -0.9079E  0  -0.1744E  2  -0.1151E  5    0.1150E  5  0.982
DIELECTRIC CONST. = 21.00  PARTICLE DIA =  0.20

POSITION     VELOCITY      ACCN          FIELD ACCN      DRAG ACCN     TIME
CM.          CM/SEC        CM/SECSQ      CM/SECSQ        CM/SECSQ      MSEC

0.1550E -1    0.0000E  0  -0.1091E  5
0.1543E -1   -0.7765E -1  -0.1224E  1  -0.1126E  5    0.1126E  5  0.982
DIELECTRIC CONST. = 21.00  PARTICLE DIA =  0.10
```

```
FIELDS
CYLINDRICAL(1) OR PLANAR(2) GEOMETRY ?      1
OUTER ELECTRODE RADIUS IN CM. ?             0.08
INNER ELECTRODE RADIUS IN CM. ?             .005
INITIAL POSITION IN CM. ?                   .0155
AIR(1) OR HYDROGEN(2) ?                     2
PRESSURE IN ATMOSPHERES ?                   0.01
PARTICLE DENSITY IN GM/CM**3 ?              2.00
APPLIED VOLTAGE ?                           210

POSITION     VELOCITY      ACCN          FIELD ACCN      DRAG ACCN     TIME
CM.          CM/SEC        CM/SECSQ      CM/SECSQ        CM/SECSQ      MSEC

0.1550E -1    0.0000E  0  -0.3099E  4
0.1396E -1   -0.3270E  1  -0.4026E  4  -0.4029E  4    0.2307E  3  0.982
DIELECTRIC CONST. =  2.25  PARTICLE DIA = 10.00

POSITION     VELOCITY      ACCN          FIELD ACCN      DRAG ACCN     TIME
CM.          CM/SEC        CM/SECSQ      CM/SECSQ        CM/SECSQ      MSEC

0.1550E -1    0.0000E  0  -0.3099E  4
0.1400E -1   -0.2952E  1  -0.3307E  4  -0.4147E  4    0.8399E  3  0.982
DIELECTRIC CONST. =  2.25  PARTICLE DIA =  5.00

POSITION     VELOCITY      ACCN          FIELD ACCN      DRAG ACCN     TIME
CM.          CM/SEC        CM/SECSQ      CM/SECSQ        CM/SECSQ      MSEC

0.1550E -1    0.0000E  0  -0.3099E  4
0.1456E -1   -0.1988E  1  -0.9109E  3  -0.3741E  4    0.2822E  4  0.982
DIELECTRIC CONST. =  2.25  PARTICLE DIA =  2.00

POSITION     VELOCITY      ACCN          FIELD ACCN      DRAG ACCN     TIME
CM.          CM/SEC        CM/SECSQ      CM/SECSQ        CM/SECSQ      MSEC

0.1550E -1    0.0000E  0  -0.3099E  4
0.1512E -1   -0.4633E  0  -0.4463E  2  -0.3337E  4    0.3290E  4  0.982
DIELECTRIC CONST. =  2.25  PARTICLE DIA =  1.00

POSITION     VELOCITY      ACCN          FIELD ACCN      DRAG ACCN     TIME
CM.          CM/SEC        CM/SECSQ      CM/SECSQ        CM/SECSQ      MSEC

0.1550E -1    0.0000E  0  -0.3099E  4
0.1540E -1   -0.1116E  0  -0.2430E  1  -0.3160E  4    0.3160E  4  0.982
DIELECTRIC CONST. =  2.25  PARTICLE DIA =  0.50

POSITION     VELOCITY      ACCN          FIELD ACCN      DRAG ACCN     TIME
CM.          CM/SEC        CM/SECSQ      CM/SECSQ        CM/SECSQ      MSEC

0.1550E -1    0.0000E  0  -0.3099E  4
0.1548E -1   -0.1772E -1  -0.6125E -1  -0.3109E  4    0.3109E  4  0.982
DIELECTRIC CONST. =  2.25  PARTICLE DIA =  0.20

POSITION     VELOCITY      ACCN          FIELD ACCN      DRAG ACCN     TIME
CM.          CM/SEC        CM/SECSQ      CM/SECSQ        CM/SECSQ      MSEC

0.1550E -1    0.0000E  0  -0.3099E  4
0.1550E -1   -0.4483E -2  -0.6200E -2  -0.3101E  4    0.3101E  4  0.982
DIELECTRIC CONST. =  2.25  PARTICLE DIA =  0.10
```

2.25. Note also in these results that in keeping with the theoretical design criteria that were found to be desirable (see Section A-7), the dimensions of the electrodes have been diminished by a considerable factor, with a total particle transit distance being a maximum of 100 μm. The voltage selected (210V) is the maximum sustainable voltage in dry air at one atmosphere.

The result of the outputs from FIELD 3 are summarized in Figure 2-1. In this figure, the particles travel from right to left, from the nominal distance of 150 μm, towards the inner electrode, which is located at 50 μm. The shaded bar represents the initial distribution of particles, which are depicted as starting with an initial position uncertainty of ± 5 μm. The remaining bars indicate the final position of the population of particles, broken down by size, after a specific time interval. At the end of this time, the population of 10 μm diameter UO_2 particles has just reached the inner electrode. Note also that there is an increasing spread in the position uncertainty of each particle population as it travels towards the inner electrode.

Figure 2-1 indicates that, using the dimensions for the electrodes as shown therein, separation of 1 μm diameter particles of UO_2 and SiO_2 can be achieved, provided the operating pressure is 1/100 atmospheres of H_2 and near breakdown voltage conditions (in air) are used. In the presence of submicron size particles, only incomplete separations can be obtained.

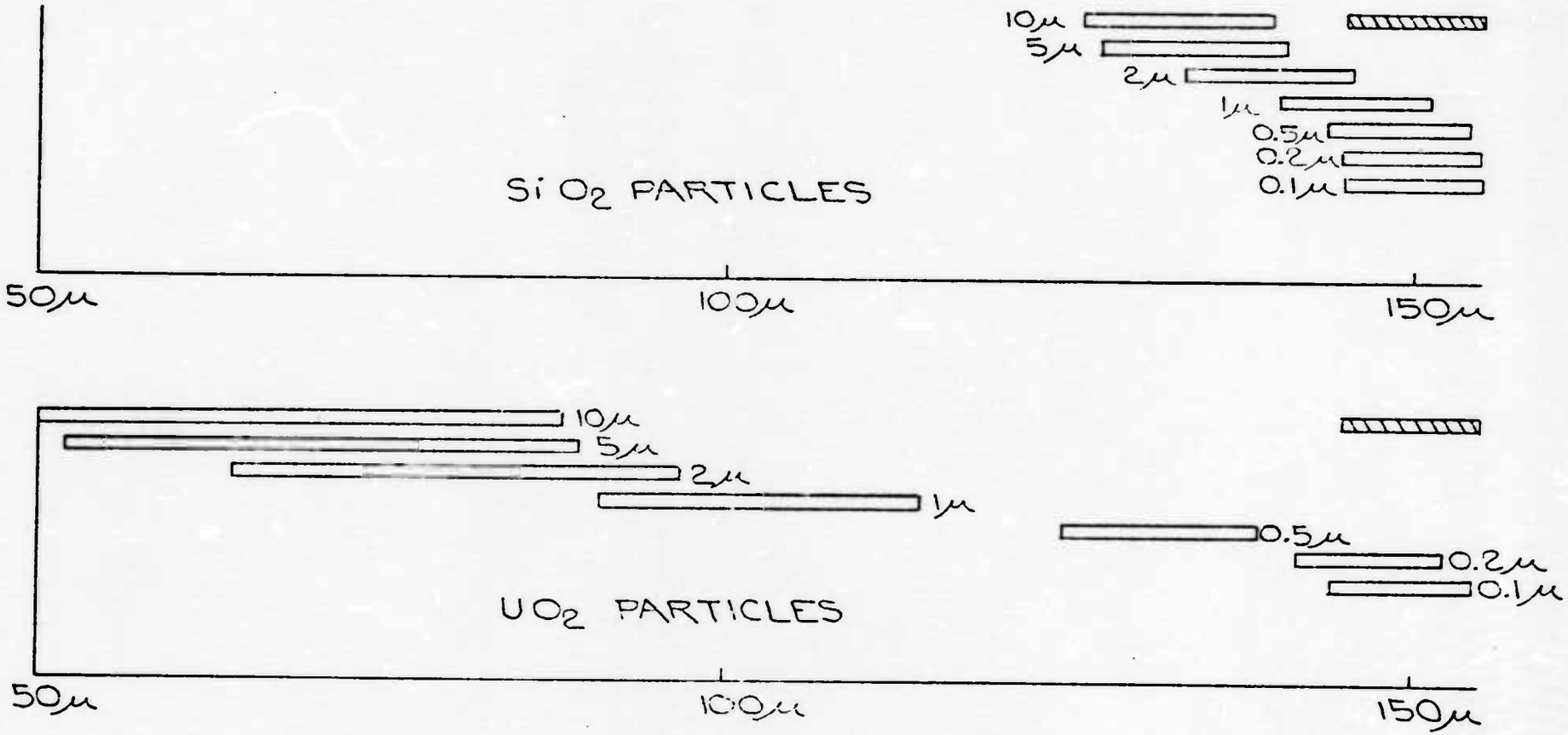

FIGURE 2-1

PARTICLE TRANSIT DISTANCES IN H_2 AT 1/100 ATMOSPHERES PRESSURE

Transit Time: 0.982 msecs. Voltage: 210 volts

2.2 Species Dependent Factor in the Dielectric Acceleration Equations

The species dependent factor in the dielectric acceleration equations (equations 2-1 and 2-2) is $(\kappa-1)/\rho$. This factor has been calculated from the known dielectric constants and densities for a number of common inorganic materials and is tabulated in Table 2-7. While there is a large variance in the dielectric constant (10.7 ± 8.6 or ± 80%), there is a smaller variance in our species dependent factor (2.3 ± 1.3 or ± 57%). For example, although UO_2 has one of the largest dielectric constants (fifth largest on our list), it stands 33rd out of 47 for the species dependent factor. Even worse is the fact that it stands in a very dense portion of the factor spectrum, near many commonly occurring materials. This nonuniqueness of the UO_2 factor makes its bulk separation from other common materials very limited at best. Consequently, a design in which there is both a high and a low cutoff must be considered, since UO_2 is neither near the upper or lower limit.

2.3 Pressure Requirements for Effective Dielectric Sorting

Considering the cylindrical geometry, we again use the program FIELD 3 to determine the final position of particles which have been allowed to accelerate for a specific time. With helium as the carrier gas and a voltage on the central wire of 189 volts, which is 90% of the breakdown voltage, the particles are brought in at a distance of 180 ± 5 μm from the center electrode. The outer cylinder's radius is 200 μm and the center wire has a 50 μm radius. In Figure 2-2, the final positions for a two material system of UO_2 (κ = 21, d = 10.9 g/cm^3) and SiO_2 (κ = 4.3, d = 2.6 g/cm^3) are shown for a range of pressures. At P = 10 torr, there

TABLE 2-7

SEPARATION RATIOS FOR DIELECTRIC SORTING OF COMMON MATERIALS

Material[+]	Dielectric Constant (κ) (at 10^6 to 10^9 Hz)	Density (ρ) (g/cm^3)	$(\kappa-1)/\rho$
1. $Pb(NO_3)_2$	37.7	4.5	8.1
2. TlCl	46.9	7.0	6.6
3. NH_4Cl	7.0	1.5	4.0
4. *Cassiterite - $SnSnO_4$	23.7	7.0	3.3
5. Na_2CO_3	8.4	2.5	3.0
6. *Calcite - $CaCO_3$	8.5	2.7	2.8
7. *Cerussite - $PbCO_3$	18.6	6.6	2.7
8. *Tenorite - CuO	18.1	6.4	2.7
9. $BaCl_2$	11.4	3.9	2.7
10. PbO	25.9	9.5	2.6
11. $CuSO_4$	10.3	3.6	2.6
12. NH_4Br	7.1	2.4	2.5
13. *Zircon - $ZrSiO_4$	12.0	4.4	2.5
14. *Halite - NaCl	6.1	2.2	2.4
15. *Apalite - $CaF_2 \cdot 3Ca_3P_2O_8$	8.5	3.2	2.3
16. *Barite - $BaSO_4$	11.4	4.5	2.3
17. PbS	17.9	7.5	2.3
18. Tarapacaite - K_2CrO_4	7.3	2.7	2.3
19. FeO	14.2	5.7	2.3
20. *Dolomite - $CaCO_3MgCO_3$	7.5	2.9	2.2
21. *Anglesite - $PbSO_4$	14.3	6.2	2.1
22. *Beryl - $3BeO \cdot Al_2O_3 \cdot 6SiO_2$	6.6	2.8	2.0
23. *Gypsum - $CaSO_4 \cdot 2H_2O$	5.7	2.3	2.0

TABLE 2-7 (continued)

24. Al_2O_3 - α	8.8	4.0	2.0
25. CaF_2	7.4	3.2	2.0
26. *Sylvite - KCl	5.0	2.0	2.0
27. *Saltpeter - KNO_3	5.0	2.1	1.9
28. K_2CO_3	5.6	2.4	1.9
29. *Smithsonite - $ZnCO_3$	9.3	4.4	1.9
30. $KClO_3$	5.1	2.3	1.8
31. *Arconite - K_2SO_4	5.9	2.7	1.8
32. *Cerargyrite - AgCl	11.2	5.6	1.8
33. UO_2	21.0	10.9	1.8
34. *Aragonite - $CaCO_3$	6.1	2.9	1.8
35. $NaNO_3$	5.2	2.3	1.8
36. *Bromyrite - AgBr	12.2	6.5	1.7
37. *Kalinite - $KAl(SO_4)_2 \cdot 12H_2O$	3.8	1.8	1.6
38. *Malachite - $CuCO_3Cu(OH)_2$	7.2	4.0	1.6
39. *Alumina - Al_2O_3	6.5	3.7	1.5
40. $Ba(NO_3)_2$	5.9	3.2	1.5
41. *Quartz - SiO_2	4.3	2.6	1.3
42. *Diamond - C	5.5	3.3	1.3
43. KI	5.6	3.6	1.3
44. AgCN	5.6	4.0	1.2
45. Hg_2Cl_2	9.4	7.2	1.2
46. *Sand - SiO_2	2.6	2.6	0.62
47. *Cotunnite - $PbCl_2$	4.2	5.9	0.55

+ Chemical names indicate data for very pure materials
* Minerals and other naturally formed materials

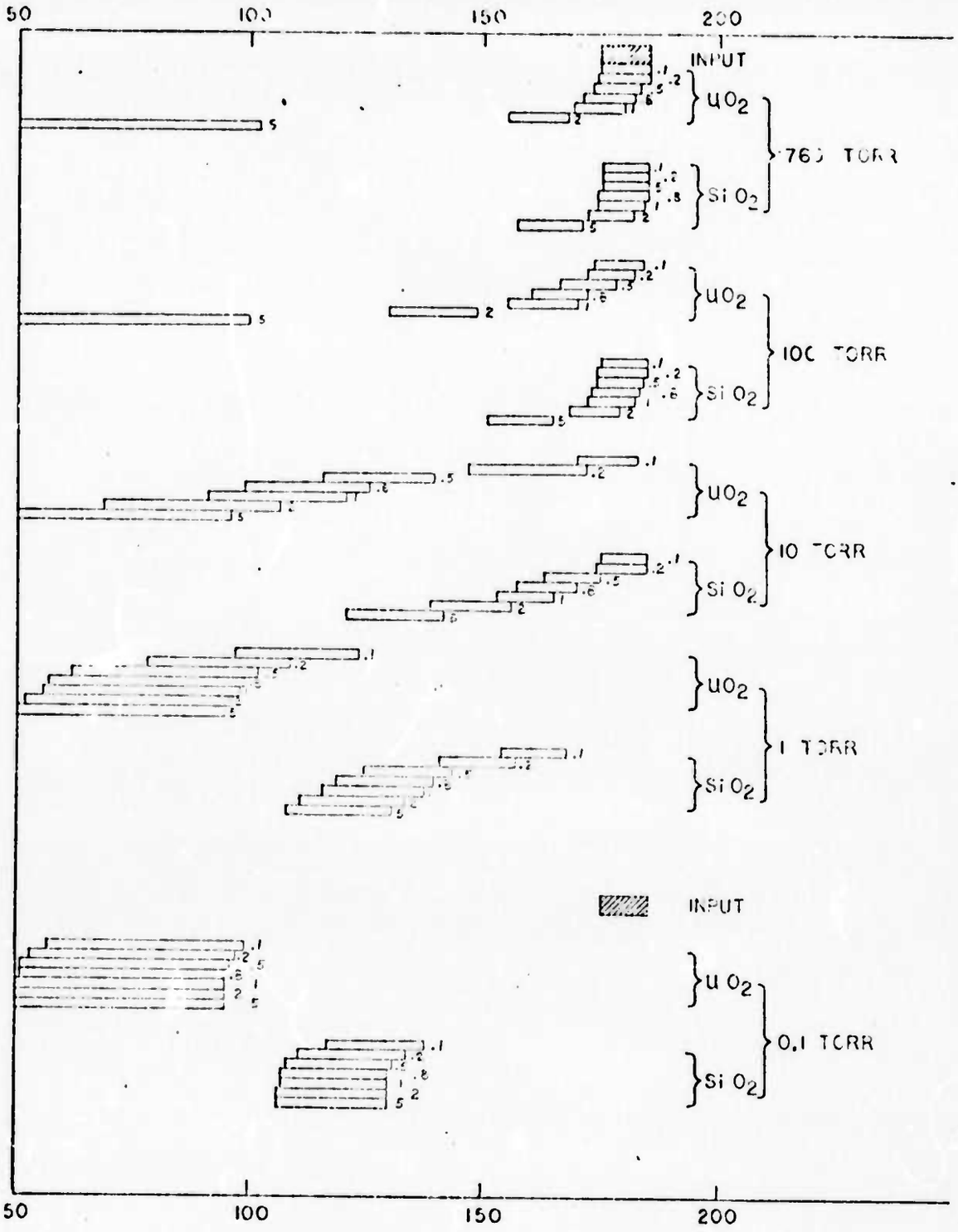

FIGURE 2-2

PARTICLE TRANSIT DISTANCES IN He AT VARIOUS PRESSURES

Voltage: 189 volts

is a partial separation like that shown in Section 2.1. However, this separation is too little for any practical use. At P = 1 torr, there is sufficient separation for a two material system. However, only at P = 0.1 torr is there sufficient separation for a multimaterial system.
In Figure 2-3, we show the results of a multiparticle separation for 1 μm diameter particles with an applied pressure of 0.1 torr. If the particles falling between 90 μm and 120 μm from the center of the wire were separated from the remainder of the particles, there is useful separation of UO_2 from particles having a $(\kappa-1)/\rho$ factor greater than 2.3 or less than 1.4.

In conclusion, these results show that an effective separation can only be possible at pressures less than about 0.1 torr (100 micron of Hg).

2.5 Laboratory Experiments

A simple qualitative experiment was conceived to demonstrate dielectric deflection of a slowly moving beam of particles. A very fine particle stream of low, but unmeasured, particle density was generated. The following equations from Appendix A are used to calculate the parameters of the experiment.

$$v_p = \left(\frac{\varepsilon_o(\kappa-1)}{\rho}\right)^{\frac{1}{2}} \frac{V_o}{p' r_p} \qquad (2-3)$$

where

$$p' = \ell n(r_1/r_o) \qquad (2-4)$$

with r_o = 0.24 cm (inner electrode radius) and r_1 = 2.54 cm (outer electrode radius), an applied voltage (V_o) greater

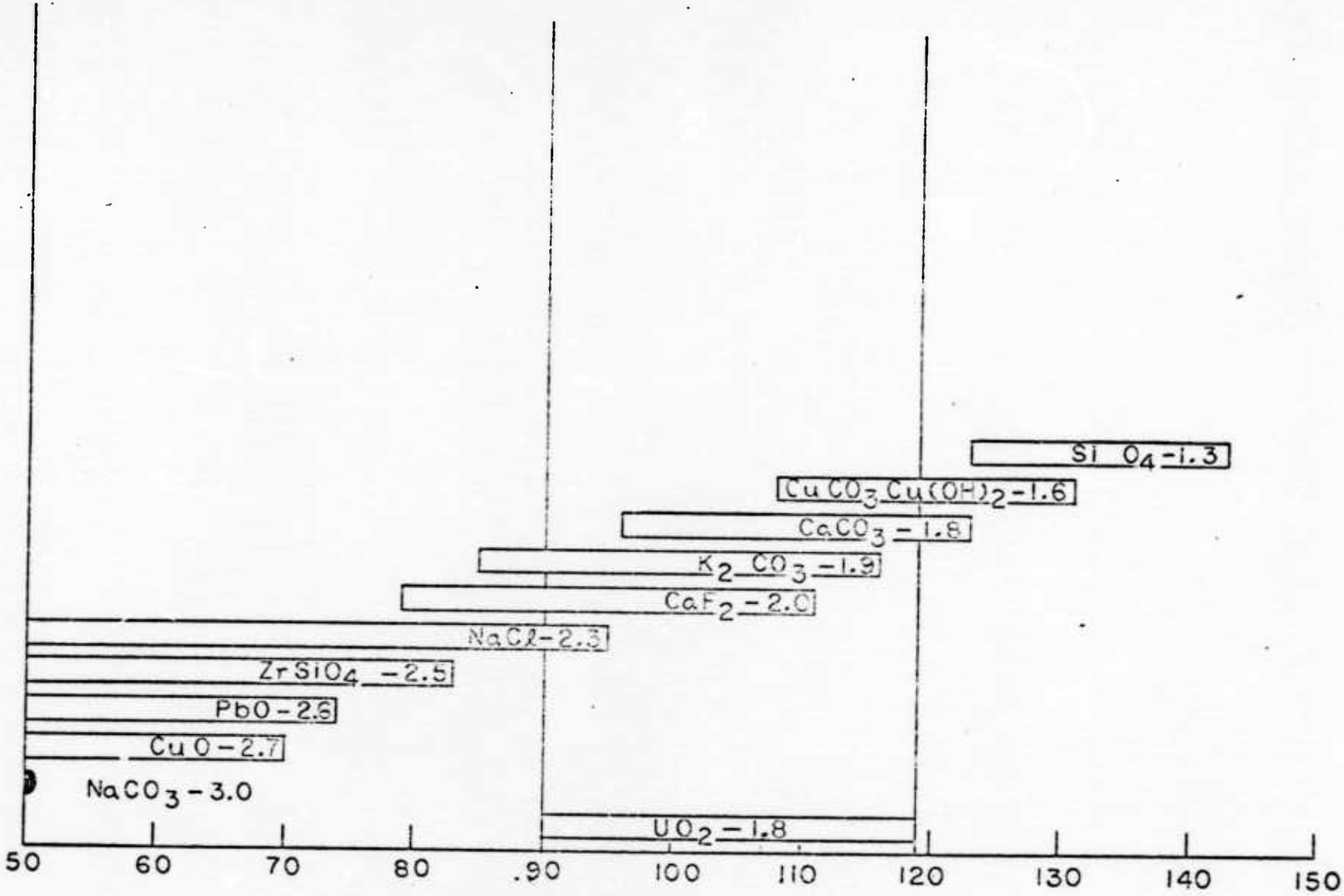

FIGURE 2-3

A MULTIPARTICLE SEPARATION FOR 1 μm PARTICLES AT A PRESSURE OF 0.1 TORR

than 5.7 kV should deflect UO_2 particles moving at a velocity, v_p, of about 3 cm/sec tangential to the inner electrode (see Figure 2-4). Operating the system at 7 kV and $v_p \simeq 3$ cm/sec, extensive deflection of a beam of 1 μm UO_2 particles was observed. It was not possible to test the particles for surface changes. On a filter paper used to collect the particles, it was observed that UO_2 particles deflected rather evenly with a tapering off starting 2 cm from the point of no deflection. The same experiment was then tried using 1 μm SiO_2 particles. With v_p again at ≃ 3 cm/sec, there was little deflection of the SiO_2 until voltage was increased to 10 kV. The qualitative results of these tests are shown in Table 2-8.

TABLE 2-8

QUALITATIVE RESULTS OF DIELECTRIC EXPERIMENT

Voltage (kV)	1 μm UO_2	1 μm SiO_2
	Estimate of the Amount of Deflection	
4	None	None
5	None	None
6	Some	-
7	Some	None
8	Extensive	None
9	Extensive	Some
10	-	Some
11	-	Extensive

Since at 8 kV, there appeared to be extensive deflection of UO_2 and almost none for SiO_2, a separation experiment was performed. A mixture of UO_2 and SiO_2 was placed in the particle chamber. With V_o = 8 kV, a 1:1 mixture of 1 μm UO_2 and 1 μm

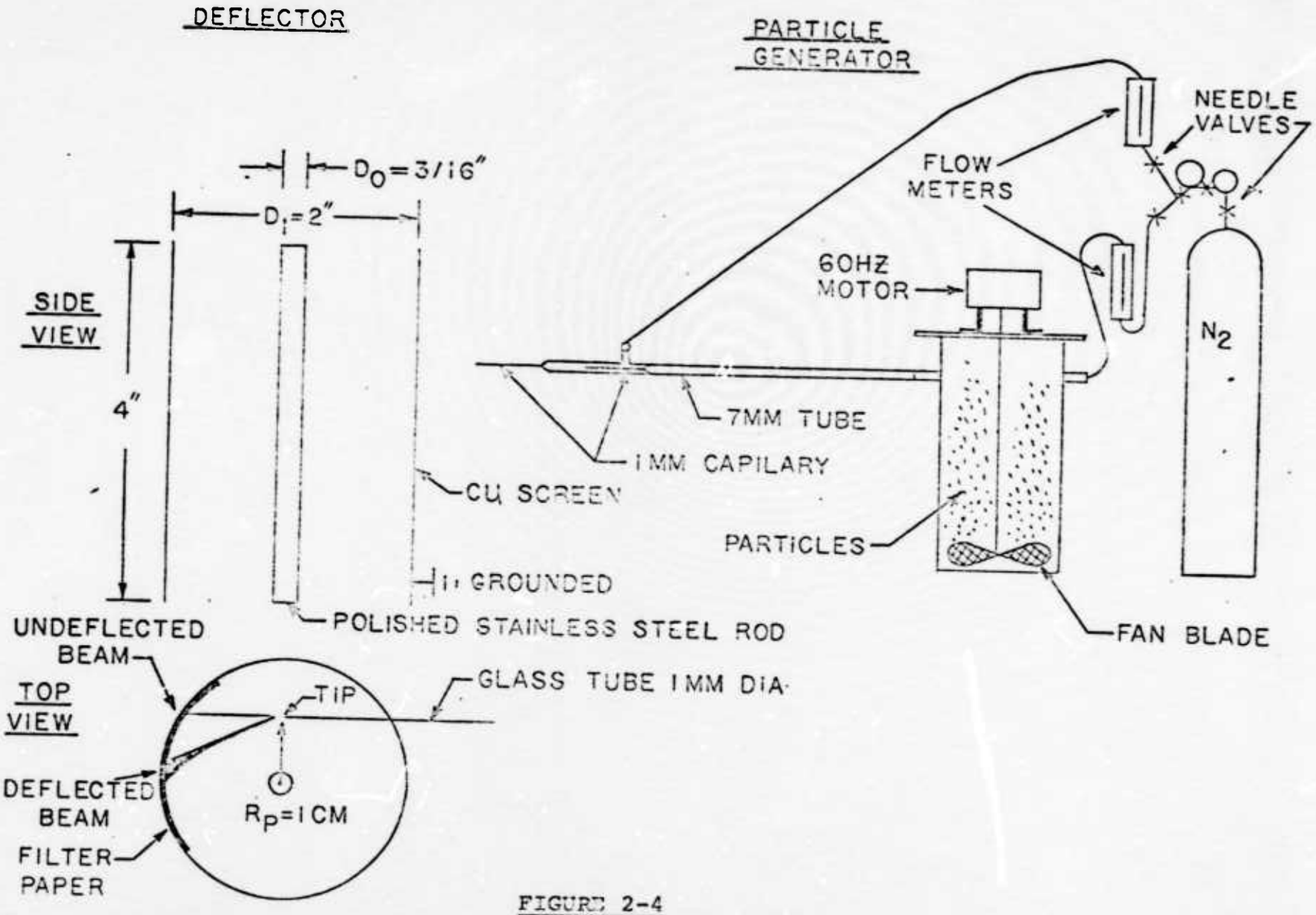

FIGURE 2-4

SCHEMATIC OF SIMPLE DIELECTRIC DEFLECTION EXPERIMENT

SiO_4 particles showed slight deflection and no separation. Since the particles under a microscope appeared to be highly conglomerated, a second particle generator was constructed so that the UO_2 and SiO_4 could be combined in the low density gas/particle beams. The results were nearly identical to those using the intimate mixture.

Under a very intense lamp the individual particles could be observed. These particles demonstrated no acceleration toward the center high voltage electrode. Even at 15 kV, no migration, either dielectric or Coulombic, was observed by the particles moving very near the wire. Although microscopic examination of the particles showed that they were still, although less, conglomerated, their central acceleration should not have been effected. Consequently, the viscous drag in nitrogen and in helium (the two gases used in these experiments) at atmospheric pressure is too great for us to observe any dielectric deflection.

The deflection that we observed in our first experiments were due to the gas dynamics in our enclosed chamber. The different results with our two materials were probably a result of their varying densities.

From these experiments we can conclude two things:

(a) dielectric deflection can, if ever, be observed only at very low pressures, and

(b) our calculation of dielectric forces may be greater than they actually are.

2.6 Dielectric Forces versus Coulombic Forces

In Appendix A, we showed that the dielectric force is

$$F_d = \varepsilon_o(\kappa-1)\, E(\partial E/\partial r)V \qquad (2\text{-}5)$$

where V is the particle volume.

It is well known that the Coulombic force is

$$F_c = Eq \qquad (2\text{-}6)$$

For the Coulombic force to be of the same order magnitude as the dielectric force (i.e., $F_d/F_c = 1$) then

$$q = ne = \varepsilon_o(\kappa-1)(\partial E/\partial r)V$$

where n is the number of electrons whose charge is e. Assuming spherical particles and using the cylindrical geometry and equation A-33,

$$\frac{\partial E}{\partial r} = - \frac{V_o}{r^2 \ell n(r_1/r_o)} \qquad (2\text{-}7)$$

with $V = \pi d^3/6$, the number of electrons that will give a Coulombic force equal to the dielectric force is

$$n = \frac{\pi \varepsilon_o (\kappa-1) V_o}{6er^2 \ell n(r_1/r_o)} \, d^3 \qquad (2\text{-}8)$$

Let V = 190 volts, r = 175 μm, r_o = 50 μm and r_1 = 200 μm, where for UO_2, κ = 21. Table 2-9 shows the number of electrons

TABLE 2-9

THE NUMBER OF ELECTRONS THAT GIVE A COULOMBIC FORCE EQUAL TO THE DIELECTRIC FORCE

Particle Diameter (μm)	n (# of electrons)
50	320,000
10	2,600
5	320
3	70
1	2.6
0.8	1.3
0.5	0.32
0.1	0.0026

for particles of UO_2 of various sizes. For particles of diameter less than 1 μm, any surface charge will give a large Coulombic force.

Particles in the atmosphere are known to be charged; electrostatic precipitators work very effectively on the principle that all particles have some charge. Charge is caused by:

(a) Friction - particles colliding with each other and with gas molecules.

(b) Reactions - chemical and nuclear

(c) External forces - ultraviolet radiation, gamma radiation, ionic discharge.

Even if the particles, which we must assume are likely to be charged when they leave the plasma asher section, could be effectively discharged, without losing them on the discharging surfaces, it is extremely unlikely they could be neutralized and kept neutral to the degree where there would literally be no free charges on their surface.

A solution would be to rapidly oscillate the electric field. In order to see a relatively uniform field, the field must oscillate at least once each time a particle transverses its diameter. For 1 μm particles moving at 1800 cm/sec, the frequency must be 1.8×10^7 Hz. This rapidly oscillating field creates a situation similar to our RF plasma stage. If the pressure is low, i.e., below 10 torr, a plasma discharge will occur. Consequently, this consideration dictates a higher pressure.

SECTION III

PLASMA ASHING

3.0 Introduction

In an RF oxygen plasma, the primary reactive species has been determined[1] to be $O_2\ \Delta_g^1$ molecules and O ^3P oxygen atoms, their individual concentrations ranging from 10 to 20% depend on the discharge conditions. Both the atomic and excited molecular oxygen react with organic substrates and gas phase species. In the glow region of the plasma, there is a free electron concentration of approximately 10^{11} cm^{-3}. However, a few millimeters away from this glow region, nearly all of the ionic species have disappeared but the other "active" species persist for a considerable distance before they are deactivated either reactively or by collision.

The direct generation of oxygen atoms in the discharge glow region results in part from electron-molecule reactions, molecule ion-electron reactions, and electronically excited molecular oxygen dissocation. High concentrations of atomic oxygen can be attained by the catalytic effects of other "foreign" gas, such as hydrogen, nitrogen, or water vapor. These impurities provide many of the kinetic pathways leading to atomic oxygen production. Nitrogen as an impurity in discharged oxygen gives such reactions as:

$$NO^+ + e^- \rightarrow N + O$$
$$N + O_2^+ \rightarrow NO^+ + O \qquad (3\text{-}1)$$

In a very pure oxygen discharge, there is the usual glow, but the plasma will contain a very low level percentage of oxygen atoms.

---

1. J. R. Hollahan and A. T. Bell, Techniques and Applications of Plasma Chemistry, John Wiley & Sons, Inc., 1974.

3.1 Optimum Conditions for Plasma Ashing

3.1.1 Pressure and Flow Rate

A fluidic system was developed where the pressure, flow rate, and gas mixture could be independently controlled. This system is shown in Figure 3-1. The asher is a Tegal PLASMOD whose RF power is continuously variable from 0-100 at 13.56 MHz. The PLASMOD was fitted with 3.25" ID by 6.25" long Pyrex reaction chamber. The mechanical pump is a Welch 1402B which has a pumping speed of 160 liters per minute. The pressure gauge is a Hastings VT-4 thermocouple gauge which has a range of 0-20 torr.

It was found that ashing rate and the completeness of ashing did not depend greatly on the flow rate or pressure. Therefore, these were relatively constant throughout the experiments. The pressure was held at 1.0 ± 0.2 torr and the flow rate at 175 ± 25 cm^3/min.

3.1.2 Gas Composition

The rate of ashing did depend greatly on the gas composition. The following gas mixtures were studied:

(a) 100% O_2

(b) 96% O_2, 4% CF_4

(c) 80% O_2, 20% N_2

(d) 50% O_2, 50% N_2

(e) 48% O_2, 48% N_2, 4% CF_4

(f) 50% O_2, 50% H_2

For each mixture, two samples each of approximately 2 grams of Whatman #44 (Ashless) filter paper were used. The results

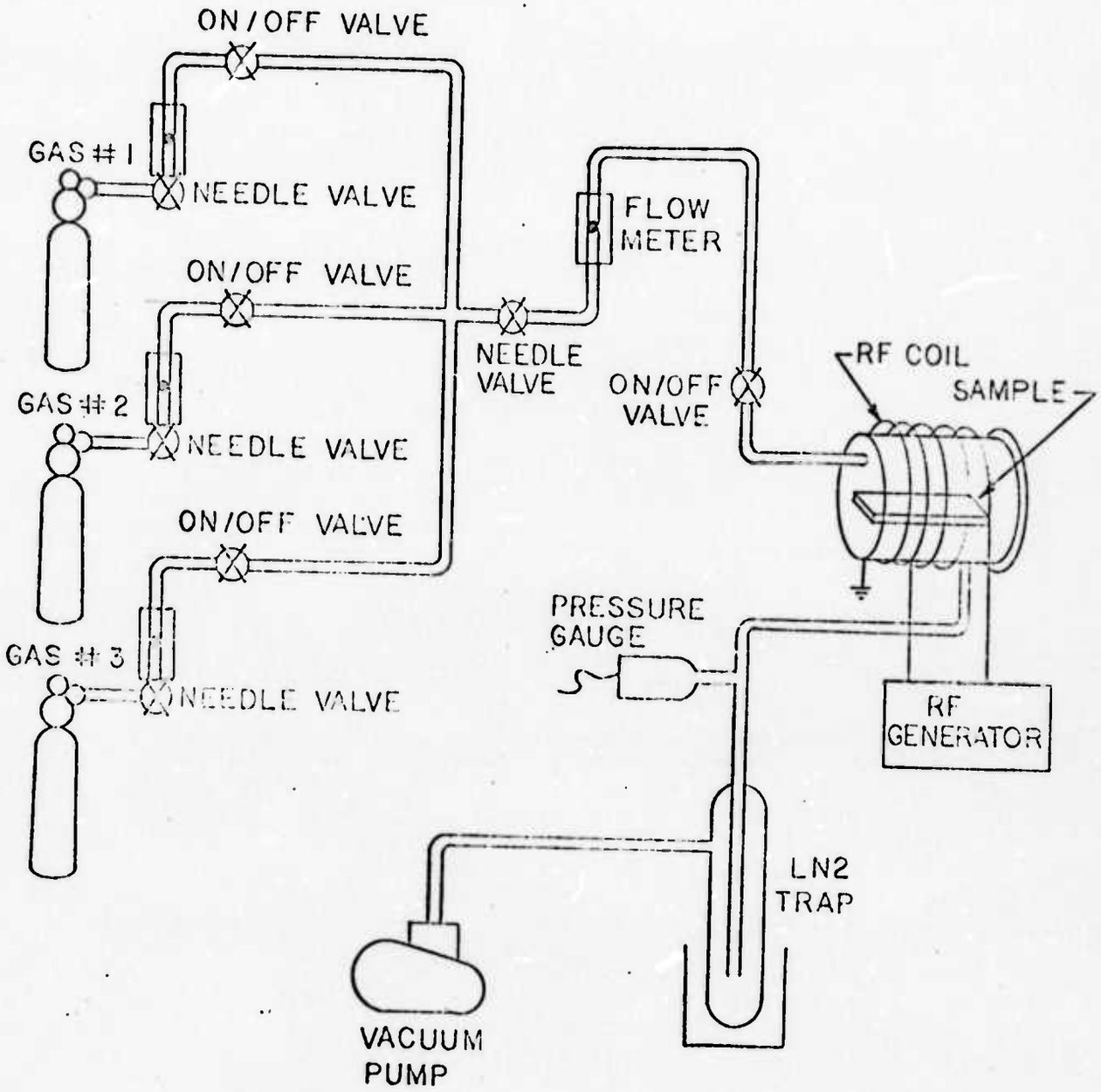

FIGURE 3-1

PLASMA ASHER AND FLOW SYSTEM

are shown in Table 3-1 and in Figure 3-2. In all cases, the variation in the percent residue after each time interval was within ± 0.05% of the average. This was small compared to the relative differences between mixtures. The 1:1 mixture of O_2 and N_2 with CF_4 was the fastest mixture tested. The addition of 4% CF_4 did increase the rate slightly but insignificantly. Adding nitrogen to oxygen markedly increased the rate of ashing.

TABLE 3-1

ASHING RATE FOR VARIOUS GAS MIXTURES

Gas Mixture	Average Percent Residue After				
	2 Hour	4 Hour	6 Hour	8 Hour	10 Hour
O_2	58.32	33.68	20.51	10.18	4.87
O_2 w CF_4	52.94	28.41	15.03	7.32	3.12
4:1 O_2/N_2	38.75	15.19	5.61	1.42	0.21
1:1 O_2/N_2	34.81	11.87	3.81	1.35	0.16
1:1 O_2/N_2 w CF_4	32.17	9.86	3.11	0.86	0.07
1:1 O_2/H_2	42.03	18.42	7.92	2.34	1.11

A more important test is the relative completeness of ashing, as well as the inertness of UO_2 to the mixture. Samples of cotton cloth (CC) and UO_2 were subjected to plasmas of the following mixtures for 18 to 24 hours:

(a) 100% O_2

(b) 96% O_2, 4% CF_4

(c) 50% O_2, 50% N_2

(d) 48% O_2, 48% N_2, 4% CF_4

(e) 80% O_2, 20% CF_4

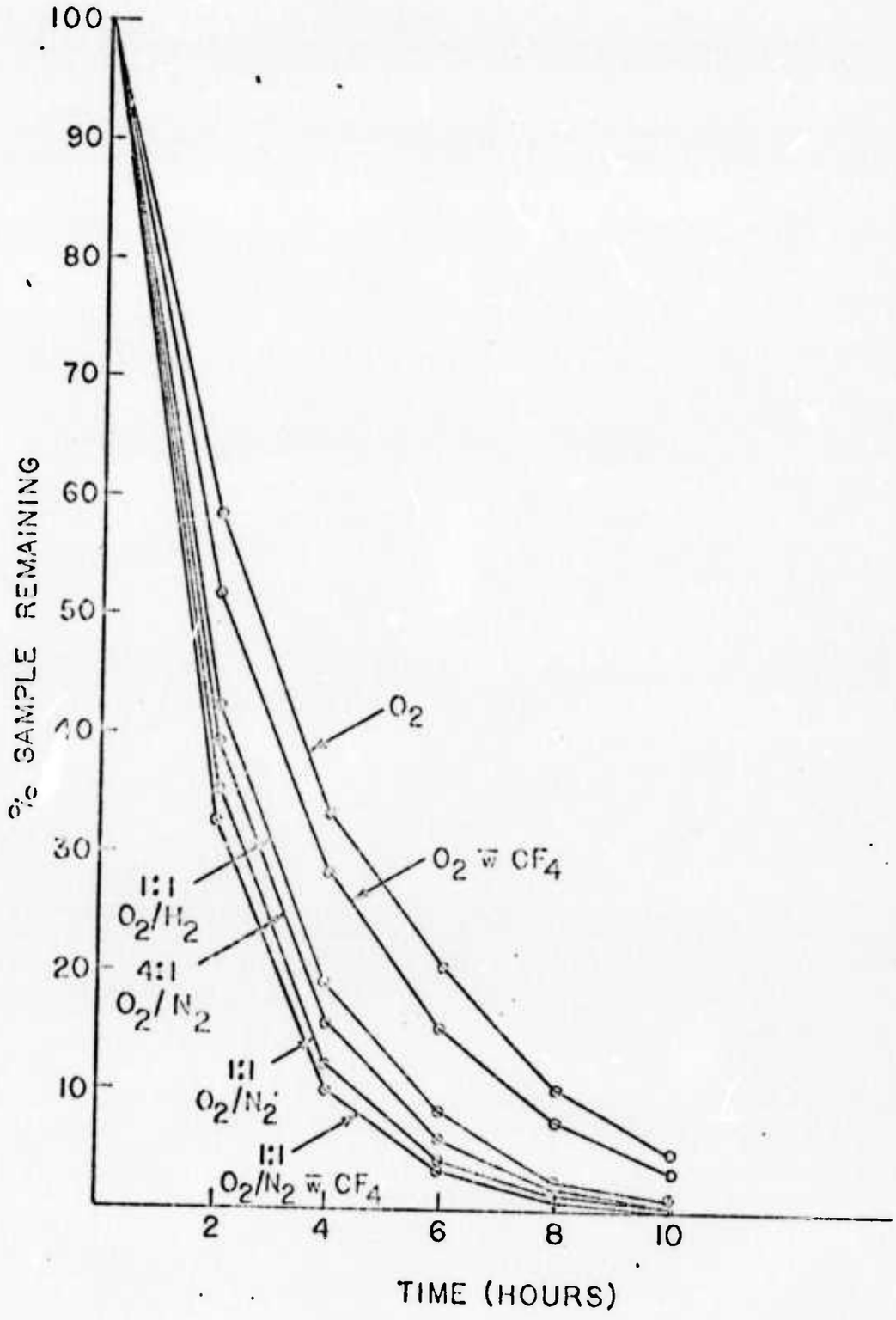

FIGURE 3-2

ASHING RATE OF VARIOUS GAS MIXTURES

The results are shown is Table 3-2. The addition of CF_4 gives considerably less ash from cotton cloth. While the 1:1 O_2/N_2 gives a much faster ashing than pure O_2, the final percent residue is nearly the same. The 1:1 O_2/N_2 with 4% CF_4 gives both the fastest and most complete ashing. However, the test for corrosion to UO_2 shows that mixtures containing CF_4 cause a serious loss in weight to UO_2 samples. Since plasmas can only etch away at the surface, a small weight loss in this experiment indicates that an exposed particle 10 μm or less in diameter would be completely destroyed if CF_4 in any concentration is present in the plasma gas. Consequently, CF_4 should not be used on samples where low losses are required.

Samples exposed only to pure O_2 or to O_2/N_2 mixtures showed a slight increased weight. This is undoubtedly due to the formation of higher oxides like UO_3. Since no material was lost, the 1:1 O_2/N_2 mixtures were deemed the best to use in the remainder of our experimental work.

3.1.3 Experimental Procedure

The samples were ashed in Pyrex petri dishes 60 mm OD x 15 mm height. Before initial weighing, the dishes were placed in the operating asher for at least 1 hour to remove all adsorbed water. All weighing was done on a Mettler H15 analytical balance which has a sensitivity of 0.1 mg and a precision (standard deviation) $\pm$ 0.05 mg.

All samples were dried for at least 24 hours in a desiccating cabinet in which the desiccant drierite was used. A silica gel desiccant was placed in the balance chamber to reduce moisture adsorbtion during weighing.

TABLE 3-2

PERCENT RESIDUE AFTER LONG TERM ASHING

Gas	Sample	Ashing Time hours	Initial Wt. gm	Final Wt. gm	% Residue
O_2	CC	23.6	3.5863	0.0114	0.32
O_2 w CF_4	CC	22.1	2.8164	0.0042	0.15
1:1 O_2/N_2	CC	21.4	2.1107	0.0061	0.29
1:1 O_2/N_2	CC	21.4	1.1559	0.0028	0.24
1:1 O_2/N_2 w CF_4	CC	24.0	0.7992	0.0005	0.06
1:1 O_2/N_2 w CF_4	CC	18.1	3.9296	0.0016	0.04
1:1 O_2/N_2 w CF_4	CC	18.1	3.9696	0.0028	0.07
O_2	UO_2	23.6	8.4692	8.5810	101.32
O_2 w CF_4	UO_2	22.1	7.9136	7.3090	92.36
1:1 O_2/N_2	UO_2	21.3	6.6439	6.7250	101.22
1:1 O_2/N_2	UO_2	21.3	7.3126	7.3777	100.89
1:1 O_2/N_2 w CF_4	UO_2	24.0	9.1268	8.1557	89.36
1:1 O_2/N_2 w CF_4	UO_2	20.2	13.1687	11.4950	87.29
1:1 O_2/N_2 w CF_4	UO_2	20.2	7.8642	7.1847	91.36
4:1 O_2/CF_4	UO_2	21.3	6.3874	4.6238	72.39
4:1 O_2/CF_4	UO_2	21.3	10.1896	7.6249	74.83

The UO_2 samples were heated in an oven at 150°C for at least 24 hours before ashing. The UO_2, 99.8% pure, was purchased from Research Organic/Inorganic Chemical Corporation, Belleville, NJ 07109.

During each run, only two samples and a blank dish could be placed in the asher. Table 3-3 shows the initial and final weights of blanks for several runs using different gases. For those runs in which CF_4 was present, there was an average weight loss of -1.9 mg. The sample weights in Table 3-2 were corrected for a -1.9 mg loss in weight by the container in those runs where CF_4 was present. In the other runs, there was a standard deviation ± 0.16 mg. The maximum error in estimated residue is ± 0.016%.

TABLE 3-3

VARIATION IN WEIGHT OF BLANKS

Gas	Ashing Time hours	Initial Wt. gm	Final Wt. gm	Δ (mg)
O_2	23.6	16.1312	16.1313	+0.1
O_2 w CF_4	22.1	17.1092	17.1074	-1.8
1:1 O_2/N_2	12.8	16.1312	16.1312	0.0
1:1 O_2/N_2	21.4	16.1314	16.1314	0.0
1:1 O_2/N_2	18.8	11.5118	11.5115	-0.3
1:1 O_2/N_2	20.3	16.7048	16.7049	+0.1
1:1 O_2/N_2	19.8	15.6736	15.6738	+0.2
1:1 O_2/N_2	17.0	14.4265	14.4267	+0.2
1:1 O_2/N_2	17.7	17.5953	17.5953	0.0
1:1 O_2/N_2 w CF_4	24.0	16.1315	16.1298	-1.7
1:1 O_2/N_2 w CF_4	18.1	16.7894	16.7875	-1.9
1:1 O_2/N_2 w CF_4	19.2	16.9765	16.9742	-2.3

In all runs, the plasma was tuned to maximum power absorbed. The characteristic plasma colors of the following pure gases are:

Oxygen	Pink
Nitrogen	Orange
Carbon Dioxide	Blue
Hydrogen	Redish Pink
Carbon Tetrafluoride	Bluish White

When an organic sample begins ashing in an oxygen or oxygen/nitrogen plasma, the color is initially blue due to the CO_2 formed. However, this shortly (10 to 20 minutes) changes to the characteristic pink of oxygen. Consequently, color has no utility in determining the completeness of ashing. It is useful in determining if the asher is well tuned.

3.2 Oxygen Ashing of Organic Materials

3.2.1 Preliminary Experiments

Table 3-4 shows the results of short ashings (8 to 10 hrs.) with pure O_2. All runs made under these conditions are listed. The pressure was approximately 3 torr and the surface temperature was estimated to be about 120° C. These experiments, not done with the system as shown in Figure 3-1, had the gas going directly through a needle valve to the reaction chamber. Consequently, the flow rate was not monitored.

3.2.2 Later Experiments

In the experiments shown in Table 3-5, the system was operated as described in Section 3.1.1 with a 1:1 O_2/N_2 mixture. For those ashings which were visibly incomplete, the final weight is marked by an I. All runs made have been listed and there is a very good agreement between the results of identical runs. When two and three samples were run, the observable rate of oxidation varied indicating that the power was not evenly distributed throughout the cavity.

TABLE 3-4

ASHING OF ORGANIC MATERIALS WITH OXYGEN

Sample Material	Initial Wt. gm	Final Wt. gm	% Residue
A. Pure Substances			
1. Polyethylene	1.0022	0.0012	0.1
2. Polyvinylchloride	0.5029	0.0031	0.6
3. Nylon	1.5160	0.0025	0.2
4. Graphite	1.0015	0.0000	0.0
5. Starch	1.0244	0.0002	0.0
B. Complex Materials			
1. Human Hair	1.0060	0.0491	4.9
2. Pine Needles	1.9836	0.0719	3.6
3. Alfalfa (dry powder)	2.0006	0.1445	7.2
4. Maple Leaf	0.5901	0.0724	12.3
5. Book Paper	6.3129	0.0892	1.4
6. Typing Paper	1.0316	0.0089	0.3
7. Filter Paper (Cotton)	2.7250	0.0089	0.3
8. Coal Dust	0.5005	0.0392	7.8
9. Powdered Whole Milk	1.0013	0.0657	6.6
10. Motor Oil (Clean)	1.0003	0.0003	0.0
11. Sawdust	1.0048	0.0304	3.0

TABLE 3-5

ASHING OF ORGANIC MATERIALS WITH 1:1 OXYGEN/NITROGEN MIXTURE

Sample Material	Ashing Time hours	Initial Wt. gm	Final Wt. gm	% Residue
A. Filter Papers				
1. Whatman #50 (Hardened--0.025%)	49.5	13.2553	0.0089	0.067
2. Whatman #541 (Hardened Ashless-0.008%)	49.5	8.6690	0.0002	0.002
3. Whatman #44 (Ashless-0.01%)	49.5	9.5029	0.0016	0.017
	12.8	4.3740	0.0017(I)	0.039
4. Millipore Duralon (NC-Nylon)	18.8	0.2008	0.0002	0.10
5. Millipore Celotate (EA-Cellulose Acetate)	18.8	0.2062	0.0004	0.19
6. Millipore Polyvic (BS-Polyvinyl Chloride)	18.8	0.3339	0.0664	19.9
7. MF-Millipore (SM-Mixed Ester of Cellulose)	12.8	0.2240	0.0001	0.04
B. Clothing Materials				
1. 100% Cotton	21.4	2.1107	0.0061	0.29
	21.4	1.1559	0.0028	0.24
2. 75% Rayon/25% Cotton	20.3	3.1164	0.0167	0.54
	17.7	2.4656	0.0134	0.54
3. 50% Cotton/50% Polyester	19.8	1.3212	0.0246(I)	1.86
	17.0	0.8214	0.0531(I)	6.46
	17.7	0.9836	0.1414(I)	14.37
4. 50% Orlon Acrylic 25% Stretch Nylon 25% Cotton	13.8	1.9510	1.0083	0.43
	17.0	1.5008	0.0062	0.41
	13.8	2.5006	0.1511(I)	6.16
5. 100% Orlon	17.0	1.1697	0.0104	0.89
	20.3	2.2564	0.0201	0.89
6. Irish Linen (flax)	17.7	1.6122	0.0042	0.26
	19.8	1.3185	0.0035	0.27

TABLE 3-5 (continued)

7. 60% Wool, 5% Cotton 5% Rayon, 10% Acetate 20% Stretch Nylon	35.6	2.6771	0.0461	1.72
	35.6	2.1087	0.0224	1.06
8. Icelandic Wool	21.4	3.0476	0.0290	0.95
	23.1	1.6308	0.0145	0.89
9. Australian Wool	21.4	2.7511	0.0167	0.61
	23.1	2.2460	0.0124	0.55
C. Natural Materials				
1. Bark	24.5	0.8829	0.0529(I)	5.99
	48.3	2.3694	0.0242	1.02
2. Dried Leaves	7.1	0.0855	0.0043	5.03
	24.5	0.6831	0.0092	1.35
3. Fresh Leaves	22.1	0.7836	0.0061	0.78
	22.1	0.8643	0.0084	0.97
D. Tissues				
1. Kimwipes	20.6	1.0871	0.0257(I)	2.36
	48.3	1.1242	0.0121	1.08
2. Kleenex	20.6	0.9718	0.0088	0.91
	48.3	1.4859	0.0131	0.88

3.2.3 Photographic Examination of the Residues

Although the residues were not chemically analyzed, they are typically oxides of trace elements such as Ca, Cu, Fe, Mg, Zn, Na, and K[1]. The particles formed upon ashing are typically considerably smaller than 0.1 μm.[1] Figure 3-2 shows 430X enlargement of ashed and crushed sample Millipore Duralon. Since no large particulate matter can be identified and since a 1 μm particle would give a .43 mm image on our film, this picture shows that particles formed are well less than 1 μm. Figure 3-3 shows a second sample of ashed Duralon which had 10 μm and smaller UO_2 particles on its surface. These particles show up clearly under a microscope. Figures 3-4 and 3-5 show that the plasma does not change the material matrix in Irish linen, and Figures 3-6 and 3-7 show the same effect for cotton cloth. Figures 3-8 and 3-9 show 100% orlon acrylic before and after ashing. Figures 3-10 and 3-11 show Australian wool before and after ashing.

3.3 Ashing of Inorganic Materials

Table 3-6 shows the result of preliminary ashings under the same conditions as described in Section 3.2.1. Data from all runs made are shown.

---

1. J.R. Hollahan and A.T. Bell, Techniques and Applications of Plasma Chemistry, John Wiley & Sons, Inc., 1974.

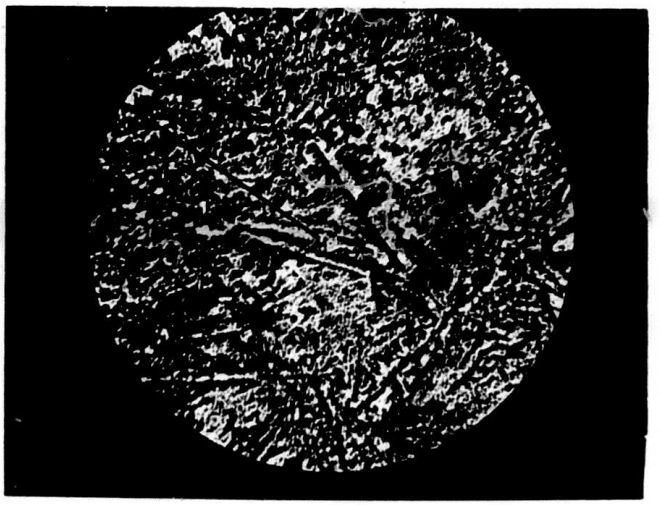

FIGURE 3-3

ASHED AND CRUSHED DURLON 430X

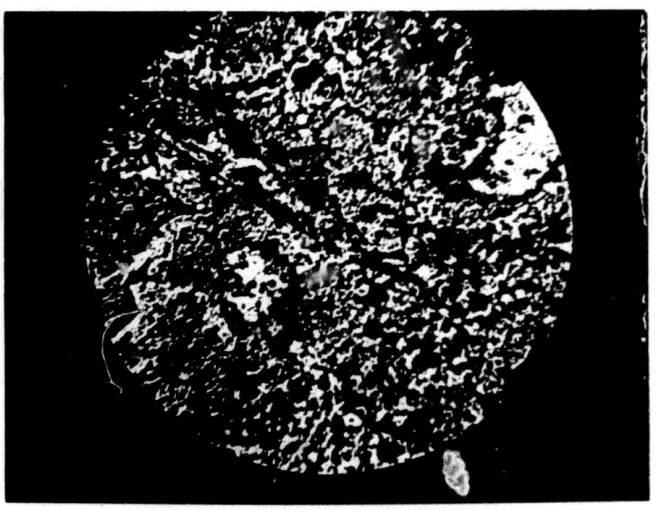

FIGURE 3-4

ASHED AND CRUSHED DURLON WITH 10 μm PARTICLES 430X

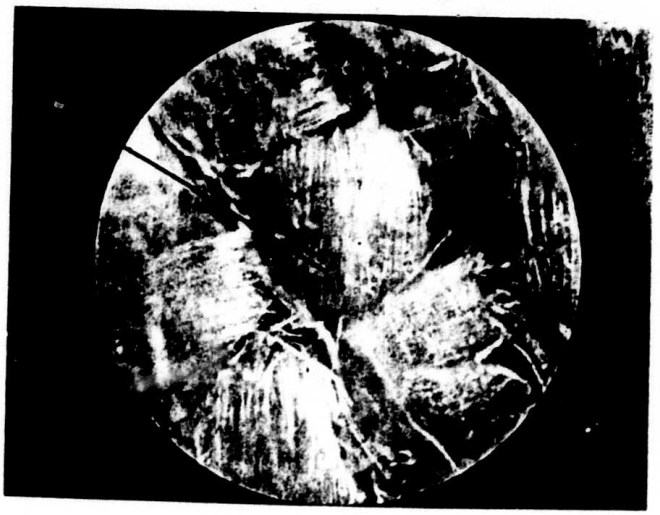

FIGURE 3-5

IRISH LINEN 100X

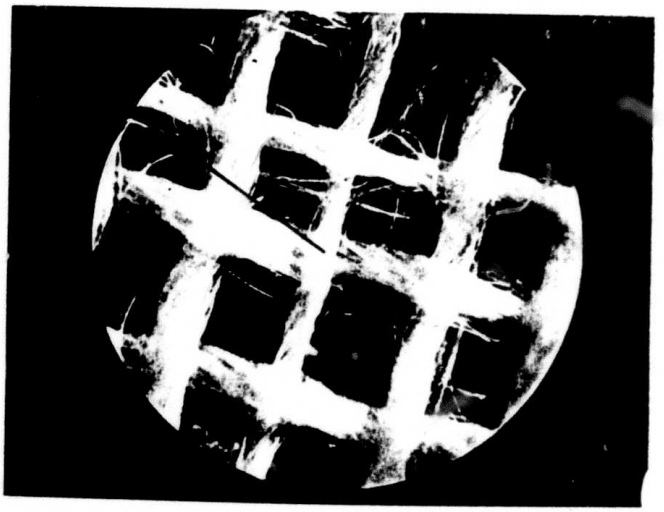

FIGURE 3-6

ASHED IRISH LINEN 100X

FIGURE 3-7

COTTON CLOTH 100X

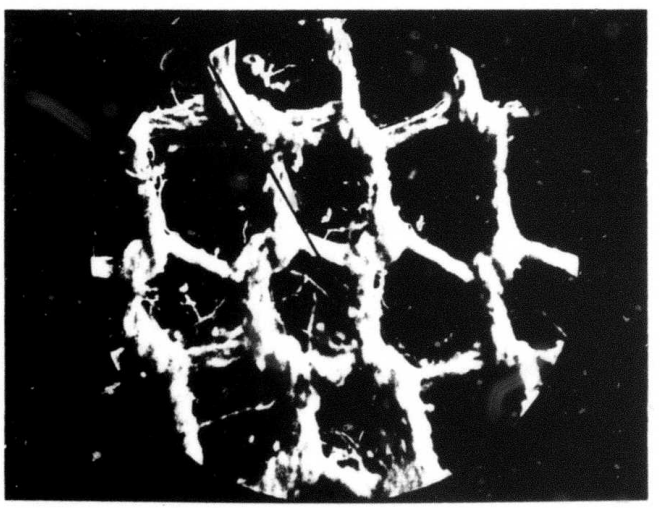

FIGURE 3-8

ASHED COTTON CLOTH 100X

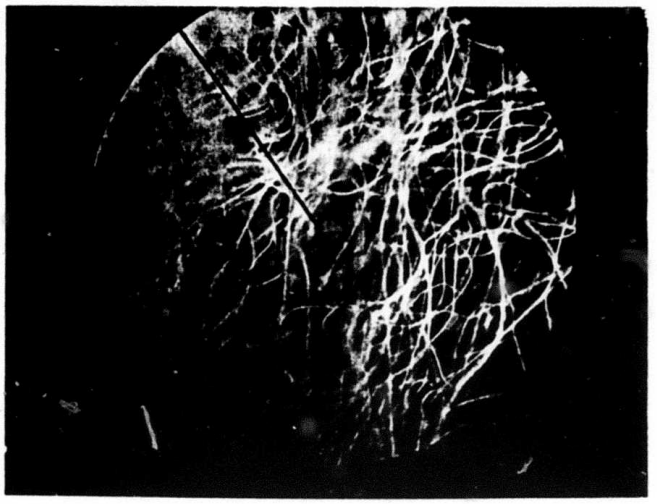

FIGURE 3-9

ASHED 100% ORLON ACRYLIC 100X

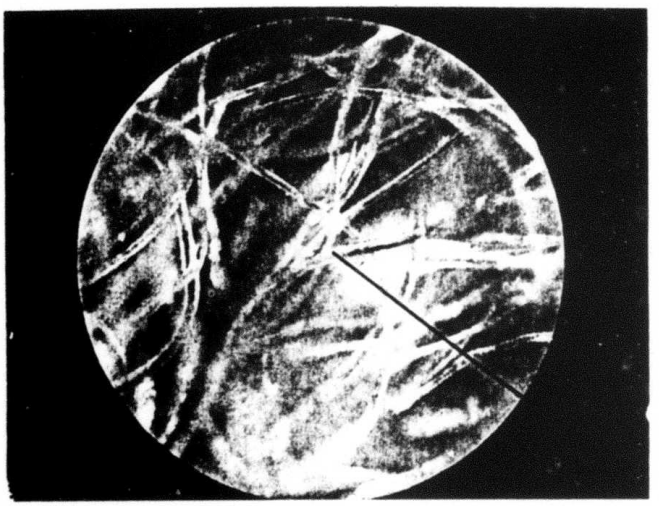

FIGURE 3-10

100% ORLON ACRYLIC 100X

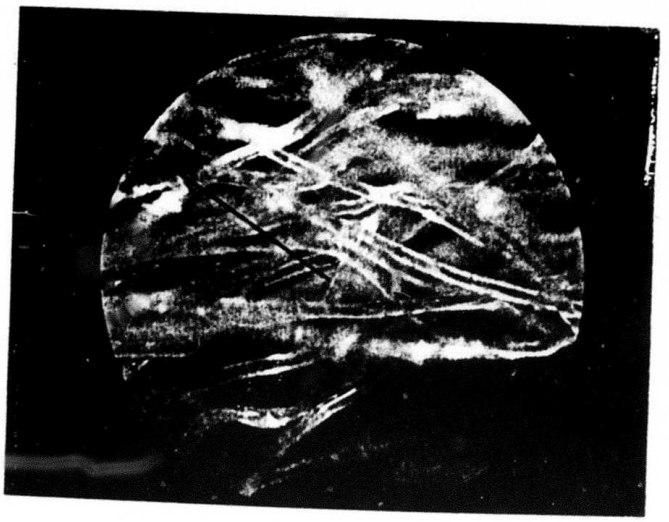

FIGURE 3-11

AUSTRALIAN WOOL 100X

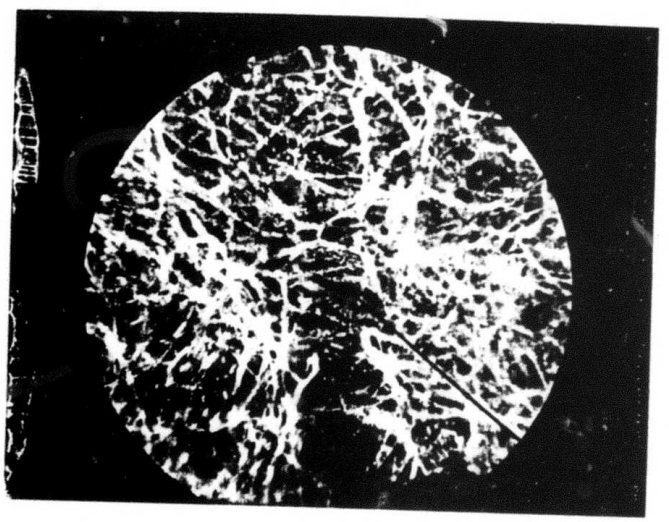

FIGURE 3-12

ASHED AUSTRALIAN WOOL 100X

TABLE 3-6

ASHING OF INORGANIC MATERIALS WITH
OXYGEN, HYDROGEN AND TETRAFLUOROMETHANE

Sample Material	Initial Wt. gm	Final Wt. gm	% Residue
A. Ashed with Oxygen			
1. Clay Encrusted Sand	1.2715	1.1845	93.2
2. Potting Soil	5.5802	4.0943	73.4
3. Silica Dust (SiO_2)	0.5609	0.5601	99.9
4. Zinc Oxide	4.1525	4.1506	100.0
5. Zirconium Nitride	0.5609	0.3409	60.8
6. Uranium Dioxide	2.9836	2.9834	100.0
B. Ashed with Hydrogen			
1. Silica Dust	0.6304	0.6301*	100.0
2. Uranium Dioxide	3.1567	3.1564*	100.0
C. Ashed with Tetrafluoromethane (CF_4)			
1. Silica Dust	0.5173	0.0000+	0.0
2. Uranium Dioxide	1.4142	1.0960+	77.5

* Ashing times were about 18 hours.

+ Adjusted for loss in weight of the pyrex container. Ashing times here were 1 hour.

3.4 Conclusions

Plasma ashing can be very useful for the removal of organic substrates and particles. The particles formed upon ashing are certainly less than 1 μm as determined microscopically and are probably considerably smaller than 0.1 μm. Therefore, the particles should be easily separated from the larger inorganic particles originally present. Oxygen and oxygen/nitrogen plasmas do extensive oxidation to UO_2, probably forming UO_3. In our experiments, about 18% of the UO_2 was oxidized to UO_3. Consequently, UO_2 does not remain invarient in oxygen plasmas.

SECTION IV

SYSTEM DESIGN AND FLUIDICS

4.0 Proposed Schematic Instrument Design

The schematic instrument design for a fluidic particle sorter at the time of termination of breadboard design is shown in Figure 4-1. Referring to this figure, the steps of the proposed operation would have been as follows:

(a) The sample is placed in the instrument just below an aluminum screen. The sample on a very low ash filter paper will be in a monolayer with particles whose diameters are greater than 5 micrometers removed.

(b) The sample's orientation with respect to the gas flow will be such that the filter paper will ash slowly from one end to the other releasing the particles slowly into the remaining stages of the instrument. The best orientation will probably be that where the normal to the plane of the filter is perpendicular to the gas flow stream.

(c) A mixture of 15%, by volume, oxygen in helium will be used as the gas mixture. The total pressure will be 1 to 2 torr in the asher section. It should take 3 to 6 hours to completely ash the filter paper and introduce the particles into the gas stream. During the first 30 minutes, almost all the organic particles present in the sample will have been oxidized to volatile products. Thus, only the interesting particles and other inorganics will remain to be carried off by the gas stream to the remaining stages of the instrument.

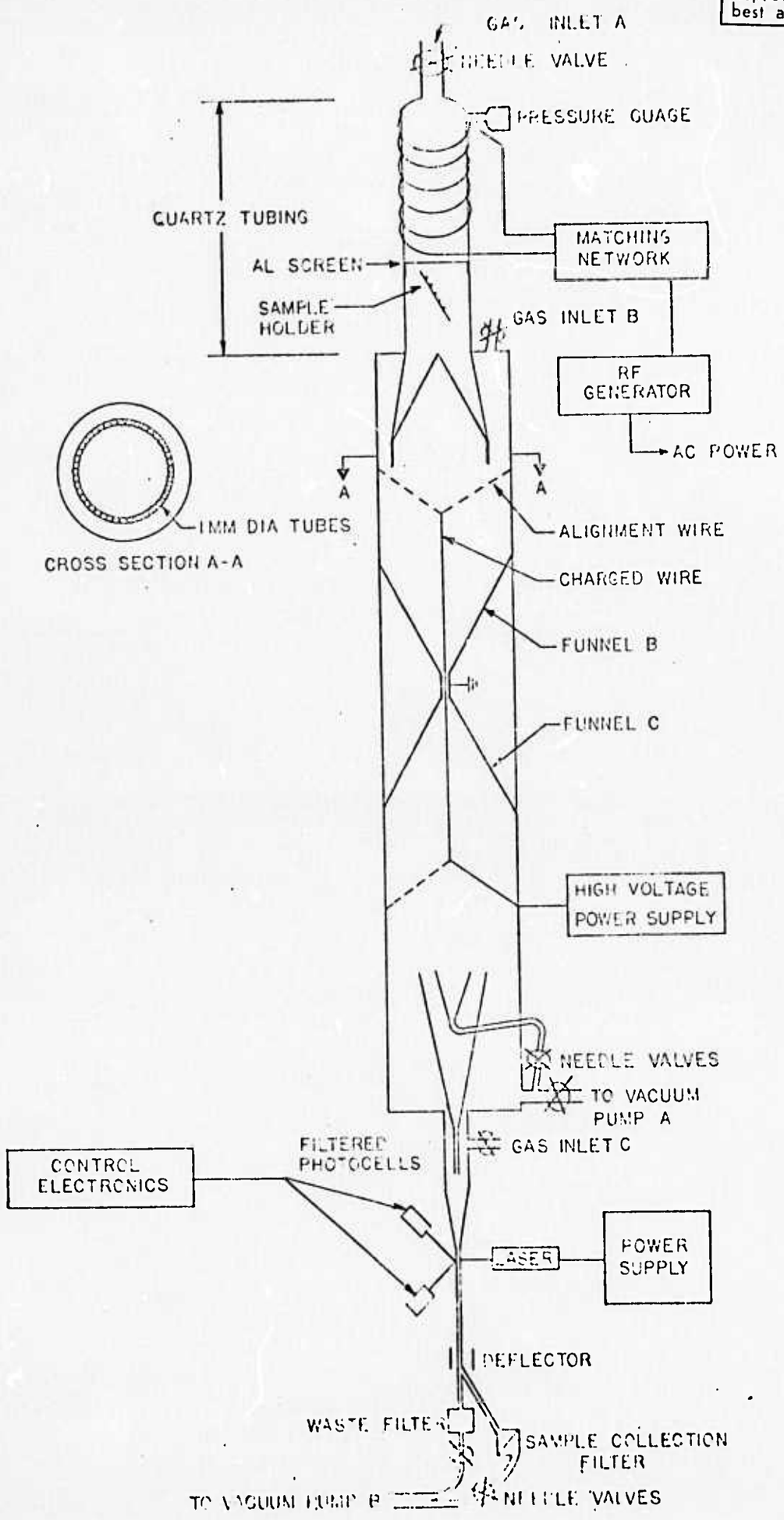

FIGURE 4-1
SCHEMATIC INSTRUMENT DESIGN

(d) The gas borne particles are carried by the gas stream to the funnel design at cross section A where they are collimated into sixteen beams of 1 mm in diameter. The helium flow at Gas Inlet B will be such as to keep the flow laminar and thereby maintain particle control. The diameter of the dielectric stage will be made large enough to maintain a pressure differential of 10:1. In the asher stage, the pressure will be about 1 torr giving an oxygen partial pressure 150 microns of Hg, which is sufficient for the ashing rates needed to ash the filter paper in 3 to 6 hours. The dielectric stage will have a diameter sufficient to maintain a pressure 0.1 torr.

(e) In the gas lens created by funnel B, each particle beam will be reduced from a diameter of 1000 micrometers to a diameter of 10 micrometers. The gas flow rates will be adjusted to maintain particle control.

(f) In the approximately 400 micrometer in diameter and 2.5 to 5 cm long cylindrical construction, dielectric forces due to the voltage on a 100 micrometer in diameter center electrode will deflect the particles. Particles of high dielectric constant to density ratio will be deflected more than those of lower ratios. Thus, a ratio spectrum is formed.

(g) The microscopic beam is then magnified by the reverse funnel at C.

(h) The separater tube will select that part of the gas borne particle beam containing the interesting

particles, which then pass into the final stage of separation.

(i) The particle stream then passes through funnel D where it is collimated into a 1 mm beam. It is then diluted by gas entering at inlet C and, again, collimated by funnel E to a 10 micrometer beam. The operational parameters will be found by adjusting flow rates and diameters so that the particle beam will have one particle at a time moving at constant velocity.

(j) A laser beam set perpendicular to the beam will excite a fluorescence from each particle as it passes by. An array of filtered detectors, each directed at the intercept of the particle beam and the laser, will sense the fluorescence. The output of the detectors will be sent into the control electronics and processed.

(k) When there is a characteristic emission from an interesting particle, the electronic processor, after a delay period, send a high voltage pulse to a pair of deflection electrodes. This delay period allows for the time it takes the selected particle to travel from the field of the detectors to that of the electrodes. The high voltage pulse creates a temporally short ion wind between the electrodes, which deflects the chosen particle into a separate beam. If the pulse width is 60 microseconds, a single particle can be selected from 10^3 particles passing by per second.

(l) The deflected particles are collected on a filter.

4.1 The Original Design of a Precision Dielectric Separator

With the favorable calculations of separation by the cylindrical geometry for the system of UO_2 and SiO_2, design of a practical dielectric separator was begun. This design required the location of a stream of particles 150 μm from a 100 μm wire. This stream had to be located initially at 150 μm to ± 5 μm. We believed that this sort of precision and accuracy is possible by taking advantage of streamlines in a laminar gas flow. Figure 4-2 shows the geometry of such a system.

The basic theory behind it is that the particles of interest are inserted in a large diameter tube, A, at a distance B between the center line of the tube and the center line of a capillary insertion device whose diameter is C. When the particle enters the gas flow, it introduces a radial disturbance to the parabolic flow pattern in the large tube. For the purposes of the following analysis it is assumed that these particles then travel along the large tube until the distance L is reached. At this point, any disturbances to the parabolic flow pattern introduced by the capillary tube is damped out, and we again have steady laminar flow, with the particles having motion only along the stream lines. This distance, L, is probably on the order of ten tube diameters or 10A.

At this point the gas flow enters a converging nozzle where the flow is focused into the dielectric sorter. The dielectric sorter length, ℓ, is sufficient for particle separation at the chosen flow rate. After deflection, the resulting particle spread is magnified by a diverging nozzle resulting in radial separation Y.

The first design criterion is that laminar flow is always maintained at critical points in the system.[1] In the area of

---

1. Kreith, Principles of Heat Transfer, International Textbook Company, Scranton, 1965.

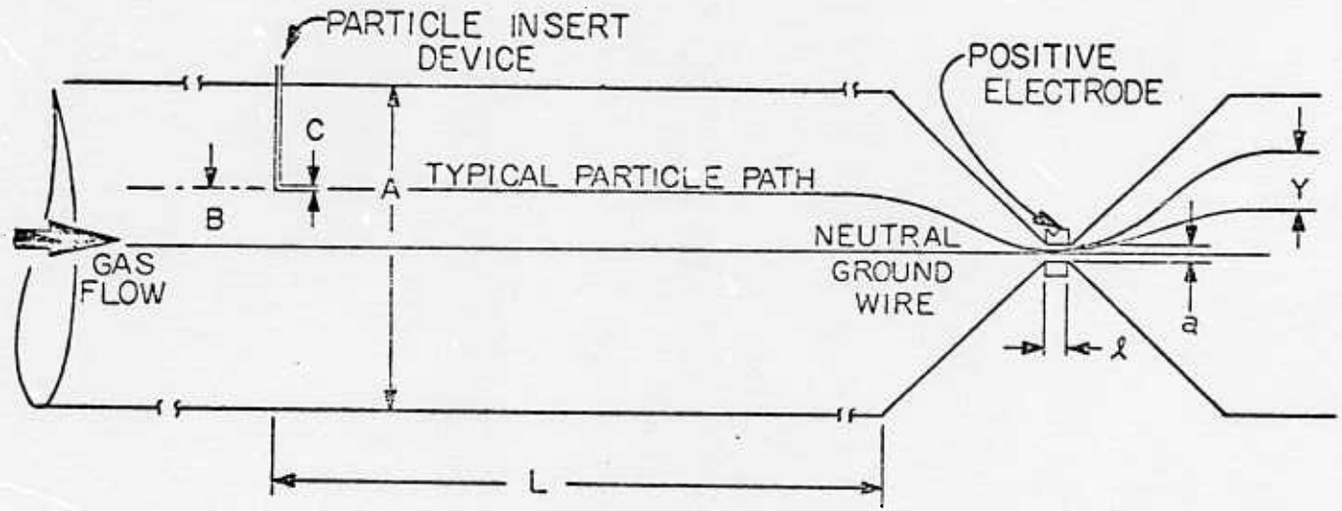

TYPICAL PARTICLE SEPARATION DUE TO DIELECTROPHORESIS

FIGURE 4-2

DIELECTRIC SORTING SYSTEM

the electrodes, the geometry is at a minimum. At this point, we must have laminar flow, therefore the Reynolds Number, Re, cannot be over 2000.

$$Re = 2000 = \frac{va}{\nu} \qquad (4\text{-}1)$$

where

v = mean fluid velocity at this point

a = local diameter

ν = kinematic viscosity

For this system, it is assumed at present that the carrier gas is helium, therefore

$$\nu = 3 \times 10^{-2} \text{ cm/sec}$$

By choosing an appropriate value for "a", this yields the mean fluid velocity at the constriction and having our dielectric deflection calculations of the electrode, ℓ. It also defines the gas flow rate for the system.

In this envisioned geometry, the particles are initially located 150 μm from the central wire, to a precision of ± 5 μm. Considering that the particles will spread radially on the order of ± 2C when initially inserted in the large tube of diameter, A, this sets up a geometrical criterion between C and B, the distance between the center lines of the capillary and the large tube. From this it can be shown that B = 60C.

We also have a criterion between B and A which is

$$A = \frac{a}{150} B \qquad (4\text{-}2)$$

where a is in microns.

In order to get a feel for some real numbers, let a = 500 μm and C = 200 μm. These are realistic numbers considering that capillaries are routinely made with I.D.'s of that size, and that is fairly simple to machine a 500 μm hole in a thin piece of aluminum.

Using these values, the velocity of the gas at the electrode will be 3.7×10^4 cm/sec.

If one uses helium as the carrier gas, this velocity is about a factor of 2.5 lower than the velocity of sound in helium. Therefore, the system is not subject to a normal shock at the constriction. This velocity defines the flow rate, which will be 74 cm^3/sec.

Next using the values of C = 200 cm, B = 1.22 cm and A = 4.0 cm, they define a mean fluid velocity at this point of 5.7 cm/sec.

The Reynolds number in the large tube will be 25.

This analysis proposed to show the definite viability of a dielectric sorter using a gas flow to locate the particles. There are, however, design problems that must be looked into and experiments that would have had to be done in order to develop the optimal design parameters.

With the sample numbers used in this analysis, the maximum allowable fluid velocity at the electrode comes out to be 3.7×10^4 cm/sec. This high velocity is undesirable for several reasons. One is that compressible effects have to be taken into account at such high velocities; two, since the sorting deflection takes place on the order of millisecond this implies an electrode length of about one foot. This is impractical with respect to the hole size that would

have to be drilled into the piece of metal. One could lower the flow rate and thus the velocity at the constriction, let us say a factor of ten or twenty, ie.

$$v = 1830 \text{ cm/sec.}$$

This would give a reasonable velocity at the electrode and a reasonable pressure at the electrode (assuming one starts with approximately 100 torr in the large tube), but the flow rate would now be only 3.7 cm^3/sec. The Reynolds number in the larger tube would only be 1.25. At this low Reynolds number an experiment would have to be done to see if there is still a parabolic velocity distribution in the large pipe. At these low velocities, temperature control might be a problem. An analysis would have to be done on the convector heating effects along the tube length.

The exact end effects of the capillary in the flow field would have to be empirically ascertained. A study would have to go into the optimum way of inserting the particles.

Various physical properties of the system would have to be experimentally measured and dealt with, i.e. the vibration mode of the central wire or the acoustic resonances of the large tube.

This flow and particle placement problem is a complex one, but it would be soluble if the dielectric sorter did not require such low total pressures. The experimental mock-up as outlined could have been readily adapted for prototype use. For example, in a prototype sorter, many more than one capillary could be introduced radially in the gas flow. Perhaps a continuous, concentric tube device could be used instead of capillaries. Thus, significantly decreasing the time to sort all of the particles in question.

The most difficult construction problem would have been the exact alignment of an approximately 12 cm long, 100 μm in diameter wire inside a 2 to 5 cm and 500 μm in diameter tube. Since the alignment accuracy must have been to ± 3 μm while having very high tension. Very high tension is required to reduce sensitivity to vibration and other deformations.

4.2 Proposed Design of a System to Determine Minimum Operating Pressure for Particle Control

In an effort to ascertain an optimum design parameters for the fluid sorting system, the equations of Section 4.1 that relate the various parameters in Figure 4-2 are plotted. Figure 4-3 was generated by relating the size of the constriction to the other parameters such as the large tube diameter, A, consisting of a family of curves depending on the insertion tube diameter, C; the total flow rate, Q, through the system; the fluid velocity at the constriction, v, and the constriction length, l.

An experiment was proposed by the use of these graphs as a reference. A constriction size diameter of 500 μm was chosen. This dictated the fluid velocity at the constriction to be 1707 cm/sec., the constriction length to be 1.8 cm and the flow rate to be 216 cc/min. These seemed all to be reasonable dimensions to work with. Since the asher was tentatively designed to have a diameter of 7.6 cm, this was chosen for the fluid control experiment also, dictating an insertion tube inner diameter of 381 μm. This also constricts the position, B, of this tube to be 2.3 cm from the centerline of the large tube A.

The next question to have been addressed, was what was the local velocity of the carrier fluid at point B. Using a parabolic fluid distribution, this was found to be 0.01 cm/sec. Ideally one would want to match this to the insertion velocity of the particles.

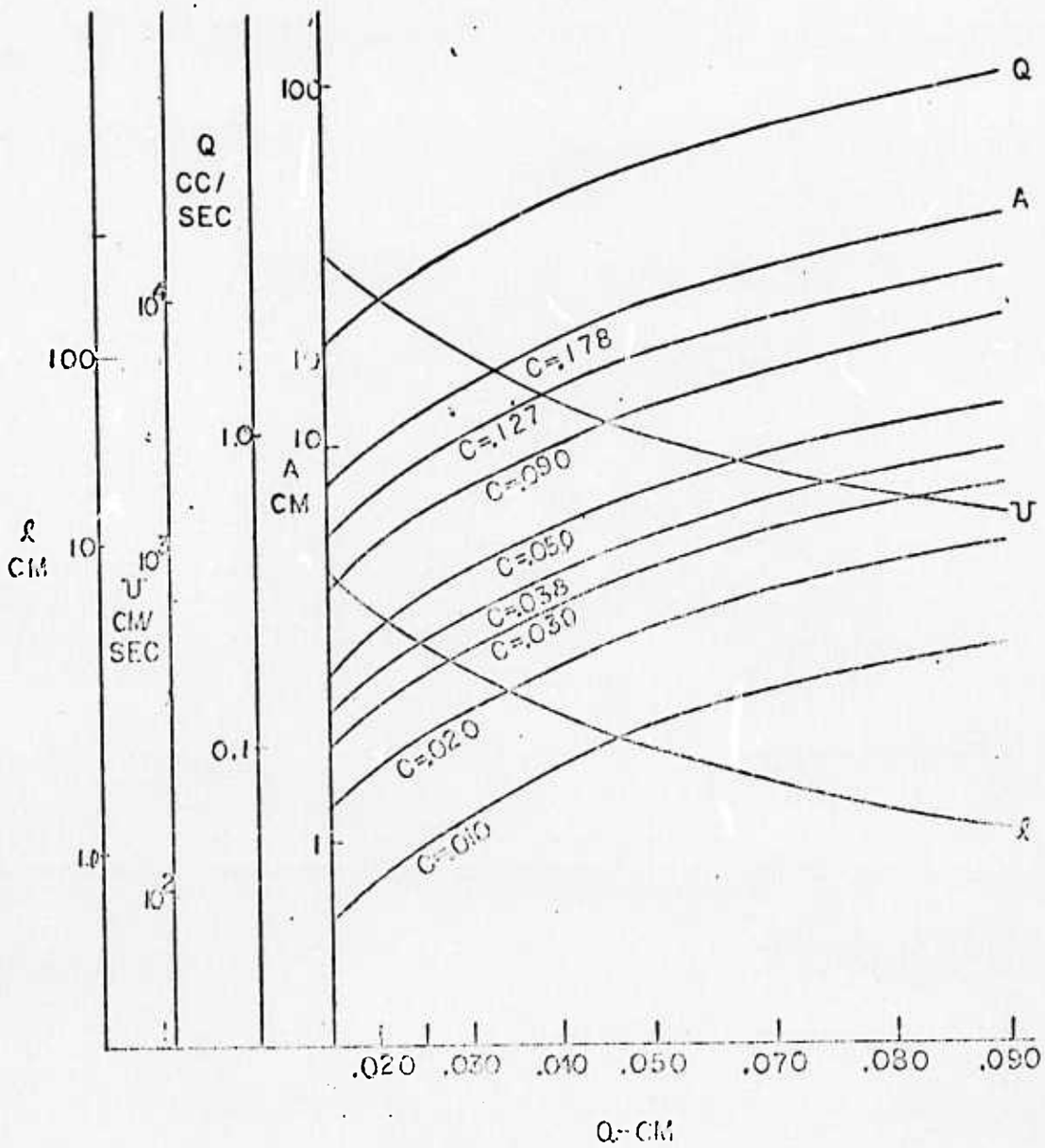

ℓ = ELECTRODE LENGTH-CM
U = FLUID VELOCITY AT ELECTRODE CM/SEC
Q = FLUID FLOW RATE CC/SEC
A = LARGE TUBE DIA-CM
Q = ELECTRODE DIA-CM
C = INSERTION TUBE DIA-CM

FIGURE 4-3

PLOTTING OF FLUDIC PARAMETER

Next, a calculation was done to determine the terminal velocities of uranium oxide particles and silicon dioxide particles, varying from 5 to 0.1 μm, if the forces acting upon them were just gravity and a fluidic drag. It was found that the terminal velocities varied from 6.4 cm/sec to 0.058 cm/sec, where ideally one is looking for insertion velocities in the neighborhood of 0.01 cm/sec nominal. This means that first of all any experiment will have to be positioned vertically, so that the insertion velocities will be minimized. It also means that one will not be able to match particle insertion velocities to bulk fluid velocities. Hopefully, all this will mean is that the particles could separate, but along one streamline. If mounted vertically, this should be an unimportant effect.

Another calculation was performed in order to estimate the perturbation effect of the capillary insertion tube. It was found that the percent perturbation to the flow field[1] is a function of $(\ell_o/L)^2$ where ℓ_o is the length of the insertion tube and L is a length measured from the tube, downstream. For example, if one wants a one percent, or less perturbation from the capillary and the capillary is, let us say 10 cm long which yields a length, L. of 100 cm. This was to be used as a design criterion for the length of the larger tube of diameter, A, before the funneling begins, and thus the focussing of the fluid streamlines.

---

1. "Theoretical Hydrodynamics", by Miline-Thomson, MacMillan, 1961.

4.3 The Effects of Brownian Motion on Particle Positioning

When the particle diameter, d, is much greater than the mean free path of the gas, λ,

$$\bar{X} = (2kTt/3\pi d\eta)^{\frac{1}{2}} \qquad (4\text{-}3)$$

where

$\bar{X}$ is the mean displacement perpendicular to the direction of flow of a particle in a beam during a time t,

k is the Boltzman constant,

T is absolute temperature, and

η is the viscosity of the gas.

Then the beam diameter, D, after a time t is given by

$$D = D_o + 2\bar{X} \qquad (4\text{-}4)$$

For He at 100 torr, however, the mean free path is 1.3 μm. Since this is not small compared to the particle sizes (5 μm to 0.1 μm), the empirical formula due Millikan[1] can be used to get the effective value of η by dividing by the factor

$$1 + (2\lambda/d)(A + B \exp[-Cd/2\lambda]) \qquad (4\text{-}5)$$

where

$$A = 1.23$$
$$B = 0.41 \qquad (4\text{-}6)$$
$$C = 0.88$$

For a particle beam moving at 5.73 cm/sec[2] down a tube of length 38 cm, the travel time is 6.63 sec. The number was obtained from our preliminary design in the previous sections

---

1. Millikan, Phys. Rev. 22, 1 (1923)

2. This value should be taken as an upper limit to the velocity. It has been determined that slower rates would be more desirable from a fluidic point of view; a slower rate would give an even greater beam spread.

and represents the type of condition that would be present in an automatic fluidic sorter. To determine λ, the mean free path, the following relationship is used.

$$\lambda = kT/(2^{\frac{1}{2}}\pi\varepsilon^2 P) \qquad (4\text{-}7)$$

where ε is the molecular (atomic diameter) and P is the pressure. For helium, $\varepsilon = 2.20$ Å. For an initial beam diameter of 1.0 mm, the calculated beam diameter at the end of tube is shown in Table 4-1 for different particle sizes and at various pressures. Since the particle distribution is not uniform and probably has a Gaussian distribution, the diameter represents that cross-section where 95% of the original particles will pass through. These results show that, at pressures greater than 10 torr, there is relatively good particle control. However, when the beam divergence is greater than 50% (i.e. 1 mm to 1.50 mm), there is insufficient particle control for proper operation of dielectric sorting and one-at-a-time sorting.

TABLE 4-1

THEORETICAL SPREAD IN A PARTICLE BEAM DIAMETER

		Particle Diameter (mm)				
P	λ (μm)	10 μm	5 μm	1 μm	0.5 μm	0.1 μm
4 atm	0.047	1.01	1.02	1.04	1.06	1.17
1 atm	0.19	1.01	1.02	1.04	1.07	1.29
100 torr	1.44	1.01	1.02	1.08	1.16	1.77
10 torr	14.4	1.03	1.05	1.25	1.49	3.44
1 torr	144	1.09	1.15	1.77	2.54	8.72
0.1 torr	1440	1.30	1.49	3.44	5.88	25.42

4.4 Conclusions

In section 2.3, a pressure of 0.1 torr was determined to be the highest pressure tolerable for good dielectric separation. However, in this section, it was theoretically determined that there is insufficient particle control for particles 1 μm or less. Consequently, for particles 1 μm or less, dielectric separation is not possible. In addition, during ashing of the substrate to make the particles gas borne, high gas pressures and velocities are required to prevent the particles from sticking to the sample holder. Although the exact pressures and velocities were not determined by experiment, they will be at least two orders of magnitude greater than the maximums calculated for dielectric separation. The theoretical irreconcilable differences in our automatic particle sorter design, which is the only possible design using the techniques considered, are summarized:

(1) High pressure and high flow rate are required to get the particles into a gas borne state. Preliminary experimental investigation showed that this transfer from substrate to gas flow is not likely to be with low loss.

(2) High pressure and low flow rate are required to position the particles to ± 5 μm in the dielectric sorter and one-at-a-time modules.

(3) Low pressure is required to overcome particle size dependence and produce a sufficient dielectric constant to density ratio spectrum for a bulk separation.

APPENDIX A

BASIC DIELECTROPHORETIC SEPARATION. THEORETICAL DEVELOPMENT

A.0 Introduction

It is well known that an uncharged, dielectric particle placed in a nonuniform electric field experiences a net force tending to move the particle towards regions of higher field intensity. In this appendix, this effect is analyzed for its application to the separation of particles in the 0.1 to 5 μm range.

The dielectric force on a particle is evaluated as a function of its dielectric constant, density, etc. and the applied electric field, for two representative electrode configurations, and the results for the two cases are compared. Later it is shown that, in some sense, these configurations are optimally effective in producing dielectrophoresis.

Next, the effect of the presence of a fluid medium on the actual movement of particles is analyzed. The viscous forces on particles of various size are evaluated, due account being taken of their extremely small diameter. The actual movement of a particle is then derived and described in terms of a normalized equation of motion.

Finally, a number of criteria are derived which are effective in determining the efficiency of dielectric separation. These criteria are of use in the actual design of a particle separation stage.

3.1 Dielectric Acceleration of Particles

The surface density of charge induced on a dielectric particle (of dielectric constant K) placed in an electric field of magnitude E (refer to Figure A-1 for the geometry) is

$$\sigma_i = \varepsilon_0(K - 1)E, \qquad \text{(A-1)}$$

where ε_0 is the permeability of free space. This result follows from Gauss' Law, relating the electric displacement to induced surface charge.

Assuming a rod like shape, A is the cross-sectional area of the particle. The total charge on one face of the particle is

$$q = A\varepsilon_0(K - 1)E. \qquad \text{(A-2)}$$

With a particle length ℓ, the moment of the induced dipole is then

$$q\ell = A\varepsilon_0\ell(K - 1)E = \varepsilon_0 V(K - 1), \qquad \text{(A-3)}$$

where $V = A\ell$ is the particle volume.

Although this derivation assumes a cylindrical particle, the dipole moment and other quantities to be derived are independent of the actual particle shape and its spatial orientation. A more general analysis, using the relation that the induced surface charge is proportional to the normal component of field and then taking a surface charge integral, proves this independence.

The following analysis thus applies to particles of arbitrary size, shape and orientation. We will see that the acceleration of a particle is independent of these parameters.

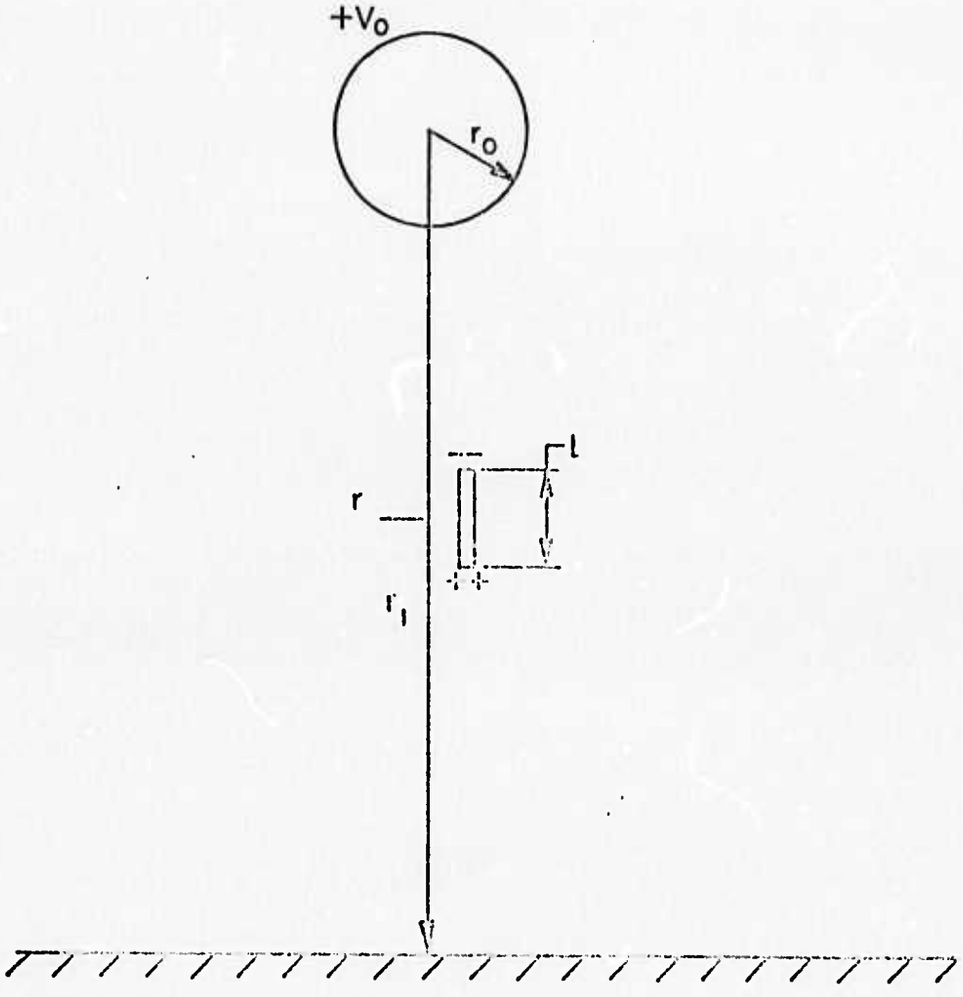

FIGURE A-1

PLANAR ELECTRODE CONFIGURATION AND DIMENSIONS FOR PARTICLE ACCELERATION

Let the radial dependence of the electric field be expressed as E(r) along the normal to the plane electrode of Figure A-1. For a particle at radius r, the forces on each face due to the induced charges are as follows:

Force on the negatively charged face is

$$F_- = -\sigma_i A E(r). \qquad \text{(A-4)}$$

Force on the positively charged face is

$$F_+ = \sigma_i A E(r + \ell). \qquad \text{(A-5)}$$

The net force on the particle is therefore

$$F = F_- + F_+ = \sigma_i A\{E(r + \ell) - E(r)\}. \qquad \text{(A-6)}$$

In a uniform field, i.e., $\Delta E = 0$, $F = 0$. Thus there is a net force only in nonuniform fields, i.e. $\Delta E \neq 0$. Now, $E(r + \ell)$ may be expressed as a function of $E(r)$ by means of a Taylor's series expansion about r:

$$E(r + \ell) = E(r) + \ell \partial E/\partial r + \frac{\ell^2}{2} \frac{\partial^2 E}{\partial r^2} + \cdots . \qquad \text{(A-7)}$$

It is assumed that the second and higher derivatives of E can be neglected with respect to $\partial E/\partial r$. Or, more specifically, it is assumed that

$$\frac{\partial^2 E}{\partial r^2} << \frac{2}{\ell} \frac{\partial E}{\partial r}. \qquad \text{(A-8)}$$

This assumption is justified since the particle sizes are small.

$$\therefore E(r + \ell) = E(r) + \ell \partial E/\partial r. \qquad \text{(A-9)}$$

The net force on the particle is

$$F = \sigma_i A \ell \frac{\partial E}{\partial r} = \varepsilon_o (K - 1) VE \frac{\partial E}{\partial r} , \qquad \text{(A-10)}$$

by substituting Equation (1) into (6).

In free space, the acceleration of such a particle (density ρ) is given by

$$\alpha_{field} = \frac{F}{m} = \frac{1}{\rho V} \varepsilon_o (K - 1) VE \frac{\partial E}{\partial r}$$

$$= \frac{\varepsilon_o}{\rho} (K - 1) E \frac{\partial E}{\partial r} . \qquad \text{(A-11)}$$

A.2 Determination of $E\frac{\partial E}{\partial r}$ for a Planar Geometry

To determine the field E between the charged wire and the plate electrode of Figure A-1, the method of image charges is used. We assume the presence of an image line charge of opposite sign an equal distance below the plate. The surface of the plate is then equipotential, and the two configurations give rise to identical fields. It is therefore sufficient to derive the field expression for a pair of wires of radius r_o separated by a distance $2r_1$.

By Gauss' Theorem, the field intensity $E_+(r)$ produced by the upper wire is related to the charge on it by

$$Q = +\int \varepsilon_0 E_+ da = + \varepsilon_0 E_+(r)\ 2\pi r \qquad \text{(A-12)}$$

or,

$$E_+(r) = \frac{Q}{2\pi\varepsilon_0 r} \quad . \qquad \text{(A-13)}$$

Similarly, the field component due to the lower wire, $E_-(r)$, can be shown to be

$$E_-(r) = \frac{Q}{2\pi\varepsilon_0 (2r_1 - r)} \quad . \qquad \text{(A-14)}$$

Using the superposition principle, the total field is then

$$\begin{aligned} E(r) &= E_+(r) + E_-(r) \\ &= \frac{Q}{2\pi\varepsilon_0} \left\{ \frac{1}{r} + \frac{1}{2r_1 - r} \right\} \quad . \qquad \text{(A-15)} \\ &= \frac{Q}{\pi\varepsilon_0} \ \frac{r_1}{r(2r_1 - r)} \quad . \end{aligned}$$

Equation 15 can now be solved in terms of the total voltage between the upper wire and the ground plane. Let this voltage be V_0. Then

$$V_0 = -\int_{r_0}^{r_1} E(r)\,dr = \frac{Q}{\pi\varepsilon_0} \int_{r_0}^{r_1} \frac{r_1\ dr}{(r^2 - 2r_1 r)} \quad . \qquad \text{(A-16)}$$

The integrand of Equation 16 can be evaluated to obtain

$$\int_{r_o}^{r_1} \frac{dr}{r^2 - 2r_1 r} = \left[-\frac{1}{2r_1} \ln \frac{2r_1 - r}{r} \right]_{r_0}^{r_1}$$

$$= \frac{1}{2r_1} \ln\left(\frac{2r_1 - r_0}{r_0}\right) . \qquad \text{(A-17)}$$

Therefore,

$$V_0 = \frac{Q}{2\pi\varepsilon_0} \ln\left(\frac{2r_1 - r_0}{r_0}\right) . \qquad \text{(A-18)}$$

This equation relates the charge per unit length on the wire conductor to its voltage. Thus the capacitance per unit length of this geometry is

$$C = \frac{Q}{V_0} = 2\ \varepsilon_0 / \ln \frac{(2r_1 - r_0)}{r_0} . \qquad \text{(A-19)}$$

Let $\ln (2r_1 - r_0)/r_0$ be defined as P, a dimensionless constant. Then, from equation 18,

$$V_0 = \frac{QP}{2\pi\varepsilon_0} \qquad \text{(A-20)}$$

or

$$Q = \frac{2\pi\varepsilon_0 V_0}{P} . \qquad \text{(A-21)}$$

We substitute (21) into equation (15) to obtain

$$E(r) = \frac{2V_0}{P} \frac{r_1}{(2r_1 - r)r} . \qquad \text{(A-22)}$$

From the above equation it is possible to obtain $\partial E/\partial r$ as

$$\frac{\partial E(r)}{\partial r} = \frac{\partial}{\partial r}\left\{\frac{2V_0 r_1}{P}\,(2r_1 r - r^2)^{-1}\right\}$$

$$= -\frac{2V_0 r_1}{P}\,(2r_1 r - r^2)^{-2}(2r_1 - 2r)$$

$$= \frac{4V_0 r_1}{P}\,\frac{(r - r_1)}{(2r_1 r - r^2)^2}\quad , \tag{A-23}$$

and

$$\frac{\partial^2 E(r)}{\partial r^2} = \frac{4V_0 r_1}{P}\,\frac{1}{(2r_1 r - r^2)^2} - \frac{16V_0 r_1}{P}\,\frac{(r_1 - r^2)}{(2r_1 r - r^2)^3}\ . \tag{A-24}$$

$$\therefore\ E(r)\frac{\partial E(r)}{\partial r} = \frac{8V_0^2 r_1^2}{P^2}\,\frac{(r - r_1)}{(2r_1 r - r^2)^3}\ . \tag{A-25}$$

Thus, from Equation (11), the net acceleration of the particle in free space will be

$$a_{field} = -\frac{8\varepsilon_0}{\rho}(K - 1)\,\frac{V_0^2 r_1^2}{P^2}\,\frac{(r_1 - r)}{(2r_1 r - r^2)^3}\ . \tag{A-26}$$

A.3 Determination of $E\,\frac{\partial E}{\partial r}$ for a Cylindrical Geometry

The dielectrophoretic effect is calculated here for the alternative cylindrical geometry shown in Figure A-2. Only a portion of the outer, completely cylindrical conductor is shown in this figure.

The net force on the particle is again given by equation (10).

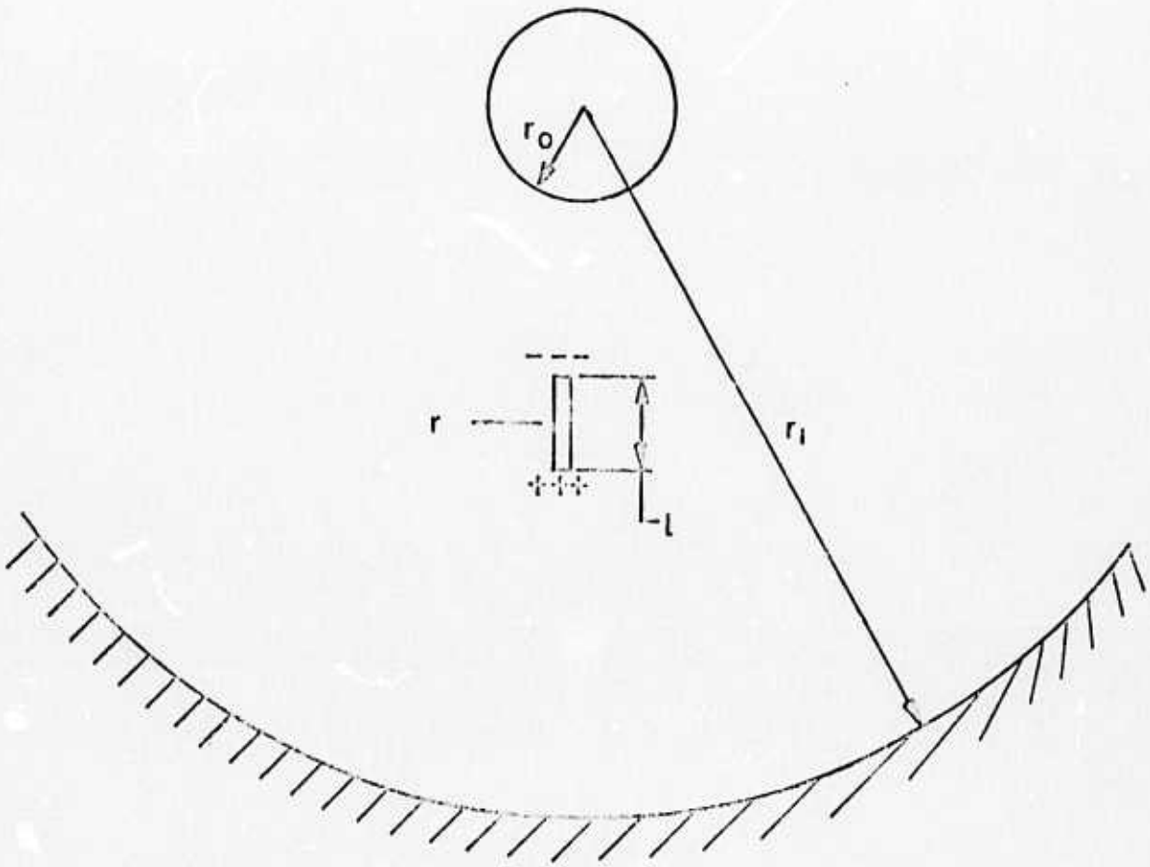

FIGURE A-2

CYLINDRICAL ELECTRODE CONFIGURATION AND DIMENSIONS FOR PARTICLE ACCELERATION

The $E \frac{\partial E}{\partial r}$ term must be determined for cylindrical geometry by Gauss' Theorem as shown by equations (12) and (13). In this case, there is only a single field component.

$$E(r) = E_+(r) = \frac{Q}{2\pi\varepsilon_0 r} . \qquad \text{(A-27)}$$

Equation 27 is solved to obtain the total voltage between the outer and inner conductors. Integrating Equation 27,

$$V_0 = -\int_{r_1}^{r_0} E(r)\, dr = \frac{Q}{2\pi\varepsilon_0}\left[\ln r\right]_{r_o}^{r_1} = \frac{Q}{2\pi\varepsilon_0} \ln(r_1/r_0). \qquad \text{(A-28)}$$

Thus, in this case, the capacitance C per unit length is

$$C = \frac{Q}{V_0} = \frac{2\pi\varepsilon_0}{\ln(r_1/r_0)} . \qquad \text{(A-29)}$$

Let $\ln(r_1/r_0)$ be defined as P', a dimensionless constant. Then, from this equation,

$$V_0 = \frac{QP'}{2\pi\varepsilon_0} \qquad \text{(A-30)}$$

or

$$Q = \frac{2\pi\varepsilon_0}{P'} V_0 . \qquad \text{(A-31)}$$

We substitute Equation (31) into Equation (27) to obtain

$$E(r) = \frac{V_0}{P'} \frac{1}{r} . \qquad \text{(A-32)}$$

By differentiating Equation (32)

$$\frac{\partial E}{\partial r} = - \frac{V_0}{P'} \frac{1}{r^2} , \qquad \text{(A-33)}$$

$$\frac{\partial^2 E}{\partial r^2} = \frac{2V_0}{P'} \frac{1}{r^3} , \qquad \text{(A-34)}$$

and thus

$$E \frac{\partial E}{\partial r} = - \frac{V_0^2}{P'^2} \frac{1}{r^3} . \qquad \text{(A-35)}$$

From Equation 11, the net acceleration of the particle in free space becomes

$$\alpha'_{field} = - \frac{\varepsilon_0 (K - 1)}{\rho} \frac{V_0^2}{P'^2} \frac{1}{r^3} . \qquad \text{(A-36)}$$

A.4 Comparison of the Cylindrical and Planar Geometries

On the basis of the previous derivation, the two geometries can be compared to determine their relative efficiencies in producing dielectrophoretic acceleration. The two key equations to be compared are

$$\alpha_{field} = - \frac{8\varepsilon_0}{\rho} (K - 1) \frac{V_0^2 r_1^2}{P^2} \frac{(r_1 - r)}{(2r_1 r - r^2)^3} \qquad \text{(A-26)}$$

and

$$\alpha'_{field} = - \frac{\varepsilon_0}{\rho} (K - 1) \frac{V_0^2}{P'^2} \frac{1}{r^3} . \qquad \text{(A-36)}$$

Let x be a normalized position parameter, such that

$$x = r/r_1 \ , \qquad \text{(A-37)}$$

where

$$r_0/r_1 \leq x \leq 1 \ . \qquad \text{(A-38)}$$

Then Equation (26) and Equation (36) are normalized as follows:

$$\alpha_{field} = - \frac{\varepsilon_0 (K - 1)}{\rho r_1^{\,3}} V_0^{\,2} \frac{(1 - x)}{P^2 (x - \tfrac{1}{2}x^2)^3} \ , \qquad \text{(A-39)}$$

and

$$\alpha'_{field} = - \frac{\varepsilon_0 (K - 1) V_0^{\,2}}{\rho r_1^{\,3}} \frac{1}{P'^2 x^3} \ . \qquad \text{(A-40)}$$

The field accelerations induced by the two electrode configurations are identical functions of the applied voltage, linear dimensions of the geometry, etc. It is sufficient to compare the terms P and P', and the factors involving x, in order to compare α with α'.

If the two geometries can be considered identical when (r_1/r_0) is the same in both cases, then we can compare P with P'.

$$P = \ln \frac{(2r_1 - r_0)}{r_0} = \ln \{(2r_1/r_0) - 1\} \qquad \text{(A-41)}$$

and

$$P' = \ln(r_1/r_0) \qquad \text{(A-42)}$$

By definition r_1/r_0 is always > 1,

$$\therefore\ 2(r_1/r_0) - 1 > (r_1/r_0), \qquad \text{(A-43)}$$

and, since ln(x) is a positive monotonic function of x, it follows that

$$P > P' \text{ also.} \qquad \text{(A-44)}$$

On the basis of comparison of P and P' alone, the accelerations produced by the cylindrical geometry will be <u>larger</u> than the accelerations produced by the planar configuration of electrodes.

The other basis on which these accelerations may be compared is the ratio of the functions involving x in the equations 39 and 40. This is a numerical comparison, and is carried out in the next section. For the present purposes it is sufficient to state that the factors involving x differ only slightly from one another, and thus on this basis the two geometries are almost identical.

A.4.1 Comparison of the Cylindrical and Planar Geometrics Based on the Factors $F_1(x)$ and $F_2(x)$

It was determined in Section A.4 that the cylindrical and planar electrode configurations can be compared on the basis of the functions

$$F_1(x) = \frac{(1 - x)}{(x - \frac{1}{2}x^3)}$$

and

$$F_2(x) = \frac{1}{x^3}$$

Then a measure of the relative efficiency of the cylindrical geometry over the planar is the ratio $F_2(x)/F_1(x)$.

The factors $F_1(x)$, $F_2(x)$ and their ratios were computed for the entire range (0 to 1) of x in increments of 0.01. The following table (Table 1) lists values of $F_1(x)$, $F_2(x)$, and their ratio for various values of x, the normalized position parameter.

It can be concluded from Table A-1 that there is no significant advantage to be obtained from selecting one of these geometries over the other.

The computer program used to generate $F_1(x)$, $F_2(x)$, and their ratio is shown in Figure A-3.

POSITION X	F1(X)	F2(X)	F1(X)/F2(X)
1.00	0.00000000	1.00000000	0.00000000
0.99	0.03002394	1.00361000	0.02776715
0.98	0.16019200	1.00840000	0.15877130
0.97	0.24064900	1.00568000	0.21963000
0.96	0.32154070	1.13020000	0.28447870
0.95	0.40301460	1.16635000	0.34553470
0.94	0.48522110	1.20397000	0.40301000
0.93	0.56831200	1.24322000	0.45712648
0.92	0.65244630	1.28421100	0.50805000
0.91	0.73778272	1.32701500	0.55597160
0.90	0.82445730	1.37174100	0.60105162
0.89	0.91270360	1.41850200	0.64344700
0.88	1.00269500	1.46741100	0.68330000
0.87	1.09456100	1.51859600	0.72077162
0.86	1.18850300	1.57218700	0.75596700
0.85	1.28478500	1.62833300	0.78901200
0.84	1.38359700	1.68718100	0.82004170
0.83	1.48509300	1.74890200	0.84914310
0.82	1.58955100	1.81366900	0.87648000
0.81	1.69725500	1.88167500	0.90199100
0.80	1.80844700	1.95310400	0.92592000
0.79	1.92343300	2.02820500	0.94831570
0.78	2.04243800	2.10724900	0.96928200
0.77	2.16585700	2.19048000	0.98873600
0.76	2.29400700	2.27808700	1.00701100
0.75	2.42725000	2.37036800	1.02399900
0.74	2.56599600	2.46776900	1.03980400
0.73	2.71064700	2.57057900	1.05440600
0.72	2.86167300	2.67915100	1.06811500
0.71	3.01955700	2.79398700	1.08073400
0.70	3.18433100	2.91544800	1.09239000
0.69	3.35907100	3.04405300	1.10313900
0.68	3.53959800	3.18033300	1.11309900
0.67	3.72698900	3.32487200	1.12214800
0.66	3.92207600	3.47808400	1.13046500
0.65	4.12596400	3.64132200	1.13803900
0.64	4.34075200	3.81469200	1.14491100
0.63	4.56737500	3.99884600	1.15114500
0.62	4.80556000	4.19489000	1.15674100
0.61	5.11823100	4.40564700	1.16174300
0.60	5.39897400	4.62962100	1.16618100
0.59	5.69717400	4.86903800	1.17008300
0.58	6.01435900	5.12525100	1.17347600
0.57	6.35221000	5.39976000	1.17638800
0.56	6.71058900	5.69403900	1.17884100
0.55	7.09756600	6.01050500	1.18086100
0.54	7.50942800	6.35064000	1.18246700
0.53	7.95073200	6.71693700	1.18368400
0.52	8.42432200	7.11195000	1.18453800
0.51	8.93337400	7.53855900	1.18502400

POSITION X	F1(X)	F2(X)	F1(X)/F2(X)
0.50	9.48145400	7.99997700	1.18519900
0.49	10.07256000	8.49983400	1.18509000
0.48	10.71118000	9.04221700	1.18469500
0.47	11.40241000	9.63174600	1.18399000
0.46	12.15197000	10.27366000	1.18295200
0.45	12.96037000	10.97300000	1.18156500
0.44	13.83000000	11.73000000	1.17980000
0.43	14.80037000	12.57746000	1.17763200
0.42	15.87805000	13.49741000	1.17507700
0.41	17.03717000	14.50031000	1.17212400
0.40	18.31047000	15.60430000	1.16875500
0.39	19.71270000	16.81750000	1.16496000
0.38	21.26100000	18.14415000	1.16073900
0.37	22.97527000	19.74267000	1.16077202
0.36	24.87875000	21.40336000	1.16074500
0.35	26.99884000	23.30349000	1.15751100
0.34	29.36775000	25.44257000	1.15407600
0.33	32.00367000	27.85031000	1.15042200
0.32	35.01213000	30.51709000	1.14703500
0.31	38.38763000	33.56697000	1.14341000
0.30	42.21576000	37.03672000	1.13953000
0.29	46.57608000	41.00186000	1.13539000
0.28	51.56558000	45.55566000	1.13197600
0.27	57.30036000	50.80487000	1.12791100
0.26	63.93674000	56.49531000	1.13076100
0.25	71.64955000	63.20945000	1.11334400
0.24	80.67899000	72.33731000	1.11550000
0.23	91.30054000	82.18674000	1.11056100
0.22	103.98870000	93.91309000	1.10643000
0.21	118.99590000	107.97850000	1.10194000
0.20	137.17270000	124.99000000	1.09739400
0.19	159.30110000	145.79010000	1.09279600
0.18	186.58060000	171.46550000	1.08815200
0.17	220.52700000	203.53000000	1.08346600
0.16	263.35990000	244.13700000	1.07873500
0.15	318.20250000	296.89150000	1.07397500
0.14	389.63500000	364.40550000	1.06917300
0.13	484.44600000	455.15750000	1.06433000
0.12	613.12160000	578.69160000	1.05945600
0.11	792.33130000	751.29740000	1.05461822
0.10	1049.69000000	999.97440000	1.04971702
0.09	1433.14900000	1371.72000000	1.04479600
0.08	2030.90600000	1953.06100000	1.03985200
0.07	3017.10400000	2915.34100000	1.03492000
0.06	4768.03900000	4629.42000000	1.03004200
0.05	8199.29760000	7999.87400000	1.02496000
0.04	15926.18000000	15603.95000000	1.01998200
0.03	37588.98000000	37033.78000000	1.01499400
0.02	126130.80000000	124083.20000000	1.00998800
0.01	1004729.60000000	999730.20000000	1.00500000

TABLE A-1. A comparison of the Functions $F_1(x)$ and $F_2(x)$.

Comparison of the Cylindrical and Planar Geometrics Based on the Functions $F_1(x)$ and $F_2(x)$

TYPE A

```
C       THIS PROGRAM CALCULATES THE FUNCTIONS
C       F1(X) AND F2(X) AND COMPARES THEIR
C       VALUES AS A FUNCTION OF THE NORMALISED
C       LOCATION PARAMETER X (SEE EQNS 39 AND 48)
C
C
C
C
C
C
        X=1.00
        DO 20 I=1,100
        ALPHA1=(1.0-X)/(X-0.5*X**2)**3
        ALPHA2=1.0/X**3
        Y=ALPHA1/ALPHA2
        WRITE(10,10)X,ALPHA1,ALPHA2,Y
10      FORMAT(5X,F4.2,4X,F15.8,4X,F15.8,4X,F15.8)
20      X=X-0.01
        STOP
        END
```

Figure A-3

A.5 Effects of the Carrier Gas

So far the viscosity of a carrier stream gas, which is necessary to move the particles, has not been considered. The behaviour of particles under dielectrophoretic forces is considered in this section in the situation where the particle motion occurs in a gaseous medium. The medium will be considered to be at rest (i.e., to have no radial velocity, although a transverse stream flow velocity does exist), and the particle is moving through this viscous medium.

The effect of viscosity on the motion of very small particles is described by Stoke's Law (shown later). The viscous force exerted on a particle moving with a velocity v is directly proportional to the particle's diameter. Since the mass of the particle is proportional to the cube of its diameter, the ratio of force to mass for a given velocity depends inversely on the square of the particle diameter. Thus for very small diameter particles, viscosity is capable of inducing very high drag accelerations. Consequentially, the effect of viscosity is very important in the case where small particles are being accelerated in a gaseous medium.

A.5.1 Stoke's Law

The force required for steady motion of a sphere through a viscous medium according to Stoke's Law is

$$F = 3\pi\eta dv, \qquad \text{(A-45)}$$

where d is the particle diameter and η is the viscosity

of the medium. It is assumed that the velocity v of the particle is relatively small. This statement of Stoke's Law is in its simplest form.

This formula is valid, however, only for the range of values for which the diameter of a falling sphere is much larger than the molecular mean free path of the gas medium. Since a typical value of the mean free path for air at STP is 0.06 μm, this form is accurate only for the larger particles of the 0.1 to 10μm in. diameter range.

The intermediate condition in which the particle size approaches the molecular mean free path length is not well analyzed theoretically. In this region the empirical formula of Millikan* is known to be almost as accurate as the macroscopic Stoke's Law.

Millikan's empirical law is as follows:

$$F = \frac{3\pi\eta dv}{1 + \frac{L}{d}\left\{a + be^{-cd/L}\right\}} , \qquad \text{(A-46)}$$

where L is the molecular mean free path of the viscous gas, and a, b and c are three empirically determined dimensionless constants with the following values:

$$a = 2.46,$$
$$b = 0.82,$$
$$c = 0.44. \qquad \text{(A-47)}$$

Note that Millikan's equation in the limiting case of $L/d \ll 1$ reduces to Stoke's Law for large particles. Milli-

---

* Millikan, Phys. Rev. 22 (1923), 1.

kan's equation for the drag force on a particle is used in the subsequent analysis. The advantage of using this is that the motion of the particle can be determined for various pressures (and therefore mean free path lengths) of the gas stream. The denominator of A-46 gives in effect the low pressure correction for η, which is then over the operational range of gas pressures independent of the gas pressure.*

A.5.2 Equation of Motion

Since the viscous drag force on the moving particle is

$$F_{drag} = -F, \tag{A-48}$$

the deceleration of the particle due to viscous drag is

$$\alpha_{drag} = \frac{F_{drag}}{m} = - \frac{18\eta v}{\rho d^2 + \rho dL(a + be^{-cd/L})}. \tag{A-49}$$

For a particle of diameter d subjected to a dielectrophoretic force and moving in a viscous medium, the net acceleration is then given by

$$\alpha_{net} = \alpha_{field} + \alpha_{drag}$$

$$= - \frac{\varepsilon_0 (K-1) V_0^2}{\rho P'^2 r_1^3 x^3} - \frac{18\eta \, \partial r/\partial t}{\rho d^2 + \rho dL(a + be^{-cd/L})}. \tag{A-50}$$

In this equation, the cylindrical electrode configuration has been assumed.

---

* See "Kinetic Theory of Gases," Kennard, McGraw-Hill, New York, 1938.

A.5.3 Normalized Equation of Motion

In terms of the normalized position coordinate x, and the normalized velocity $\dot{x}$ and accleration $\ddot{x}$, the previous equation can be written as

$$r_1\ddot{x} = -\frac{\varepsilon_0(K-1)V_0^2}{\rho P'^2 r_1^3 x^3} - \frac{18\eta r_1 \dot{x}}{\rho d^2 + \rho dL(a + be^{-cd/L})}, \qquad \text{(A-51)}$$

or, dividing throughout by r_1, we have the normalized equation of motion of the particle as

$$\ddot{x} = -\frac{\varepsilon_0(K-1)V_0^2}{\rho P'^2 r_1^4 x^3} - \frac{18\eta \dot{x}}{\rho d^2 + \rho dL(a + be^{-cd/L})}. \qquad \text{(A-52)}$$

This equation together with the state equations

$$v = \dot{r} = r_1\dot{x} \qquad \text{(A-53)}$$

and

$$a_{net} = \ddot{r} = r_1\ddot{x} \qquad \text{(A-54)}$$

define the motion of a dielectric particle moving under the influence of a dielectrophoretic force in a viscous medium.

A.6 Upper Limits on the Term $E\frac{\partial E}{\partial r}$ used in Computing the Dielectrophoretic Force on a Particle

So far in this analysis, only two out of a large number of possible geometrical configuration of electrodes have been considered. Although both of these geometries were shown to be equally effective in producing a nonuni-

form field it remains to be shown that more effective configurations do not exist. Accordingly at this point, it is preferable to take a more general approach and to consider an argument which sets an upper bound on the variation of the function

$$E \frac{\partial E}{\partial r} (r)$$

with r. It is possible to evaluate such an upper bound, based on fundamental electrostatic principles, that is independent of any particular electrode geometry.

To evaluate this maximum one must consider the total electric field function produced at a point r in space due to a discrete distribution of charges. In a physical situation, the distribution of these charges will be continuous; however, no loss of generality is incurred in considering a discrete charge distribution.

It is convenient to consider two possible classes of electrode configurations separately; one, in which an invariance of the electrode geometry exists along one of the dimensions. This is the case with the cylindrical and planar geometries that have been considered. The second, and more general case, is one in which the electrode configuration varies arbitrarily along all three dimensions. The elements of the first configuration are units of line charge, of the second, point charge units. We will call the first configuration the two dimensional, and consider this first.

A.6.1 Two-dimensional Geometries

If a number of line charges $q_1, q_2, \ldots, q_n$ are located

at points $r_1, r_2, \ldots, r_n$ then the net electric field at a point r in space due to these line charges is the vector sum of the field due to each such charge.

$$E(r) = \frac{1}{4\pi\varepsilon_0}\left\{\frac{q_1}{(r - r_1)} + \frac{q_2}{(r - r_2)} + \cdots + \frac{q_n}{(r - r_n)}\right\} \qquad \text{(A-55)}$$

from this,

$$\frac{\partial E}{\partial r} = -\frac{1}{4\pi\varepsilon_0}\left\{\frac{q_1}{(r - r_1)^2} + \frac{q_2}{(r - r_2)^2} + \cdots + \frac{q_n}{(r - r_n)^2}\right\} \qquad \text{(A-56)}$$

Now, both $E(r)$ and $\frac{\partial E}{\partial r}$ and therefore $E\frac{\partial E}{\partial r}$ have significant value only at the singularities

$$r = r_1, r_2, \cdots \text{or } r_n.$$

Also, at each of these points, the contribution due to all other line charges is relatively insignificant. This can be seen from the fact that both

$$\frac{q_n}{(r_1 + \varepsilon - r_n)} \Big/ \frac{q_1}{(r_1 + \varepsilon - r_1)}, \quad r_1 \neq r_n$$

and

$$\frac{q_2}{(r_1 + \varepsilon - r_n)^2} \Big/ \frac{q_1}{(r_1 + \varepsilon - r_1)^2}$$

tend to zero as $\varepsilon \to 0$.

Therefore both the field and the gradient of the field are a maximum in the vicinity of a line charge. It is thus sufficient to consider the maximum value of $E \frac{\partial E}{\partial r}$ in the vicinity of a single line charge (for convenience, at $r = 0$). The field due to this charge is expressible as

$$E(r) = \frac{q}{r} \tag{A-57}$$

$$\therefore \frac{\partial E}{\partial r} = - \frac{q}{r^2} \tag{A-58}$$

and

$$E \frac{\partial E}{\partial r} = - \frac{q^2}{r^3} \tag{A-59}$$

At this point we can compare our result with Eqn. 25 and more directly with Eqn. 35. In both, the variation of $E \frac{\partial E}{\partial r}$ is as $1/r^3$. Thus it can be asserted that, in the two dimensional situation, the two geometries considered are just as effective as any others that may be conceived for dielectrophoretic deflection.

A.5.2 Three-Dimensional Geometries

If a number of point charges $q_1, q_2 -- q_n$ are located at points $r_1, r_2 -- r_n$, then the net electric field at each point r in space due to these point charges is the vector sum of the field due to each such charge.

$$E(r) = \frac{1}{4\pi\varepsilon_0} \left\{ \frac{q_1}{(r - r_1)^2} + \frac{q_2}{(r - r_2)^2} + \ldots + \frac{q_n}{(r - r_n)^2} \right\} . \tag{A-60}$$

From this,

$$\frac{\partial E}{\partial r} = - \frac{2}{4\pi\varepsilon_0} \left\{ \frac{q_1}{(r - r_1)^3} + \frac{q_2}{(r - r_2)^3} + \ldots + \frac{q_n}{(r - r_n)^3} \right\} . \tag{A-61}$$

Again, both $E(r)$ and $\partial E/\partial r$ (and therefore $E\ \partial E/\partial r$) are significantly large only at the singular points

$$r = r_1,\ r_2, \ldots \text{or } r_n .$$

Also, since both

$$\frac{q_n}{(r_1 + \varepsilon - r_n)^2} \Bigg/ \frac{q_1}{(r_1 + \varepsilon - r_1)^2} , \qquad \begin{matrix} r_1 \neq r_n , \\ \varepsilon \to 0 , \end{matrix}$$

and

$$\frac{q_n}{(r_1 + \varepsilon - r_n)^3} \Bigg/ \frac{q_1}{(r_1 + \varepsilon - r_1)^3}$$

tend to zero, the contribution due to all other point charges is insignificant in the neighborhood of a singularity. An upper bound on E is therefore of the form

$$E(r) = \frac{q}{r^2} . \qquad \text{(A-62)}$$

$$\therefore\ \partial E/\partial r = -2q/r^3 , \qquad \text{(A-63)}$$

and,

$$E\ \partial E/\partial r = -\frac{2q^2}{r^5} . \qquad \text{(A-64)}$$

Comparing this result with Eqns. 25 and 35, it can be concluded that there is something to be gained from a transition

from two dimensional to three dimensional electrode configurations.

Although the general three dimensional geometry appears to be preferable, there are a number of practical reasons which preclude its use. Whereas in the cylindrical or planar geometries there is an obvious path along which particle must be introduced, no such symmetric flow path exists in the case of a spherical charged electrode. Secondly, because the fields produced by the spherical charge are correspondingly stronger, they also lead to breakdown in the interelectrode gas very easily. Hence lower accelerating voltages must be used to avoid breakdown. Thirdly, if the particles possess any appreciable velocity when they are injected in the vicinity of the electrode, they will spend a very small time in and will thus be only negligibly accelerated by the field. In the two dimensional geometries, the particles can very easily be made to possess zero radial velocity by immersing them in a gas stream flowing parallel to the axis.

Because of these reasons, it is desirable to operate with two dimensional electrode configurations. Our approach to the design of such a system will thus be confined to the two dimensional, cylindrical geometry.

A.7 Design Approach to Dielectric Separation

The differential equation of motion for the cylindrical geometry was found to be

$$\ddot{x} + \frac{k_1}{x^3} + k_2 \dot{x} = 0, \qquad \text{(A-65)}$$

$$\text{where } k_1 \triangleq \frac{\varepsilon_o (K - 1) V_o^2}{\rho P'^2 r_1^4} \qquad \text{(A-66)}$$

$$\text{and } k_2 \triangleq \frac{18\eta}{\rho d^2 + \rho dL(a + be^{-c/dL})} . \qquad \text{(A-67)}$$

We must examine this differential equation for the domain in which the particle motion is not drag limited, but is instead determined primarily by the electric field. That is, to find operating conditions such that:

$$k_2 \dot{x} << \frac{k_1}{x^3} . \tag{A-68}$$

Let β be a constant such that $\beta << 1$, and let us substitute for the previous inequality the equation

$$k_2 \dot{x} = \beta \frac{k_1}{x^3} , \tag{A-69}$$

$$\text{or} \quad k_2 \frac{\partial x}{\partial t} = \beta \frac{k_1}{x^3} , \tag{A-70}$$

We will write this differential equation in separable form, and obtain

$$k_2 x^3 dx = \beta k_1 dt. \tag{A-71}$$

Upon integration, we find that

$$k_2 \frac{x^4}{4} \Bigg]_{x_1}^{x_2} = \beta k_1 T \Bigg]_{T_1}^{T_2} \tag{A-72}$$

where the particle motion occurs between T_1 and T_2 from x_1 to x_2.

If

$$\frac{(x_2^4 - x_1^4)}{(T_2 - T_1)} \text{ is defined as } \frac{\Delta x}{\Delta T} ,$$

then

$$\frac{\Delta x}{\Delta T} = \frac{4\beta\, k_1}{k_2} \qquad \text{(A-73)}$$

is a condition for essentially drag-free motion of the particle.

We notice in the result above that, since $x_2 < x_1$, the dominant term in the determination of Δx is x_1, the initial position.

We are now able to determine which parameters must be maximized or minimized in order to obtain effective dielectric separation when particles of different sizes, densities, and dielectric constants are present in the gas stream.

From Equation 73, we find that for field-determined motion of the particles, the ratio k_1/k_2 must be as large as possible. Thus this ratio

$$\frac{k_1}{k_2} = \frac{\varepsilon_o (K - 1) V_o^2}{\rho p'^2 r_1^4} \cdot \frac{\rho d^2 + \rho dL(a + be^{-c/dL})}{18\eta} \qquad \text{(A-74)}$$

should be maximized.

Before analyzing the various parameters individually, it is preferable to examine the combination of some of them that are limited by other considerations. For instance, Equation 74 suggests that for effective dielectric separation, the applied voltage V_o should be as high as possible. However, limits to the applicable voltage are imposed by the possibility of eventual breakdown in the interelectrode gas. Thus, a more global consideration must apply in the determination of the maximum usable voltage.

We will write Equation 74 in slightly modified form to enable breakdown effects to be analyzed. From Equation 32, we see that the field in the interelectrode space is given by

$$E(r) = \frac{V_o}{P' r} , \qquad \text{(A-32)}$$

and thus

$$E^2(r_o) = \frac{V_o^2}{P'^2 r_o^2} \qquad \text{(A-75)}$$

Since r_o is the minimum radius, the field strength at the inner electrode surface is a maximum and thus possible breakdown will occur on this surface. We substitute Equation 75 into Equation 74 to obtain

$$\frac{k_1}{k_2} = \frac{\varepsilon_o (K - 1)}{\rho} E^2(r_o) \cdot \frac{r_o^2}{r_1^2} \cdot \frac{1}{r_1^2} \cdot \frac{\rho d^2 + \rho dL(a + be^{-c/dL})}{18\eta} . \qquad \text{(A-76)}$$

The various parameters that affect the efficiency of dielectric separation can now be enumerated.

Since the objective for effective separation is to maximize the ratio k_1/k_2, from Equation 76 we have the conditions

a) $E(r_o)$ should be as large as possible. The limit to this is set by breakdown considerations. Thus, in dry air at standard temperature and pressure, the voltage gradient should not exceed 30 KV/cm.

b) The ratio r_o/r_1 should be maximized. This suggests that the inner electrode should be as large as possible while the outer electrode is as small as possible.

c) r_1 should also be minimized from entirely separate considerations. This criterion coincides with the previous one.

d) The mean-free-path length of the carrier gas should preferably be as large as possible. There are two ways of accomplishing this goal. First, it is possible to select gases which have large mean free paths. An example is hydrogen, with a mean free path of 0.118×10^{-6} metres, or 1.85 times that of air. Second, it is possible to rarify the gas such that a corresponding increase in the mean free path length occurs.

In the analysis of dielectric separation, we will consider two gases, air and hydrogen. Also, each of these will be considered both at standard temperature and pressure, and at the reduced pressure of 1/100 atmospheres.

Another design parameter, which is not included in the previous discussion, can be evaluated from Equation 73. Since the condition for obtaining drag-free motion also involves minimizing the ratio $\Delta x/\Delta T$ in this equation, we see that Δx should be as small as we can make it. From the expression for Δx, we can derive a fifth condition for effective dielectric separation, namely

e) particle trajectories should be confined as close to the vicinity of the inner electrode as possible. Ideally, the motion of the particle should terminate at the inner electrode.

These are some of the design criteria that must be kept in mind in the actual design of a dielectric separator.

A.8 An Alternative Approach to Dielectrophoretic Separation

In an alternative approach to particle separation evolving out of the previous design, the dielectrophoretic, inward force on the particle is balanced by an outward, centrifugal force, by placing the particle in a circular orbit. A successful design based on this approach should eliminate any considerations of the viscosity of the carrier gas. We will analyze this scheme in detail in this section.

We must calculate the magnitude of the centrifugal acceleration required and consequently the angular speed required to be imparted to the particle in order to achieve this dynamic balance. An equally important question is the dynamic stability of this equilibrium situation. Here, the magnitude of the angular speed is derived for a given particle. The problem of dynamic stability is considered later.

A.8.1 The Equilibrium Orbit of a Particle

The centripetal acceleration of a particle moving in a circular orbit of radius r with an angular velocity $\omega(r)$ is

$$\alpha_r = -\omega^2(r) \cdot r. \qquad \text{(A-77)}$$

If this particle is in equilibrium under the simultaneous acceleration due to a dielectrophoretic force, this force must be equal in magnitude to the force of centripetal acceleration. The value of the acceleration due to dielectrophoresis is obtained from Equation 36. Here, the net outward force F will be expressed as a sum of the (outward) centrifugal force and the (inward) dielectrophoretic force.

$$F = m\,\omega^2(r) \cdot r - m \cdot \frac{\varepsilon_o}{\rho}\,(K - 1)\,\frac{V_o^{\,2}}{P'^{\,2}}\,\frac{1}{r^3} \qquad \text{(A-78)}$$

In dynamic equilibrium, that is, when F = 0,

$$\omega^2(r) \cdot r = \frac{\varepsilon_o}{\rho}\,(K - 1)\,\frac{V_o^{\,2}}{P'^{\,2}}\,\frac{1}{r^3} \qquad \text{(A-79)}$$

or

$$\omega(r) = \sqrt{\frac{\varepsilon_o (K - 1)}{\rho}} \cdot \frac{V_o}{p'} \cdot \frac{1}{r^2} \cdot \qquad \text{(A-80)}$$

This result can be interpreted in two ways.

a) The equilibrium radius of a given particle is unique, for a given angular velocity profile $\omega(r)$, and is determined solely by the particle dielectric constant and density, being independent of the particle size.

b) For a given radius to which particles are confined, the angular speed of a particle is determined by its dielectric constant and density.

Of these two, the first viewpoint is of greater importance for dielectrophoretic separation.

A.8.2 Self-stability or Stability in Vacuum of the Equilibrium Orbit of a Particle

It is of interest to determine whether a particle in a dielectrophoretic field in the absence of any drag forces due to a gas flow stream is in stable orbit or not.

In the absence of a tangential field, there is no torque on the particle and hence the angular momentum relation takes the form

$$\frac{\partial}{\partial t} (mr^2\omega) = 0 \qquad \text{(A-81)}$$

Assume a particle to enter the cylindrical interelectrode region with a tangential component of velocity v_p, at the radius r_p. Then the initial angular momentum is $mv_p r_p$, and since this must remain constant throughout the path of the particle,

$$mr^2\,\omega(r) = mv_p r_p \qquad \text{(A-82)}$$

or

$$\omega(r) = \frac{v_p r_p}{r^2} . \qquad \text{(A-83)}$$

In order to obtain an idea of the radial stability of the particle, the net radial force is equated to the rate of change of radial momentum. The radial force has two components, one due to the electric field, and the other the centrifugal force on the particle.

Equating the sum of these to the product of mass and radial acceleration yields

$$mr\,\omega^2(r) - m \cdot \frac{\varepsilon_o (K - 1)\, V_o^2}{3\, p'^2} \cdot \frac{1}{r^3} = \frac{\partial^2 r}{\partial t^2} \cdot m \qquad \text{(A-84)}$$

as the equation of radial motion.

Several interesting conclusions can be drawn from this result. Since

$$\frac{\partial^2 r}{\partial t^2} = \left\{ v_p^2\, r_p^2 - \frac{\varepsilon_o (K - 1)}{\rho\, p'^2} V_o^2 \right\} \cdot \frac{1}{r^3} , \qquad \text{(A-85)}$$

the particle trajectory is in general an unstable one, with the particle either spiralling inwards with constantly increasing radial velocity, or spiralling outward at a slower increasing radial rate. However, there is one particular injection velocity

$$v_p = \sqrt{\frac{\varepsilon_o (K - 1)}{\rho}} \cdot \frac{V_o}{p'\, r_p} \qquad \text{(A-86)}$$

at which the particle is in a circular orbit about the inner electrode.

For an ensemble of particles which have various values for the ratio $\frac{(K - 1)}{\rho}$, this offers a means of selection.

Particles with high dielectric constant/density ratio will spiral inwards from r_p, while less dielectric particles will spiral outwards.

A.8.3 Radius of the Equilibrium Orbit for a Given Angular Velocity Profile $\omega(r)$

It is assumed that the particle is constrained to move in a gas stream flowing in the annular region between the cylindrical electrodes (see Figure A-4). In this case, $\omega(r)$ an externally determined parameter in the previous equation. The orbital radius of a particle in equilibrium is then found to be

$$r = \left[\sqrt{\frac{\varepsilon_o (K - 1)}{\rho}} \quad \frac{V_o}{P' \omega(r)} \right]^{1/2} . \qquad \text{(A-87)}$$

For a given angular speed $\omega(r)$, the equilibrium radius r is determined by the particle dielectric constant and density.

As an example, it is assumed that $\omega(r)$ is a constant (i.e., ω_o) between r_o and r_1. This represents an ideal motion of the gas stream. The dependence of r, the equilibrium radius, on K, the dielectric constant, is

$$r \approx \sqrt[4]{K} \qquad \text{(A-88)}$$

A.8.4 Stability of a Particle in Equilibrium Orbit

The distribution at equilibrium will be considered to be determined by the angular velocity profile $\omega(r)$. Each particle comes to an equilibrium at a specific radius, depending only on its dielectric constant and its density.

A given velocity profile $\omega(r)$ can be obtained by considering the particle to be immersed in a fluid stream flowing in the annular space between the inner and outer electrodes (see Figure 1). Fluid streams of various angular velocity

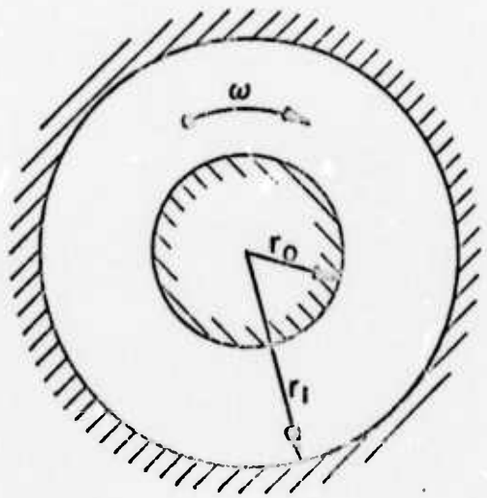

FIGURE A-4.

ANGULAR VELOCITY PROFILE OF A GAS STREAM FLOWING BETWEEN CONCENTRIC ELECTRODES

profiles can be obtained by having a gas flow between stationary electrodes, by rotating one or both electrodes, or by a combination of both these methods.

The stability condition for the equilibrium orbit of a particle is as follows:

If $\frac{\partial^n F(r)}{\partial r^n}$ is the first non-zero derivative of $F(r)$,

then

$\frac{\partial^n F(r)}{\partial r^n} < 0$ is a condition for stability.

Here we will simply assume that

$$\frac{\partial F(r)}{\partial r} \neq 0, \tag{A-89}$$

and therefore the condition for stability is:

$$\frac{\partial F(r)}{\partial r} < 0. \tag{A-90}$$

Since

$$\frac{F}{m} = r\,\omega^2(r) - \frac{\varepsilon_o}{\rho}(K-1)\frac{V_o^2}{P'^2}\frac{1}{r^3} \tag{A-91}$$

$$\frac{\partial F(r)}{\partial r} = m\left\{\omega^2(r) + 2r\,\omega(r)\frac{\partial \omega}{\partial r} + \frac{3\,\varepsilon_o}{\rho}\cdot (K-1)\frac{V_o^2}{P'^2}\frac{1}{r^4}\right\} \tag{A-92}$$

(The factor m is dropped from here on out.)

The condition for stability is thus:

$$\omega^2(r) + 2r\omega(r)\frac{\partial\omega}{\partial r} + \frac{3\varepsilon_o}{\rho}(K-1)\frac{V_o^2}{p'^2}\frac{1}{r^4} < 0. \tag{A-93}$$

To make this equation more tractable, we substitute for r from Equation 87, to obtain

$$\omega^2(r) + 2r\omega(r)\frac{\partial\omega}{\partial r} + 3\omega^2(r) < 0, \tag{A-94}$$

or

$$r\frac{\partial\omega(r)}{\partial r} + 2\omega(r) < 0 \tag{A-95}$$

on the implicit assumption that $\omega(r) > 0$.

The preceding equation can be written as either

$$\text{(i)}\quad \frac{\partial\omega(r)}{\partial r} < -\frac{2\omega(r)}{r} \tag{A-96}$$

$$\text{(ii)}\quad \frac{\partial r}{r} < -\frac{1}{2}\frac{\partial\omega(r)}{\omega(r)} \tag{A-97}$$

where $\omega(r)$ is constrained to > 0.

Some conclusions that can be drawn from these equations are:

a) A uniform angular velocity profile (vs. radial distance) is not sufficient to obtain dynamic stability. Since $\partial\omega/\omega$ is then zero. Thus the idealized case of uniform angular flow considered previously is not sufficient for orbital stability.

b) To obtain stable particle orbits, $\partial\omega/\omega$ must be negative. Since $\omega(r)$ is positive by implicit assumption, it follows that $\partial\omega/\partial r$ must be negative. Thus a configuration which produces high angular speeds toward the center is required

if stability is to be achieved.

Such a configuration could be obtained, for instance, if the inner electrode were rotated with respect to the outer electrode.

A.8.5 Possible Stability Conditions for a Specific Flow Profile

It is possible to solve the preceding equation for any specific radial flow profile $\omega(r)$ and thus to predict the regions in which a particle, in a circular orbit, can be expected to be stable. As an example, assume that a flow profile is created in which the gas stream flow velocity as a function of radial position is expressed as

$$\omega(r) = \omega_o \frac{(r_1 - r)}{(r_1 - r_o)} \quad \text{(A-98)}$$

This velocity profile is obtainable, for instance, if the outer electrode is stationary while the inner electrode spins with an angular speed of ω_o, giving rise to a linearly decreasing velocity profile as a function of r.

Using Equation 96, the stability condition is

$$\frac{\partial}{\partial r} \omega_o \frac{(r_1 - r)}{(r_1 - r_o)} < \frac{2}{r} \omega_o \frac{(r_1 - r)}{(r_1 - r_o)} \quad \text{(A-99)}$$

i.e.,

$$- \omega_o \cdot \frac{1}{(r_1 - r_o)} < - \frac{2}{r} \omega_o \frac{(r_1 - r)}{(r_1 - r_o)} \quad \text{(A-100)}$$

This simplifies to the condition

$$\frac{2}{r} (r_1 - r) < 1 \quad \text{(A-101)}$$

or

$$\boxed{r > \frac{2}{3} r_1 .} \qquad \text{(A-102)}$$

for stable orbits. That is, the region of stability for a linear gas flow profile is the outer one-third region between the two conductors.

The above derived stability condition is somewhat surprising in one respect; namely that the stability of the particle is independent of ω_o, the magnitude of the angular speed with which the inner electrode is rotated. In theory, stable particle motion could be obtained with very low rotation speeds of this inner electrode. In practice however, a certain minimum angular speed must be used. This is true because the stability condition we have derived is one of the bounded-input bounded-output kind, and says nothing about the excursions of the particle about its stable orbit. As the angular speed ω_o is decreased, the excursions of the particle around its equilibrium orbit become larger and larger, and at some point the uncertainty in the particle orbit becomes comparable to the total width of the stability region. A minimum angular speed ω_o for the inner electrode must therefore be used. This minimum value of ω_o must be derived from separate, perhaps experimental considerations.

A.8.6 Improved Particle Stability Conditions for the Flow Profile Obtained by a Rotation of the Electrodes

It is possible to solve the stability condition derived in the previous section for any specific flow profile $\omega(r)$, and thus predict the existence of regions of gas flow in which a circularly orbiting particle can be expected to be stable.

In this section we will consider the gas flow profiles resulting from rotating the cylindrical electrodes about their axes, and derive the corresponding stability regions for the particles. The gas in the annular region is assumed to have no externally impressed velocity profile. Thus the angular velocity of the interelectrode gas is determined solely by the speeds of the inner and outer electrodes, which are assumed to be concentric.

Such a gas flow must necessarily be laminar and satisfy the governing fluid dynamic equations and boundary conditions. However, these conditions are not sufficient to ensure the stability of the gas flow itself. The instability of the flow of a viscous gas between concentric cylinders is a kind of inertial instability, and its possibility must be taken into account. This will be dealt with later in the analysis.

In the analysis, we will consider that the inner and outer electrodes spin about their common axes with angular velocities ω_0 and ω_1, respectively. Under such conditions, and assuming laminar behavior, the velocity profile of the gas in the annular region can be shown* to have the time-average form

---

* Taylor, G.I., 1923, Phil. Trans. Roy. Soc., London, A223, p. 289-343

$$\omega(r) = A + \frac{B}{r^2} \tag{A-103}$$

where

$$A = \frac{\omega_1 r_1^2 - \omega_0 r_0^2}{r_1^2 - r_0^2} \tag{A-104}$$

and

$$B = \frac{(\omega_o - \omega_1) r_1^2 r_0^2}{r_1^2 - r_0^2} \tag{A-105}$$

We will apply the previously derived particle stability condition, namely

$$\frac{\partial \omega(r)}{\partial r} < \frac{-2\omega(r)}{r} \tag{A-106}$$

to this particular velocity profile and obtain the regions of stability for particle motion.

Solving for both sides of this equation and equating, we have

$$-\frac{2B}{r^3} < -2\left[\frac{A}{r} + \frac{B}{r^3}\right] \tag{A-107}$$

as the stability condition; that is,

$$\frac{A}{r} < 0 \tag{A-108}$$

Since, in the expression for A, r_1^2 is always greater than r_0^2, the condition for stability thus reduces to the very simple one:

$$\omega_1 r_1^2 < \omega_0 r_0^2 \tag{A-109}$$

or

$$\omega_1 < \frac{\omega_0 r_0^2}{r_1^2} \tag{A-110}$$

We will for simplicity suppose that the outer electrode is held stationary ($\omega_1 = 0$) while the inner electrode is spun at the speed ω_0. This situation satisfies the stability criterion, and the particle orbits are then stable at any radial position.

A.8.6 Inertial Stability Conditions for the Gas Flow Profile

In order to obtain stable orbital motion of the particles, it is necessary to rotate the inner electrode at an angular speed ω_0. Although this arrangement stabilizes the particle motion, we must additionally ensure that the resulting gas motion is itself stable.

As discussed previously, it is possible for a gas stream under such boundary conditions to exhibit a form of inertial instability arising from the acceleration of the container. The following is a condition* sufficient to ensure the absence of this kind of stability, known as Taylor instability.

For stable gas flow, we must have

$$\frac{\partial}{\partial r} r^2 \omega(r) > 0 \qquad \text{(A-111)}$$

in the entire region $r_0 \leq r \leq r_1$.

We substitute the known form of $\omega(r)$ from the previous section to obtain the condition

$$\frac{\partial}{\partial r} (Ar^2 + B) > 0 \qquad \text{(A-112)}$$

which reduces to the condition

$$A > 0 \, . \qquad \text{(A-113)}$$

---

* C-S. Yih, "Fluid Mechanics", Ch. 9, Sec. 3, McGraw-Hill, 1969

This condition for the stability of the gas flow is the exact opposite of the condition required for the stability of the particle orbits, derived in the previous section. We are thus forced to conclude that the conditions for stable gas flow and stable particle orbits are mutually incompatible.

Appendix B. FORTRAN Programs to Generate Particle Trajectories in the Planar and Cylindrical Geometries

```
TYPE FIELD

      REAL KAPPA
C
      EO=8.855-12
      RHO=253
      KAPPA=10.0
      P2=(ALOG(2.0*50.0-1.0))**2
      ETA=2.182E-4
      POSN=0.9
      ACCEPT "ETA? (TYPE 0.0 FOR DEFAULT)", ETA1
      IF (ETA1.NE.0.0) ETA=ETA1
      ACCEPT "POSN? ", POSN1
      IF (POSN1.NE.0.0) POSN=POSN1
C
      WRITE(10,10)
10      FORMAT(' ELECTRODE SPACING IN CM. ? (FA.2)'/)

      READ(11,20)H
20    FORMAT(FA.2)
      H=H/100.0
      WRITE(10,25)
25    FORMAT(' PARTICLE DIAMETER IN MICRONS ? (F5.1)'/)
      READ(11,30)D2
30    FORMAT(F5.1)
      D2=(D2*1E-6)**2
      WRITE(10,35)
35    FORMAT(' VOLTAGE ? (F7.1)'/)
      READ(11,40)VOLTS
40    FORMAT(F7.1)
C
      ALPHA=2.0*EO*(KAPPA-1)*VOLTS**2/RHO/P2
      ALPHA=ALPHA/H**4
      BETA=18.0*ETA/RHO/D2
C
      TPOSN=POSN*H*100.0
      VEL=0.0
      ACCN=ALPHA*POSN/(1.0-POSN**2)**3
      TACCN=ACCN*H*100.0
C
      WRITE(10,50)
50    FORMAT(10,'POSITION',T16,'VELOCITY',T29,'ACCELERATION',
     1 T42,'FIELD ACCN',T55,'DRAG ACCN    TIME'/
     2 T3,'CM.',T16,'CM/SEC',T29,'CM/SEC**2',
     3 T42,'CM/SEC**2',T55,'CM/SEC**2    MSEC'/)
      WRITE(10,60)TPOSN,TVEL,TACCN
60    FORMAT(10,E11.4,T15,E11.4,T28,E11.4,T41,E11.4,T54,E11.4,F7.3)

C


      TIME=0.0
      DO 70 I=1,100
      TIME=TIME+0.1
      DO 65 J=1,100
      POSN=POSN+1E-6*VEL+0.5*(1E-6)**2*ACCN
      VEL=VEL+(1E-6)*ACCN
      FACCN=-ALPHA/POSN**3
      DACCN=BETA*VEL
      ACCN=FACCN-DACCN
      TPOSN=POSN*H*100.0
      TVEL=VEL*H*100.0
      TACCN=ACCN*H*100.0
      TFACCN=FACCN*H*100.0
      TDACCN=DACCN*H*100.0
65    CONTINUE
      WRITE(10,60)TPOSN,TVEL,TACCN,TFACCN,TDACCN,TIME
70    CONTINUE
C
      STOP
      END
```

```
TYPE FIELD3

      REAL KAPPA
C
      E0=8.85E-12
      RHO=3E3
      KAPPA=10.0
      P2=(ALOG(50.0))**2
      ETA=0.182E-4
      POSN=0.1
      ACCEPT "ETA? (TYPE 0.0 FOR DEFAULT)",ETA1
      IF (ETA1.NE.0.0) ETA=ETA1
      ACCEPT "POSN? ",POSN1
      IF (POSN1.NE.0.0) POSN=POSN1
C
      WRITE(10,10)
10      FORMAT(' ELECTRODE DIAMETER IN CM. ? (F4.2)'/)

      READ(11,20)H
20    FORMAT(F4.2)
      H=H/2/100.0
      WRITE(10,25)
25    FORMAT(' PARTICLE DIAMETER IN MICRONS ? (F5.1)'/)
      READ(11,30)D2
30    FORMAT(F5.1)
      D2=(D2*1E-6)**2
      WRITE(10,35)
35    FORMAT(' VOLTAGE ? (F7.1)'/)
      READ(11,40)VOLTS
40    FORMAT(F7.1)
C
      ALPHA=E0*(KAPPA-1)*VOLTS**2/RHO/P2
      ALPHA=ALPHA/H**4
      BETA=18.0*ETA/RHO/D2
C
      TPOSN=POSN*H*100.0
      TVEL=0.0
      VEL=0.0
      ACCN=-ALPHA/POSN**3
      TACCN=ACCN*H*100.0
C
      WRITE(10,50)
50    FORMAT(T3,'POSITION',T16,'VELOCITY',T29,'ACCELERATION',
     1 T42,'FIELD ACCN',T55,'DRAG ACCN    TIME'/
     2 T3,'CM.',T16,'CM/SEC',T29,'CM/SECSQ',
     3 T42,'CM/SECSQ',T55,'CM/SECSQ    MSEC'/)
      WRITE(10,60)TPOSN,TVEL,TACCN
60    FORMAT(T2,E11.4,T15,E11.4,T28,E11.4,T41,E11.4,T54,E11.4,F7.3)

C


      TIME=0.0
      DO 70 I=1,100
      TIME=TIME+0.1
      DO 65 J=1,100
      POSN=POSN+1E-6*VEL+0.5*(1E-6)**2*ACCN
      VEL=VEL+(1E-6)*ACCN
      FACCN=-ALPHA/POSN**3
      DACCN=BETA*VEL
      ACCN=FACCN-DACCN
      TPOSN=POSN*H*100.0
      TVEL=VEL*H*100.0
      TACCN=ACCN*H*100.0
      TFACCN=FACCN*H*100.0
      TDACCN=DACCN*H*100.0
65    CONTINUE
      WRITE(10,60)TPOSN,TVEL,TACCN,TFACCN,TDACCN,TIME
70    CONTINUE
C
      STOP
      END
```

APPENDIX C. FORTRAN Programs to Generate Particle Trajectories and Determine Particle Distributions as a Function of Particle Characteristics.

```
      TYPE FIELD

            ACCEPT "CYLINDRICAL(1) OR PLANAR(2) GEOMETRY ?          ",NA
            ACCEPT "OUTER ELECTRODE RADIUS IN CM. ?                 ",R1
            R1=R1/100
            ACCEPT "INNER ELECTRODE RADIUS IN CM. ?                 ",R2
            R2=R2/100
            IF(NA.EQ.1)F=ALOG(R1/R2)
            IF(NA.EQ.2)F=ALOG(R2-R1/R2-1.0)
            ACCEPT "INITIAL POSITION IN CM. ?                       ",XPOSN
            POSN=XPOSN/100/R1
            ACCEPT "AIR(1) OR HYDROGEN(2) ?                         ",NF
            IF(NF.EQ.1)ETA=1.810E-4
            IF(NF.EQ.2)ETA=1.000E-4
            ACCEPT "PRESSURE IN ATMOSPHERES ?                       ",ATM
            IF(NA.EQ.1)PTL=0.760*ATM
            IF(NA.EQ.2)PTL=1.100*ATM
            ACCEPT "PARTICLE DIAMETER IN MICRONS ?                  ",D
            D=D*1E-6
            ACCEPT "DIELECTRIC CONSTANT ?                           ",KAPPA
            ACCEPT "PARTICLE DENSITY IN GM/CM**3 ?                  ",RHO
            RHO=RHO*1E3
            ACCEPT "APPLIED VOLTAGE ?                               ",V
C
            EO=8.85E-12
C
            ALPHA=EO*(KAPPA-1.0)*V**2/RHO/D**2/R1**4
            N=0.7
            IF(0.44*D/PTL.GT.100.)GO TO 5
            X=EXP(-0.4481/PTL)
5           BETA=18.0*ETA/(RHO*D**2+RHO*D*PTL*(0.46+0.62*X))
            VEL=0.0
            TVEL=0.0
            IF(NA.EQ.1)X=1.0/POSN**3
            IF(NA.EQ.2)X=(1.0-POSN)/(POSN-0.5*POSN**2)**3
            ACCN=-ALPHA*X
            TACCN=ACCN*R1*1E2
C
            WRITE(10,10)
10          FORMAT(//////T3,'POSITION',T15,'VELOCITY',T25,'ACCN',
     .            T41,'FIELD ACCN',T54,' DRAG ACCN   TIME'/
     .            T3,'CM.',T15,'CM/SEC',T25,'CM/SEC**2',
     .            T41,'CM/SEC**2',T54,' CM/SEC**2    MSEC'/)
            WRITE(10,20)TPOSN,TVEL,TACCN
20          FORMAT(T2,E11.4,T15,E11.4,T25,E11.4,T41,E11.4,T54,E11.4,F7.3)
C
            NTIME=0
      .     DO 50 I=1,100
            DO 30 J=1,100
      .     POSN=POSN+VEL*0.5E-12*ACCN
            VEL=VEL+1E-6*ACCN
            IF(NA.EQ.1)X=1.0/POSN**3
            IF(NA.EQ.2)X=(1.0-POSN)/(POSN-0.5*POSN**2)**3
            FACCN=-ALPHA*X
            DACCN=-BETA*VEL
      .     ACCN=FACCN+DACCN
      .     NTIME=NTIME+1
            IF(POSN.LE.RO/R1)GO TO 40
30          CONTINUE
40          TPOSN=POSN*R1*1E2
            TVEL=VEL*R1*1E2

            TACCN=ACCN*R1*1E4
            TFACCN=FACCN*R1*1E2
            TDACCN=DACCN*R1*1E2
            TIME=NTIME*1E-8
            WRITE(10,20)TPOSN,TVEL,TACCN,TFACCN,TDACCN,TIME
            IF(POSN.LE.RO/R1)GO TO 60
50          CONTINUE
C
60          STOP
            END
```

```
TYPE FIELDS

        ACCEPT "CYLINDRICAL(1) OR PLANAR(2) GEOMETRY ?   ",KA
        ACCEPT "OUTER ELECTRODE RADIUS IN CM. ?           ",R1
        R1=R1/1E2
        ACCEPT "INNER ELECTRODE RADIUS IN CM. ?           ",R2
        R2=R2/1E2
        IF(KA.EQ.1)R=ALOG(R1/R2)
        IF(KA.EQ.2)R=ALOG(2*R1/R2-1.0)
        ACCEPT "INITIAL POSITION IN CM. ?                 ",TPOSN
        POSN=TPOSN/1E2/R1
        ACCEPT "AIR(1) OR HYDROGEN(2) ?                   ",KB
        IF(KB.EQ.1)ETA=0.1827E-4
        IF(KB.EQ.2)ETA=0.0877E-4
        ACCEPT "PRESSURE IN ATMOSPHERES ?                 ",ATM
        IF(KB.EQ.1)PPL=0.0653E-6*ATM
        IF(KB.EQ.2)PPL=0.1181E-6*ATM
        ACCEPT "PARTICLE DIAMETER IN MICRONS ?            ",D
        D=D*1E-6
        ACCEPT "DIELECTRIC CONSTANT ?                     ",AKAPPA
        ACCEPT "PARTICLE DENSITY IN GM/CM**3 ?            ",RHO
        RHO=RHO*1E3
        ACCEPT "APPLIED VOLTAGE ?                         ",V
C
        E0=8.85E-12
C
        ALPHA=E0*(AKAPPA-1.0)*V**2/RHO/R**2/R1**4
        X=0.0
        IF(0.44*D/PPL.GT.150.0)GO TO 5
        X=EXP(-0.44*D/PPL)
5       BETA=18.0*ETA/(RHO*D**2+RHO*D*PPL*(2.46+0.82*X))
        VEL=0.0
        TVEL=0.0
        IF(KA.EQ.1)X=1.0/POSN**3
        IF(KA.EQ.2)X=(1.0-POSN)/(POSN-0.5*POSN**2)**3
        ACCN=-ALPHA*X
        TACCN=ACCN*R1*1E2
C
        WRITE(10,10)
10      FORMAT(//T2,'POSITION',T15,'VELOCITY',T28,'ACCN',
     .         T41,'FIELD ACCN',T54,' DRAG ACCN   TIME'/
     .         T3,'CM.',T15,'CM/SEC',T28,'CM/SECSQ',
     .         T41,'CM/SECSQ',T54,' CM/SECSQ    MSEC'/)
        WRITE(10,20)TPOSN,TVEL,TACCN
20      FORMAT(T2,E11.4,T15,E11.4,T28,E11.4,T41,E11.4,T54,E11.4,F7.3)
C
        N=1
        KTIME=0
        GO TO 40
30      N=N*10
40      POSN=POSN+1E-6*VEL+0.5E-12*ACCN
        VEL=VEL+1E-6*ACCN
        IF(KA.EQ.1)X=1.0/POSN**3
        IF(KA.EQ.2)X=(1.0-POSN)/(POSN-0.5*POSN**2)**3
        FACCN=-ALPHA*X
        DACCN=-BETA*VEL
        ACCN=FACCN+DACCN
        KTIME=KTIME+1
        IF(POSN.GT.R2/R1.AND.KTIME.NE.N)GO TO 40
        TPOSN=POSN*R1*1E2
        TVEL=VEL*R1*1E2
        TACCN=ACCN*R1*1E2
        TFACCN=FACCN*R1*1E2
        TDACCN=DACCN*R1*1E2
        TIME=KTIME*1E-3
        WRITE(10,20)TPOSN,TVEL,TACCN,TFACCN,TDACCN,TIME
        IF(POSN.GT.R2/R1)GO TO 30
C
        STOP
        END
R
```

```
TYPE FIELD3

      DIMENSION FIEL(2),DIA(7)
      FIEL(1)=20.0
      FIEL(2)=5.00
      DIA(1)=10.0
      DIA(2)=5.00
      DIA(3)=2.00
      DIA(4)=1.00
      DIA(5)=0.50
      DIA(6)=0.20
      DIA(7)=0.10
      ACCEPT "CYLINDRICAL(1) OR PLANAR(2) GEOMETRY ?    ",NA
      ACCEPT "OUTER ELECTRODE RADIUS IN CM. ?           ",R1
      R1=R1/100
      ACCEPT "INNER ELECTRODE RADIUS IN CM. ?           ",R0
      R0=R0/100
      IF(NA.EQ.1)F=ALOG(R1/R0)
      IF(NA.EQ.2)F=ALOG((R1/R0-1.0)
      ACCEPT "INITIAL POSITION IN CM. ?                 ",ATPOSN
      TPOSN=ATPOSN
      POSN=TPOSN/100/R1
      ACCEPT "AIR(1) OR HYDROGEN(2) ?                   ",NB
      IF(NB.EQ.1)ETA=0.183E-4
      IF(NB.EQ.2)ETA=0.103E-4
      ACCEPT "PRESSURE IN ATMOSPHERES ?                 ",ATM
      IF(NB.EQ.1)FFL=0.064E-5*ATM
      IF(NB.EQ.2)FFL=0.115E-6*ATM
      ACCEPT "PARTICLE DENSITY IN GM/CM**3 ?            ",RHO
      RHO=RHO*1E3
      ACCEPT "APPLIED VOLTAGE ?                         ",V
C
      E0=8.85E-12
C
      DO 65 I=1,2
      KAPPA=FIEL(I)
      DO 50 J=1,7
      TPOSN=ATPOSN
      POSN=TPOSN/100/R1
      D=DIA(J)*1E-6
      ALPHA=E0*(KAPPA-1.0)*V**2/RHO/ETA**2/F1**4
      X=0.0
      IF(0.44*D/FFL.GT.150.0)GO TO 5
      X=EXP(-0.44*D/FFL)
5     BETA=18.0*ETA/(RHO*D**2+RHO*D*FFL*(0.46+0.32*X))
      VEL=0.0
      TVEL=0.0
      IF(NA.EQ.1)N=1.0/POSN**3
      IF(NA.EQ.2)N=(1.0-POSN)/(POSN-0.5*POSN**2)**3
      ACCN=-ALPHA*N
      TACCN=ACCN*R1*100
C
      WRITE(12,10)
10    FORMAT(//,5X,'POSITION',7X,'VELOCITY',5X,'ACCN',
     *       7X,'FIELD ACCN',5X,' DRAG ACCN   TIME'/
     *       7X,'CM.',7X,'CM/SEC',5X,'CM/SEC**2',
     *       7X,'CM/SEC**2',5X,' CM/SEC**2    MSEC'/)
      WRITE(12,20)TPOSN,TVEL,TACCN
20    FORMAT(5X,E11.4,3X,E11.4,5X,E11.4,7X,E11.4,7X,E11.4,F7.3)
C
      DO 30 XTIME=1,4150


      POSN=POSN+1E-6*VEL+1.5E-12*ACCN
      VEL=VEL+1E-6*ACCN
      IF(NA.EQ.1)N=1.0/POSN**3
      IF(NA.EQ.2)N=(1.0-POSN)/(POSN-0.5*POSN**2)**3
      ACCN=-ALPHA*N
      DACCN=-ETA*VEL
      ACCN=ACCN+DACCN
30    TIME=XTIME*1E-3
      TPOSN=POSN*R1*100
      TVEL=VEL*R1*100
      TACCN=ACCN*R1*100
      TDACCN=DACCN*R1*100
      TACCN=TACCN+TDACCN
      WRITE(12,40)TPOSN,TVEL,TACCN,TDACCN,TIME
      WRITE(12,40)FIEL(I),I=1,4)
40    FORMAT('  DIELECTRIC CONST. = ',F5.2,'  PARTICLE DIA = ',F5.2//)
50    CONTINUE
      PAUSE
60    CONTINUE
C
      STOP
      END
```